

## INFORMATION TO USERS

This material was produced from a microfilm copy of the original document. While the most advanced technological means to photograph and reproduce this document have been used, the quality is heavily dependent upon the quality of the original submitted.

The following explanation of techniques is provided to help you understand markings or patterns which may appear on this reproduction.

1. The sign or "target" for pages apparently lacking from the document photographed is "Missing Page(s)". If it was possible to obtain the missing page(s) or section, they are spliced into the film along with adjacent pages. This may have necessitated cutting thru an image and duplicating adjacent pages to insure you complete continuity.
2. When an image on the film is obliterated with a large round black mark, it is an indication that the photographer suspected that the copy may have moved during exposure and thus cause a blurred image. You will find a good image of the page in the adjacent frame.
3. When a map, drawing or chart, etc., was part of the material being photographed the photographer followed a definite method in "sectioning" the material. It is customary to begin photoing at the upper left hand corner of a large sheet and to continue photoing from left to right in equal sections with a small overlap. If necessary, sectioning is continued again — beginning below the first row and continuing on until complete.
4. The majority of users indicate that the textual content is of greatest value, however, a somewhat higher quality reproduction could be made from "photographs" if essential to the understanding of the dissertation. Silver prints of "photographs" may be ordered at additional charge by writing the Order Department, giving the catalog number, title, author and specific pages you wish reproduced.
5. PLEASE NOTE: Some pages may have indistinct print. Filmed as received.

### University Microfilms International

300 North Zeeb Road  
Ann Arbor, Michigan 48106 USA  
St. John's Road, Tyler's Green  
High Wycombe, Bucks, England HP10 8HR

77-3708

VARMA, Girish Kumar, 1949-  
THEORETICAL STUDIES IN MEDIUM AND HIGH  
ENERGY HADRON-NUCLEUS AND NUCLEUS-NUCLEUS  
COLLISIONS.

City University of New York, Ph.D., 1976  
Physics, nuclear

**Xerox University Microfilms,** Ann Arbor, Michigan 48106

© COPYRIGHT BY  
GIRISH KUMAR VARMA

1976

THEORETICAL STUDIES IN MEDIUM AND HIGH ENERGY  
HADRON-NUCLEUS AND NUCLEUS-NUCLEUS COLLISIONS

by

GIRISH KUMAR VARMA

A dissertation submitted to the Graduate Faculty  
in Physics in partial fulfillment of the require-  
ments for the degree of Doctor of Philosophy, The  
City University of New York.

1976

This manuscript has been read and accepted for the Graduate Faculty in Physics in satisfaction of the dissertation requirement for the degree of Doctor of Philosophy.

Sept. 24, 1976  
date

Victor Franco  
Chairman of Examining Committee

September 27, 1976  
date

Impegin P. Saracchia  
Executive Officer P.H.

Carl A. Alalin

Joseph Spay

Louis K. Cole

David R. Harrington  
Supervisory Committee

The City University of New York

Abstract

THEORETICAL STUDIES IN MEDIUM AND HIGH ENERGY  
HADRON-NUCLEUS AND NUCLEUS-NUCLEUS COLLISIONS

by

Girish Kumar Varma

Advisor: Professor Victor Franco

A variety of nuclear collisions ranging from hadron-deuteron to those involving heavy-ions are studied in a theoretical framework which is based upon extensions of the high energy diffraction theory due to Glauber. The approximations leading to the Glauber theory of particle-nucleus scattering are discussed in the first section and its extension to nucleus-nucleus collisions is compared with an exact nucleus-nucleus multiple scattering series. In the second section an exact solution (within the Glauber framework) is obtained for the charged hadron-deuteron scattering problem with both the incident hadron and the bound proton having extended charge distributions. An approximation is obtained which leads to simple analytic formulas for the analysis of experimental data and applications are

made to p-d scattering measurements below 70 GeV. The p-n scattering parameters extracted in this way are found to differ significantly from those of earlier analyses. Coulomb effects in scattering of charged hadrons from other nuclei are then studied in the third section. Several frequently used approximate models are also considered and their accuracy investigated. In the fourth section we treat the problem of deuteron scattering from complex nuclei. For simple wave functions, the exact Glauber amplitude is expressed as a finite series which converges rapidly. These exact results are compared to those obtained from several approximations to the Glauber amplitude which have been used in the past. The effects on elastic scattering intensities due to the Coulomb field and the quadrupole deformation of the deuteron are also investigated. Deuteron-nucleus total cross sections are calculated at 0.87 and 2.1 GeV/n using harmonic oscillator wave functions for the targets, and excellent agreement is obtained with the available data. The formulas are also applied to 650 MeV  $d-^{12}\text{C}$  elastic scattering and a comparison is made with the data. In the fifth section we study the general case of nucleus-nucleus collisions. A recently observed discrepancy between high energy total cross section measurements and existing theoretical calculations is shown to be due to the breakdown of the optical limit approximation rather than that of the Glauber theory. The optical limit amplitude which has been widely used for analyses of nucleus-nucleus collisions is

shown to be inaccurate. Systematic corrections to the optical phase shift function are obtained which provide a basis for accurate calculations with realistic wave functions for light and medium-A nuclei. With these corrections, our theoretical predictions for nucleus-nucleus total cross sections, inelastic cross sections and forward elastic scattering slope parameters show good agreement with recent experimental measurements at 0.87 and 2.1 GeV/n.

## ACKNOWLEDGEMENTS

I would like to take this opportunity to express my appreciation and gratitude to Professor Victor Franco who has greatly influenced my development as a physicist. I have benefitted a great deal from his advice, interest, encouragement, and criticism during the entire course of this work. I am indebted to Professor David Harrington for spending a considerable amount of time on a critical review of this thesis and for a number of instructive discussions and suggestions on its contents. I also thank Professors Carl Shakin and Louis Celenza for useful conversations in the past few years on scattering theories in general.

## TABLE OF CONTENTS

	Page
List of Tables	10
List of Figures	11
 Section	
I. Introduction: Nuclear Collisions and the Glauber Approximation	13
II. Small Angle Scattering of Hadrons by Deuterium	
(a) Introduction	20
(b) Basic Formulas	21
(c) Comparison of Theoretical Expressions	31
(d) Analysis of p-d Scattering Data	33
III. Scattering of Charged Hadrons from Nuclei other than Deuterium	
(a) Introduction	45
(b) Basic Formulas	45
(c) Comparison of Approximate Models	51
IV. Scattering of Medium and High Energy Deuterons from Complex Nuclei	
(a) Introduction	55
(b) Basic Formulas	56
(c) Total Cross sections	
(i) Gaussian Wave Functions and Comparison of Theoretical Expressions	61
(ii) Realistic Wave Functions and Comparison with the data	63
(d) Elastic Scattering Intensities	
(i) Comparison of Theoretical Cross sections	67
(ii) Coulomb and Deuteron D-state Effects	72
(iii) 650 MeV d- <sup>12</sup> C Scattering	78

TABLE OF CONTENTS (cont'd)

	Page
V. Medium and High Energy Collisions between Heavy Ions	
(a) Introduction	82
(b) Basic Formulas	83
(c) Theoretical Results and Comparison with Data	86
VI. Summary of Results	96
Appendix A: Exact Multiple Scattering Series	99
Appendix B: Coulomb Phase Shift Function for Extended Charges	102
Appendix C: Average Phase Shift Functions	103
Appendix D: Charge Exchange Effects	107
Appendix E: Approximation II for d-A Scattering	108
Appendix F: Deuteron-Deuteron Cross sections	109
Appendix G: Nucleus-Nucleus Cross sections	110
Appendix H: Center of Mass Correction	112
Bibliography	115

## LIST OF TABLES

Number		Page
1	Input nucleon-nucleon parameters used in calculation of $\rho_n$ and $a_n$	36
2	Results for $\rho_n$ and $a_n$ from the analyses of p-d data	37
3	Deuteron-nucleus total cross sections at 0.87 and 2.1 GeV/n	68
4	Uncertainties in deuteron-carbon total cross sections due to uncertainties in the input parameters	69
5	Nucleus-nucleus total cross sections at 0.87 and 2.1 GeV/n	91
6	Nucleus-nucleus forward elastic scattering slope at 0.87 and 2.1 GeV/n	92
7	Nucleus-nucleus inelastic cross sections at 0.87 and 2.1 GeV/n	93

## LIST OF FIGURES

Number		Page
2.1	Percent error in p-d elastic scattering at 20.5 GeV/c for the formulas used in Ref. 17 and for the point charge solution of Eq. (2.19) compared to the extended charge result of Eq. (2.18)	30
2.2	Differential cross sections for elastic p-d scattering at 11.2 and 64.8 GeV/c. The data are from Ref. 18 and the curves correspond to Eq. (2.18)	40
2.3	Differential cross sections for elastic-plus-quasi elastic scattering at 19.3 GeV/c. The data are from Ref. 16 and the curve corresponds to Eq. (2.27)	42
2.4	Results for $\rho_n$ together with dispersion relation calculations of Ref. 27 and 28	43
3.1	Percent error in (a) p- $^{12}\text{C}$ , (b) p- $^{58}\text{Ni}$ and (c) p- $^{208}\text{Pb}$ elastic scattering intensities at 1.04 GeV for approximate formulas discussed in Sec. III compared to the extended charge result given by Eq. (3.8)	52
4.1	Partial cross sections given by Eqs. (4.24) and (4.25) for target nuclei $^{64}\text{Cu}$ and $^{27}\text{Al}$	64
4.2	Percent errors in d-A total cross sections obtained from Approximations I [Eq. (4.21)] and II [Eq. (D.1)] compared to the exact Glauber result Eq. (4.23)	65
4.3	Deuteron-carbon elastic scattering angular distribution at 2.1 GeV/n. Predictions of approximations I and II are compared with the exact Eq. (4.12)	70
4.4	Approximations made in Ref. 41 for d- $^{12}\text{C}$ scattering compared with exact Glauber results	73
4.5	(a) d- $^4\text{He}$ and (b) d- $^{12}\text{C}$ elastic scattering at 2.1 GeV/n with and without deuteron D-state	76

LIST OF FIGURES (cont'd)

Number		Page
4.6	650 MeV d- <sup>12</sup> C elastic scattering. Theoretical results, with and without Coulomb effects, compared with the data	80
5.1	(a) <sup>4</sup> He - <sup>4</sup> He and (b) <sup>12</sup> C - <sup>12</sup> C elastic scattering at 2.1 GeV/n. The dot-dash curve, when not shown, is indistinguishable from the solid curve	94

## I. INTRODUCTION: Nuclear Collisions and the Glauber Approximation

In recent years a large number of experiments, involving the scattering of medium and high energy nucleons and pions from various nuclear targets, have been performed. The theoretical analyses of such experiments are expected to yield information about the nuclear structure as well as about the incident particle-nucleon interactions. Theoretical studies in the field have generally involved the Glauber theory<sup>1</sup>, some approximate versions of the Watson series<sup>2,3</sup> and some optical potential calculations<sup>4,5</sup>. Also of current interest are high energy collisions between heavy ions. In addition to being relevant to speculations regarding super-heavy nuclei, and to providing a new tool for probing nuclear structure, these collisions are useful for testing general concepts such as factorization and limiting fragmentation. The past theoretical analyses have again employed the Glauber approximation or some variants of it<sup>6-10</sup>, and there have been some folding model<sup>11</sup> calculations at lower energies.

The present theoretical work is based upon extensions and generalizations of the Glauber approximation. An attempt is made to understand both the hadron-nucleus and nucleus-nucleus scattering processes in terms of the basic hadron-nucleon (or nucleon-nucleon) scattering amplitudes. Theoretical results are obtained for the various nuclear colli-

sions to the same degree of accuracy and applied to the available data with the view that a good agreement between theory and measurements, for nucleon-nucleus and nucleus-nucleus collisions simultaneously, would give increased confidence in the theory and in its inherent approximations. Alternatively, it could provide an excellent check of the input nuclear density and nucleon-nucleon scattering parameters which are obtained by independent means. It also provides a practical way of extracting scattering parameters involving elementary particles which are scarce or short-lived.

The approximations leading to the Glauber theory are discussed in the remainder of this section. In Section III, we study the case of charged hadron-deuteron scattering with emphasis on extraction of hadron-neutron amplitudes. The theoretical results are then extended to include targets other than deuterium in Section III. The scattering of deuterons from complex nuclei is treated in Sec. IV. In Sec. V, we study the general case of nucleus-nucleus collisions. Finally a brief summary of our results is given in Sec. VI.

Let us first consider the scattering of a single particle (with hamiltonian  $h$ ) from a nucleus with mass number  $A$  (and hamiltonian  $H_A$ ). The corresponding eigenstates are given by

$$h |\phi_{\vec{k}}\rangle = (\hbar^2 k^2 / 2m) |\phi_{\vec{k}}\rangle, \quad (1.1)$$

$$H_A |\gamma_n\rangle = E_n |\gamma_n\rangle \quad (1.2)$$

where  $m$  is the reduced mass. The schrödinger equation for the scattering is then

$$(H_A + \frac{\hbar^2 k^2}{2m} + V) |\Psi\rangle = (E_0 + \frac{\hbar^2 k^2}{2m}) |\Psi\rangle \quad (1.3)$$

where, assuming two body interactions between projectile and the target constituents, we have

$$V = \sum_{i=1}^A V_i(\vec{r} - \vec{r}_i) \quad (1.4)$$

The free particle Greens function (with outgoing boundary condition) is

$$G^+ = [E_0 + \frac{\hbar^2 k^2}{2m} - H_A - \frac{\hbar^2}{2m} + i.0]^{-1} \quad (1.5)$$

The total wave function is then given by

$$|\Psi^+\rangle = |\gamma_0 \phi_{\vec{k}}\rangle + G^+ V |\Psi^+\rangle \quad (1.6)$$

Now using a complete set of states  $\mathbb{1} = \sum_n \int d^3k' |\gamma_n \phi_{\vec{k}'}\rangle \langle \gamma_n \phi_{\vec{k}'}|$ , we obtain

$$|\Psi^+\rangle = |\gamma_0 \phi_{\vec{k}}\rangle + \sum_n |\gamma_n\rangle G^+(k_n) \langle \gamma_n | V | \Psi^+\rangle, \quad (1.7)$$

where  $k_n^2 = k^2 + \epsilon_{n0}$ ,  $\epsilon_{n0} = 2m(E_n - E_0)/\hbar^2$ ,

$$G^+(k_n) = \frac{2m}{\hbar^2} \int d^3k' |\phi_{\vec{k}'}\rangle \frac{1}{k_n^2 - k'^2 + i.0} \langle \phi_{\vec{k}'}|. \quad (1.8)$$

In coordinate space this becomes

$$G^+(k_n; \vec{r}, \vec{r}') = -\frac{2m}{\hbar^2} \frac{e^{ik_n|\vec{r}-\vec{r}'|}}{|\vec{r}-\vec{r}'|} \quad (1.9)$$

In Eq. (1.7) one has to sum over all the intermediate states

$|\gamma_n\rangle$ . Considerable simplification can be achieved by noting that, at high energies, the energy transferred to the target, in the intermediate states of the scattering process, is quite small compared to the incident energy i.e.,  $\epsilon_{n0} \ll k^2$  or  $k_n^2 \simeq k^2$ . With this approximation, we have  $G^+(k_n) \simeq G^+(k)$  and one can use the closure property  $\sum_n |\gamma_n\rangle\langle\gamma_n| = 1$  in Eq. (1.7). The solution of (1.7) now takes the form

$$|\Psi^+\rangle = |\Phi_{\vec{k}}^+\rangle |\gamma_0\rangle, \quad (1.10)$$

where the projectile wavefunction  $|\Phi_{\vec{k}}^+\rangle$  satisfies

$$|\Phi_{\vec{k}}^+\rangle = |\phi_{\vec{k}}\rangle + G^+(k)V|\Phi_{\vec{k}}^+\rangle. \quad (1.11)$$

The elastic scattering amplitude is related to the matrix element  $\langle\vec{k}'|T|\vec{k}\rangle = T_{\vec{k}'\vec{k}} = \langle\gamma_0\phi_{\vec{k}'}|V|\Phi_{\vec{k}}^+\rangle$ , which with Eq. (1.10), becomes

$$T_{\vec{k}'\vec{k}} = \langle\gamma_0|\tilde{T}_{\vec{k}'\vec{k}}|\gamma_0\rangle, \quad (1.12)$$

where the operator  $\tilde{T}$  now corresponds to scattering from A fixed nucleons, and is given by

$$\tilde{T}_{\vec{k}'\vec{k}} = \langle\phi_{\vec{k}'}|V|\Phi_{\vec{k}}^+\rangle. \quad (1.13)$$

The Green's function  $G^+(k)$  now can be written in form (1.8) with  $k_n^2$  replaced by  $k^2$ . At high energies, the scattering is concentrated in the forward direction and so one may expand the momentum space dependence of  $G^+$  about  $k$ . Letting  $\vec{k}' = \vec{k} + \vec{a}$ , we obtain

$$G^+(k) = -(2m/\hbar^2) \int d^3a |\phi_{\vec{k}+\vec{a}}\rangle [2\vec{k}\cdot\vec{a} + a^2 - i.0]^{-1} \langle\phi_{\vec{k}+\vec{a}}|$$

$$\begin{aligned}
&= -(2m/\hbar^2) \int d^3Q |\phi_{\vec{k}+\vec{Q}}\rangle [2\vec{k}\cdot\vec{Q}-i.0]^{-1} \left[1 - \frac{Q^2}{2\vec{k}\cdot\vec{Q}-i.0} + \dots\right] \langle\phi_{\vec{k}+\vec{Q}}| \\
&= G_0^+(\vec{k}) + G_1^+(\vec{k}) + \dots \quad (1.14)
\end{aligned}$$

Under the conditions  $kR \gg 1$  and  $\frac{\bar{V}}{(\hbar^2 k^2/2m)} \ll 1$  ( $R$  and  $\bar{V}$  being the typical range and strength of the interaction), it can be shown<sup>1</sup> that replacing  $G^+$  by  $G_0^+$  is a good approximation. This approximation also indicates that the resulting wave function, obtained via Eq. (1.11), will not in general have a correct estimate of Fourier amplitudes corresponding to large momentum transfers and is therefore best suited for small angle scattering.

In order to obtain an explicit solution, one can go over now to the coordinate representation where  $G_0^+$  becomes<sup>12-14</sup>

$$G_0^+(\vec{k}; \vec{r}, \vec{r}') = -\frac{im}{\hbar^2 k} e^{i\vec{k}(\vec{z}-\vec{z}')} \delta^2(\vec{b}-\vec{b}') \theta(\vec{z}-\vec{z}'), \quad (1.15)$$

where  $\vec{r} = \vec{b} + z \hat{z}$ . With this, Eq. (1.11) yields<sup>1,12</sup>

$$\Phi_{\vec{k}}^+(\vec{r}) = \exp\left[i\vec{k}\cdot\vec{r} - \frac{i}{\hbar v} \int_{-\infty}^{\vec{z}} V(\vec{b}, z') dz'\right], \quad \vec{v} = \frac{\hbar \vec{k}}{m} \quad (1.16)$$

The scattering amplitude operator, by means of Eq. (1.13), is given by

$$\begin{aligned}
F_A(\vec{q}; \vec{r}_1, \dots, \vec{r}_A) &= -(2m/4\pi\hbar^2) \widetilde{T}_{\vec{k}, \vec{k}'}(\vec{r}_1, \dots, \vec{r}_A) \\
&= \frac{1}{2\pi} \int d^2b e^{i\vec{q}\cdot\vec{b}} \left[1 - e^{i\sum_{j=1}^A \chi_j(\vec{b}-\vec{s}_j)}\right], \quad (1.17)
\end{aligned}$$

where we have defined  $\vec{q} = \vec{k} - \vec{k}'$ ,  $\vec{r}_j = \vec{s}_j + z_j \hat{z}$ ,

$$\chi_j(\vec{b}) = -\frac{1}{\hbar v} \int_{-\infty}^{\infty} V_j(\vec{b}, z) dz \quad (1.18)$$

The result can be generalized immediately to the case of

nucleus-nucleus scattering. With  $V = \sum_{i=1}^{A_1} \sum_{j=1}^{A_2} v_{ij}(\vec{r} - \vec{r}_i + \vec{r}_j)$ , we obtain

$$F_{A_1 A_2}(\vec{q}; \{\vec{r}_i\}, \{\vec{r}_j\}) = \frac{i k}{2\pi} \int d^2 b e^{i \vec{q} \cdot \vec{b}} \left[ 1 - e^{i \sum_{ij} \chi_{ij}(\vec{b} - \vec{s}_i + \vec{s}_j')} \right]. \quad (1.19)$$

Inverting Eq. (1.17) for the case of nucleon-nucleon (NN) scattering ( $A=1$ ), we have

$$1 - e^{i \chi_{ij}(\vec{b})} = \Gamma_{ij}(\vec{b}) = (2\pi k_{ij})^{-1} \int d^2 q e^{-i \vec{q} \cdot \vec{b}} f_{ij}(\vec{q}). \quad (1.20)$$

We can also rewrite

$$\begin{aligned} 1 - e^{i \sum_{ij} \chi_{ij}} &= 1 - \prod_{i=1}^{A_1} \prod_{j=1}^{A_2} (1 - \Gamma_{ij}) \\ &= \sum_{ij} \Gamma_{ij} - \frac{1}{2} \sum_{\substack{ijkl \\ (ij) \neq (kl)}} \Gamma_{ij} \Gamma_{kl} + \dots \end{aligned} \quad (1.21)$$

Eq. (1.21), when substituted in (1.19) provides the Glauber multiple scattering series which terminates after  $A_1 A_2$  terms. Furthermore, the terms in the series are on-shell as they can be expressed in terms of measured NN amplitudes by means of Eq. (1.20). This is to be compared with the exact multiple scattering series (described in Appendix A) which is an infinite series and also has contributions coming from NN  $t$  matrices off the energy shell. Now, since the Glauber series is the solution of the exact series when  $G^+$  is replaced by  $G_0^+$ , it follows that the off shell contributions and the contributions from the terms of order higher than  $A_1 A_2$  must cancel exactly (in the high energy limit  $G^+ \rightarrow G_0^+$ ). This cancellation which was shown explicitly,

for the special case of particle-deuteron scattering, by Harrington<sup>12</sup> is, in part, responsible for the remarkable accuracy of the Glauber theory. It also emphasizes the caution required in obtaining corrections to the theory. In particular, the Glauber theory is not a truncated version of the Watson series but is an alternative series (generated by the approximate propagator  $G_0^+$ ) where a large number of terms cancel resulting in a series which is both on-shell and finite.

## II. Small Angle Scattering of Hadrons by Deuterium

### II (a). Introduction

When charged hadrons collide with nuclei, the scattering cross sections are influenced by both the strong and the Coulomb interactions. At very small momentum transfers, the contributions of the Coulomb interactions and of the strong interactions are comparable, and hence the elastic scattering intensities are quite sensitive to the interference between them. Information regarding strong interactions, such as the real parts of the strong interactions amplitudes, can be extracted from the analysis of the interference region. Since direct hadron-neutron scattering experiments, for the most part, are not feasible because of the unavailability of neutron targets or the scarcity or short lives of most elementary particles, small angle hadron-deuteron scattering is of particular interest. Hadron-deuteron scattering experiments can be used, together with hadron-proton measurements, to extract information about the hadron-neutron amplitudes by means of the Glauber approximation. In earlier analyses,<sup>16,17</sup> a number of additional approximations and simplifications were made. In this section we obtain an exact solution for charged hadron-deuteron scattering in the Glauber approximation, with both the incident hadron and the bound proton having extended charge distributions. Some approximate and simpler formulas are also considered and their accur-

acy discussed. We then apply the results to p-d measurements<sup>18</sup> between 10-70 GeV to extract p-n scattering parameters.

(b). Basic Formulas

From Sec. I, the hadron-deuteron scattering amplitude operator can be written as

$$F_d(\vec{q}, \vec{s}) = \frac{i k}{2\pi} \int d^2b e^{i\vec{q}\cdot\vec{b}} \Gamma_d(\vec{b}, \vec{s}) \quad (2.1)$$

where  $\vec{k}$  is the incident momentum,  $\vec{q}$  is the momentum transfer,  $\vec{b}$  is the impact parameter and  $\vec{s}$  is the projection of the internal deuteron coordinate  $\vec{r}$  on a plane perpendicular to  $\vec{k}$ . The profile function  $\Gamma_d$  for the deuteron is given by

$$\Gamma_d(\vec{b}, \vec{s}) = 1 - \exp\left[i\chi_p(\vec{b} + \frac{1}{2}\vec{s}) + i\chi_n(\vec{b} - \frac{1}{2}\vec{s})\right] \quad (2.2)$$

where  $\chi_n$  and  $\chi_p$  are the phase shift functions for the scattering of the incident hadron by the neutron and proton, respectively. At high energies, we further assume<sup>19</sup> that

$$\chi_p(\vec{b}) = \chi_c(\vec{b}) + \chi_{ps}(\vec{b}) \quad (2.3)$$

where  $\chi_c$  is the phase shift function for the Coulomb scattering from the proton and  $\chi_{ps}$  is that for scattering by the strong interaction alone. If we separate out of the Coulomb phase shift function  $\chi_c^{pt}$  due to a point charge, we can write

$$\chi_c(\vec{b}) = \chi_c^{pt}(\vec{b}) + \chi_c^E(\vec{b}) \quad (2.4)$$

where  $\chi_c^E$  denotes the correction to the Coulomb phase shift

function due to extended charge effects. (In Appendix B we calculate  $\chi_c^E$  explicitly for a specific charge distribution of the incident particle and the target proton.)

Let us write the hadron-nucleon profile function as

$$\Gamma_j(\vec{b}) = 1 - \exp\left[i\chi_j(\vec{b})\right], \quad j = n, ps \quad (2.5)$$

and also write

$$\Gamma_c^i(\vec{b}) = 1 - \exp\left[i\chi_c^i(\vec{b})\right], \quad i = pt, E. \quad (2.6)$$

There are many ways of separating point charge and charge distribution effects. For example, one way that exhibits various multiple scattering effects explicitly is given by

$$\begin{aligned} \Gamma_d(\vec{b}, \vec{s}) = & \Gamma_c^{pt} + \Gamma_c^E + \Gamma_{ps} + \Gamma_n - \Gamma_c^{pt} [\Gamma_{ps} + \Gamma_n] \\ & - \Gamma_{ps} \Gamma_n - \Gamma_c^E [\Gamma_c^{pt} + \Gamma_{ps} + \Gamma_n] + \Gamma_c^{pt} \Gamma_{ps} \Gamma_n \\ & + \Gamma_c^E [\Gamma_c^{pt} \Gamma_{ps} + \Gamma_c^{pt} \Gamma_n + \Gamma_{ps} \Gamma_n] - \Gamma_c^{pt} \Gamma_c^E \Gamma_{ps} \Gamma_n \quad (2.7) \end{aligned}$$

where the argument of  $\Gamma_n$  is  $\vec{b} - (1/2)\vec{s}$  and the argument of all other  $\Gamma$ 's is  $\vec{b} + (1/2)\vec{s}$ .

The terms involving a single  $\Gamma$  can be viewed as representing single scattering by the interactions denoted by the subscripts or superscripts, while a product of  $\Gamma$ 's corresponds to multiple scattering. The effects of charge distribution are embedded in the second, eighth, ninth, tenth and twelfth through fifteenth terms. The second term represents single scattering by the extended charge corrections to the Coulomb field. The eighth, ninth and

tenth are double scattering terms. For example, the tenth term represents double scattering by the extended charge corrections to the Coulomb field and by the neutron. The twelfth, thirteenth and fourteenth terms have similar triple scattering interpretations; the last term can be thought of as quadruple scattering by a point Coulomb field, the extended charge effects of the Coulomb field, the proton strong interaction and neutron. In the absence of an extended charge distribution,  $\Gamma_c^E$  vanishes and Eq. (2.7) reduces to the results of Ref. 19.

Another way of writing Eq.(2.7) which is more convenient for numerical evaluation is<sup>20</sup>

$$\begin{aligned} \Gamma_d(\vec{b}, \vec{s}) = & \Gamma_c^{Pt}(\vec{b} + \frac{1}{2}\vec{s}) + e^{i\chi_c^{Pt}(\vec{b} + \frac{1}{2}\vec{s})} \Gamma_c^E(\vec{b} + \frac{1}{2}\vec{s}) \\ & + e^{i\chi_c(\vec{b} + \frac{1}{2}\vec{s})} [\Gamma_{ps}(\vec{b} + \frac{1}{2}\vec{s}) + \Gamma_n(\vec{b} - \frac{1}{2}\vec{s}) \\ & - \Gamma_{ps}(\vec{b} + \frac{1}{2}\vec{s}) \Gamma_n(\vec{b} - \frac{1}{2}\vec{s})] . \end{aligned} \quad (2.8)$$

For a screening radius  $R$  and  $q \gg 1/R$ , we have<sup>1</sup>

$$\begin{aligned} \chi_c^{Pt}(\vec{b}) = & 2n \ln(b/2R) , \quad b < R \\ = & 0 , \quad b > R \end{aligned} \quad (2.9)$$

where  $n = e^2/\pi v$  and  $v$  is the relative velocity between the projectile and the bound proton in the target.

For  $R$  of atomic dimensions, this is valid for  $n^2 q^2 \gg 10^{-11} (\text{GeV}/c)^2$ . Using Eqs. (2.6) and (2.9) we obtain

$$\begin{aligned} \frac{i k}{2\pi} \int d^2 b e^{i\vec{q} \cdot \vec{b}} \Gamma_c^{Pt}(\vec{b}) d^2 b = & -2n k q^{-2} e^{-2i[n \ln(qR) - \arg \Gamma(1+in)]} \\ = & e^{-2in \ln(2kR)} f_c^{Pt}(q) , \end{aligned}$$

where we have defined the Coulomb amplitude for a point

charge as

$$f_c^{pt}(q) = -\frac{2n\kappa}{q^2} e^{-2i[n \ln(q/2\kappa) - \arg \Gamma(1+in)]} \quad (2.10)$$

with  $\Gamma(z)$  being the gamma function.

Hadron-nucleon profile functions are related to hadron-nucleon scattering amplitudes by

$$\Gamma_j(\vec{b}) = (2\pi\kappa)^{-1} \int d^2q e^{-i\vec{q}\cdot\vec{b}} f_j(\vec{q}), \quad j = n, ps$$

Using this relation together with Eq. (2.1) we obtain

$$\begin{aligned} F_d(\vec{q}, \vec{s}) = & e^{-2in \ln(2\kappa R)} e^{-\frac{i}{2}\vec{q}\cdot\vec{s}} \left\{ f_c^{pt}(q) + i \int_0^\infty J_0(qb) \Gamma_c^E(b) (\kappa b)^{2in+1} db \right. \\ & + \frac{1}{4\pi^2} \int d^2q' d^2b e^{i(\vec{q}-\vec{q}')\cdot\vec{b}} (\kappa b)^{2in} e^{i\chi_c^E(\vec{b})} [f_{ps}(\vec{q}') \\ & + f_n(\vec{q}') e^{i\vec{q}'\cdot\vec{s}}] + \frac{i}{8\pi^2\kappa} \int d^2q' d^2q'' d^2b e^{i(\vec{q}-\vec{q}'-\vec{q}'')\cdot\vec{b}} \\ & \left. \times (\kappa b)^{2in} e^{i\vec{q}''\cdot\vec{s}} e^{i\chi_c^E(\vec{b})} f_{ps}(\vec{q}') f_n(\vec{q}'') \right\}. \quad (2.11) \end{aligned}$$

We will omit the phase  $\exp[-2in \ln(2\kappa R)]$  from now on as it does not contribute to physically measured quantities.

We point out that the scattering amplitude for hadron-proton scattering  $f_p(q)$  can be obtained as a special case by setting  $s$  and  $f_n$  equal to zero in Eq. (2.11).

The differential cross section for elastic scattering by deuterium is given by

$$(d\sigma/d\Omega)_{el} = |F_{el}(\vec{q})|^2, \quad (2.12)$$

where the elastic scattering amplitude is the expectation value of  $F_d(\vec{q}, \vec{s})$  in the deuteron ground state and is given by

$$\begin{aligned} F_{el}(\vec{q}) = & S(\frac{1}{2}\vec{q}) \left[ f_c^{pt}(\vec{q}) + i \int_0^\infty J_0(qb) (\kappa b)^{2in+1} \Gamma_c^E(b) db \right. \\ & \left. + \frac{1}{4\pi^2} \int d^2q' d^2b e^{i(\vec{q}-\vec{q}')\cdot\vec{b}} (\kappa b)^{2in} e^{i\chi_c^E(b)} f_{ps}(\vec{q}') \right] \end{aligned}$$

$$\begin{aligned}
& + \frac{1}{4\pi^2} \int d^2q' d^2b e^{i(\vec{q}-\vec{q}') \cdot \vec{b}} (kb)^{2L_n} e^{i\chi_c^E(b)} f_n(\vec{q}') S(\frac{1}{2}\vec{q}-\vec{q}') \\
& + \frac{i}{8\pi^2 k} \int d^2q' d^2q'' d^2b e^{i(\vec{q}-\vec{q}'-\vec{q}'') \cdot \vec{b}} (kb)^{2L_n} e^{i\chi_c^E(b)} \\
& \times f_{ps}(\vec{q}') f_n(\vec{q}'') S(\frac{1}{2}\vec{q}-\vec{q}'') \quad (2.13)
\end{aligned}$$

Here  $S(\vec{q})$  is the form factor of the ground state of the deuteron.

If we parametrize the hadron-nucleon scattering amplitudes by

$$f_j(\vec{q}) = c_j \exp(-a_j q^2/2), \quad j = n, ps \quad (2.14)$$

with

$$c_j = k \sigma_j (i + \rho_j) / 4\pi$$

where  $\sigma_j$  are incident hadron-nucleon total cross sections and  $\rho_j$  are ratios of real to imaginary parts of the forward hadron-nucleon elastic scattering amplitudes, and if we also define

$$T(b) = (kb)^{2L_n} b \exp[i\chi_c^E(b)], \quad (2.15)$$

then Eq. (2.11) simplifies to

$$\begin{aligned}
F_d(\vec{q}, \vec{s}) = & e^{-\frac{i}{2}\vec{q} \cdot \vec{s}} \left[ f_c^{pt}(\vec{q}) + i \int_0^\infty J_0(qb) (kb)^{2L_n+1} \Gamma_c^E(b) db \right. \\
& + (c_p/a_p) \int_0^\infty J_0(qb) T(b) e^{-b^2/2a_p} db \\
& + (c_n/a_n) e^{-s^2/a_n} \int_0^\infty J_0(|\vec{q} - \frac{i\vec{s}}{a_n}|b) T(b) e^{-b^2/2a_n} db \\
& \left. + \frac{i c_n c_p}{k a_n a_p} e^{-s^2/a_n} \int_0^\infty J_0(|\vec{q} - \frac{i\vec{s}}{a_n}|b) T(b) e^{-\frac{(a_n+a_p)b^2}{2a_n a_p}} db \right] \quad (2.16)
\end{aligned}$$

where

$$|\vec{q} - \frac{i\vec{s}}{a_n}| = (q^2 - 2i\vec{q} \cdot \vec{s}/a_n - s^2/a_n^2)^{1/2}$$

In this and future equations we suppress the subscript  $s$  in  $c_{ps}$  and  $a_{ps}$ . For hadron-nucleon amplitudes given by Eq. (2.14) and a deuteron form factor given by a sum of Gaussians

$$S(q) = \sum_{j=1}^N \alpha_j \exp(-\beta_j q^2) \quad (2.17)$$

the expression for the elastic scattering amplitude can be reduced to one dimensional integrals and is given by

$$F_{el}(q) = \left[ f_c^{pt}(q) + i \int_0^\infty J_0(qb) (\kappa b)^{2in+1} \Gamma_c^E(b) db \right. \\ \left. + (c_p/a_p) \int_0^\infty J_0(qb) T(b) e^{-b^2/2a_p} db \right] \sum_{j=1}^N \alpha_j e^{-\beta_j q^2/4} \\ + c_n \sum_{j=1}^N (\alpha_j/A_j) e^{-\beta_j q^2/4} e^{\beta_j^2 q^2/2A_j} \left[ \int_0^\infty J_0(G_j qb/A_j) T(b) \right. \\ \left. \times e^{-b^2/2A_j} db + \frac{i c_p}{\kappa a_p} \int_0^\infty J_0(G_j qb/A_j) T(b) e^{-H_j b^2/2A_j a_p} db \right], \quad (2.18)$$

where  $G_j = a_n + \beta_j$ ,  $A_j = G_j + \beta_j$  and  $H_j = A_j + a_p$ .

For the special case of point charges,  $\chi_c^E$  vanishes and Eq. (2.18) can be evaluated analytically to yield

$$F_{el}(q) = \left[ f_c^{pt}(q) + (2a_p)^{in} \Gamma(1+in) c_p e^{-\frac{1}{2}a_p q^2} {}_1F_1(-ln; 1; \frac{1}{2}a_p q^2) \right] \\ \times \sum_{j=1}^N \alpha_j e^{-\beta_j q^2/4} + \sum_{j=1}^N \alpha_j e^{-\beta_j q^2/4} (2A_j)^{in} c_n \Gamma(1+in) \\ \times \left[ e^{-\frac{1}{2}a_n q^2} {}_1F_1(-in; 1; G_j q^2/2A_j) + \frac{i c_p}{\kappa H_j} \left( \frac{a_p}{H_j} \right)^{ln} \right. \\ \left. \times e^{(\beta_j^2 - a_p a_n) q^2/2H_j} {}_1F_1(-ln; 1; \frac{a_p G_j^2 q^2}{2A_j H_j}) \right], \quad (2.19)$$

which is a simple generalization of the results of Ref. 19 to the case of the deuteron form factor given by Eq. (2.17).

We can obtain an explicit expression for  $\chi_c^E(b)$  by considering the incident hadron and the bound proton to have Gaussian charge distributions. If the respective charge form factors are given by  $\exp(-d^2 q^2/4)$  and  $\exp(-c^2 q^2/4)$ , we obtain

$$\chi_c^E(b) = n E_1 \left[ \frac{b^2}{c^2 + d^2} \right], \quad (2.20)$$

where  $E_1(x) = -\text{Ei}(-x)$  is the exponential integral. This result is derived in Appendix B.

Since Eq. (2.18) requires numerical integration for its evaluation, it will be convenient to also consider

an average phase approximation which leads to analytic results. For this approximation, which will be described in Appendix C, the scattering amplitude operator for hadron-deuteron collisions, is given by

$$F_d^{av}(\vec{q}, \vec{s}) = e^{-\frac{i}{2}\vec{q}\cdot\vec{s}} \left[ f_c(\vec{q}) + e^{i\chi_{cp}} f_{ps}(\vec{q}) \right] + e^{\frac{i}{2}\vec{q}\cdot\vec{s}} e^{i\chi_{cn}} f_n(\vec{q}) \\ + \frac{i}{2\pi R} e^{i\chi_{cpn}} \int d^2q' e^{i\vec{q}'\cdot\vec{s}} f_{ps}(\frac{1}{2}\vec{q}-\vec{q}') f_n(\frac{1}{2}\vec{q}+\vec{q}'), \quad (2.21)$$

where  $\chi_{cp}$ ,  $\chi_{cn}$ ,  $\chi_{cpn}$  are average values of the Coulomb phase shift functions. Analytic expressions for them are derived in Appendix C for the case of Gaussian charge distributions for the incident hadron and the bound proton. The Coulomb amplitude may also be written in an analytic form as

$$f_c(q) = f_c^{pt}(q) \mathcal{F}_x(q) \mathcal{F}_p(q) \quad (2.22)$$

where  $f_c^{pt}(q)$  is given by Eq. (2.10) and  $\mathcal{F}_p(q)$  and  $\mathcal{F}_x(q)$  are the electromagnetic form factors of the proton and the incident hadron. The result that the Coulomb amplitude is proportional to the form factors of the colliding particles can be easily derived in the Born approximation. In Appendix C we show that this result can be derived from the more accurate Coulomb amplitude, given by the first two terms in Eq. (2.11), by dropping terms of  $O(n^2)$ .

For deuteron form factors given by Eq. (2.17) and hadron-nucleon amplitudes given by Eq. (2.14), the ground state expectation value of  $F_d^{av}$  reduces to

$$F_d^{av}(q) = \left[ f_c(q) + e^{i\chi_{cp}} f_{ps}(q) + e^{i\chi_{cn}} f_n(q) \right] \sum_{j=1}^N \alpha_j e^{-\beta_j q^2/4} \\ + \frac{\chi_{cpn}}{R} e^{i\chi_{cpn}} e^{-\frac{1}{8}(a_p+a_n)q^2} \sum_{j=1}^N \frac{\alpha_j}{H_j} e^{-(a_p-a_n)^2 q^2/8H_j}. \quad (2.23)$$

Below 2 GeV, charge exchange effects are important and it is straightforward to extend this formula to include them. The final expression is given in Appendix D.

Measurements of the sum of p-d elastic and quasi-elastic (i.e. deuteron breakup) scattering have also been used<sup>13</sup> to obtain values for  $\rho_n$ . The angular distribution for such processes is given by

$$\left(\frac{d\sigma}{d\Omega}\right)_{sc} = \sum_f |\langle \gamma_d^f | F_d(\vec{q}, \vec{s}) | \gamma_d \rangle|^2. \quad (2.24)$$

At high energies we can neglect the energy differences between the final state of the deuteron, and the completeness relation

$$\sum_f |\gamma_d^f\rangle \langle \gamma_d^f| = 1 \quad (2.25)$$

can be utilized to yield

$$\left(\frac{d\sigma}{d\Omega}\right)_{sc} = \langle \gamma_d | \{ |F_d(\vec{q}, \vec{s})|^2 \} | \gamma_d \rangle. \quad (2.26)$$

This expression can be evaluated using  $F_d(\vec{q}, \vec{s})$  given by Eq. (2.11) but the result is a tediously long expression involving double integrals and an infinite sum. We shall write down the result in the average phase approximation where one can obtain an analytic result. Using  $F_d^{av}(q, s)$  in Eq. (2.26) we obtain

$$\begin{aligned}
\left(\frac{d\sigma}{d\Omega}\right)_{sc} &= |f_c(q) + e^{i\chi_{cp}} f_{ps}(q)|^2 + |f_n(q)|^2 \\
&+ 2 \operatorname{Re} [f_c(q) + e^{i\chi_{cp}} f_{ps}(q)]^* [e^{i\chi_{cn}} f_n(q) \\
&\times \sum_j \frac{\alpha_j}{j} e^{-\beta_j q^2} + \frac{i c_p c_n}{k} e^{i\chi_{cpn}} e^{-\frac{1}{2} a_p q^2} \sum_j \frac{\alpha_j}{H_j} \\
&\times e^{a_p^2 q^2 / 2 H_j}] + 2 \operatorname{Re} \left\{ [e^{i\chi_{cn}} f_n(q)]^* \frac{i c_n c_p}{k} \right. \\
&\times \left. e^{i\chi_{cpn}} e^{-\frac{1}{2} a_n q^2} \sum_j \frac{\alpha_j}{H_j} e^{a_n^2 q^2 / 2 H_j} \right\} \\
&+ \frac{|c_n c_p|^2}{k^2} e^{-a_n a_p q^2 / (a_n + a_p)} \sum_j \frac{\alpha_j}{(H_j^2 - 4\beta_j^2)} .
\end{aligned}$$

(2.27)

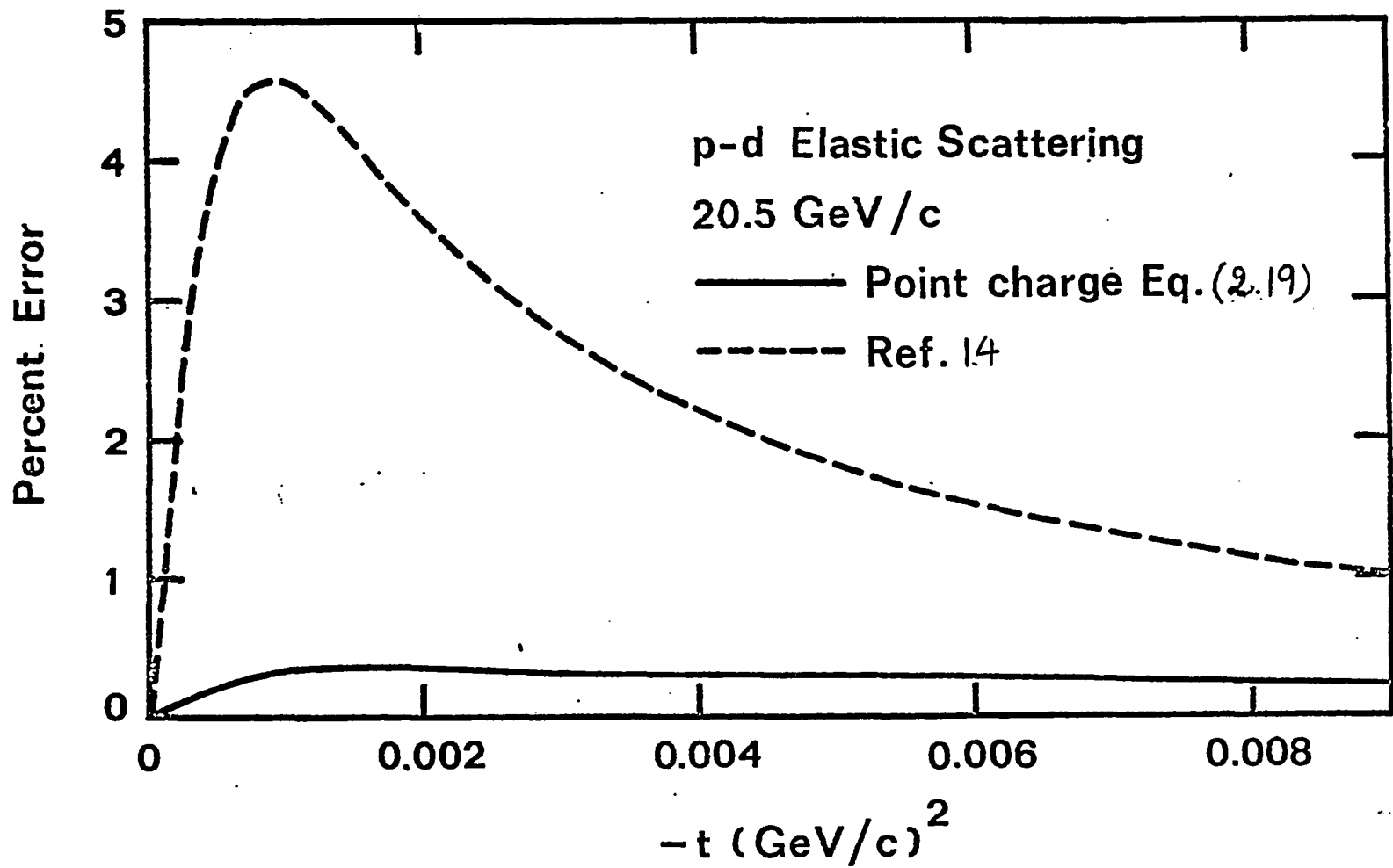


Fig. 2.1

## II.(c). Comparison of Theoretical Expressions

In this section we compare the various approximations discussed in the text with the more exact results. Throughout our analysis, the proton charge form factor is assumed to have the form  $e^{-c^2 q^2/4}$ . The value of  $c$  is taken to be 0.66fm which corresponds to a r.m.s. radius of 0.81fm. This value fits the experimentally observed form factor in the region  $0.001 \lesssim -t \lesssim 0.05$  (GeV/c)<sup>2</sup> which is the momentum transfer region in which we perform our analysis of the pd data.

The form factor used for the deuteron is a sum of Gaussians fit to form factors obtained from "realistic" deuteron wave functions and will be described in detail in Sec. II(d). In Fig. 2.1 we show the percent error in the pd differential cross sections near the interference region, for the point charge solution given by Eq. (2.19) and for the formula used in Ref. 14 in an analysis of p-d data. The "exact" values of the cross sections are obtained from Eq. (2.18). The error in the average phase approximation of Eq. (2.23) is exceedingly small in this region and hence is not shown. The maximum error in the formula of Ref. 14 in the interference region is  $\sim 4.6\%$ . For  $-t \lesssim 0.1$  (GeV/c)<sup>2</sup> the error in the point charge approximation is  $\lesssim 0.5\%$ , while the error in Eq. (2.23) is even smaller ( $\lesssim 0.1\%$ ). However, near the minimum in the differential cross sections ( $-t \sim 0.33$  (GeV/c)<sup>2</sup>), the error in Eq. (2.23) is as large as  $\sim 22\%$  while

the error in Eq. (2.19) is only  $\sim 2\%$ . For even larger angles, the error in the Coulomb amplitude due to the point charge approximation increases, but Coulomb contributions themselves become unimportant compared to nuclear contributions. The errors in Eq. (2.19) and (2.23) depend negligibly upon the energy while the error in the formula of Ref. 14 increases slightly with energy.

The reason for the increase in the error of the point charge solution with the momentum transfer is that the large angle scattering results from small impact parameter collisions where the point charge assumption starts to break down. On the other hand, the error in the formula of Ref. 14 is in some measure due to the assumption that  $\chi_{cp}$ ,  $\chi_{cn}$ , and  $\chi_{cpn}$  are all equal to 0.06 (at 70.2 GeV/c, for example, their values are respectively 0.086, 0.098, 0.085), but is mostly due to the Coulomb amplitude in which Bethe's phase has been used incorrectly. We point out that Bethe's phase is the relative phase between the Coulomb amplitude (without its phase) and the strong interaction amplitude for the hadron-nucleus collisions, and it should not be present in the formula of Ref. 14 which has been obtained from a multiple scattering series where the strong interaction terms are already modified by a phase factor arising from the Coulomb interaction. The correct Coulomb amplitude that should be used is given by Eq. (2.22).

## II (d). Analysis of p-d Scattering Data

We first describe the deuteron form factor which will be used in our analyses. We note that the extended charge expressions derived in Sec. II (b) are relatively easy to evaluate for deuteron form factors given by a Gaussian or sums of Gaussians. In order to both preserve this ease in numerical evaluations and have an accurate form factor, we have fitted sums of Gaussians to form factors given by "realistic" deuteron wave functions. The first wave function we choose is that obtained from the hard core potential of Reid<sup>21</sup> which is fitted accurately to the nucleon-nucleon (NN) phase shifts up to 350 MeV. Our second choice is the wave function obtained by Humberston<sup>21</sup> by slightly modifying the Hamada-Johnston<sup>21</sup> potential to give the observed binding energy of the deuteron. Since both these wave functions are obtained from hard core potentials, we also consider a wave function due to Bressel and Kerman<sup>21</sup> which is obtained from finite soft core potentials that reproduce the NN phase shifts very well. All these wave functions have a small admixture of D state. We obtained the form factors from these wave functions by numerical integration and we fitted sums of Gaussians to them. A sum of Gaussians which is consistent with each of the three form factors is given by

$$S(q) = 0.34 e^{-141.5q^2} + 0.58 e^{-26.1q^2} + 0.08 e^{-15.5q^2} \quad (2.28)$$

with  $q$  in GeV/c.

In the interference region  $-t \lesssim 0.01 (\text{GeV}/c)^2$ , the form factor  $S(q/2)$  given by Eq. (2.28) agrees with those given by realistic wave functions to better than 0.2%. For larger momentum transfers  $0.01 \lesssim -t \lesssim 0.21 (\text{GeV}/c)^2$  it agrees to within 2.4%; but in this region the values of  $S(q/2)$  given by the Reid and by the Bressel-Kerman wave functions themselves differ by  $\sim 3\%$ . The region where the form factor given by Eq. (2.28) differs significantly from that given by the above wave functions is at large momentum transfers. However since the deuteron form factor is sharply peaked in the forward direction, the contribution from this region to the scattering amplitudes is negligible.

We can now utilize the proton-deuteron elastic scattering data obtained at Serpukhov in the energy range 10 to 70 GeV to extract proton-neutron scattering parameters such as  $\rho_n$ , the ratio of real to imaginary part of the forward proton-neutron elastic scattering amplitude, and  $a_n$ , the slope parameter. We do our calculations in two steps. For the purpose of calculating  $\rho_n$  we restrict the analysis to small momentum transfers  $-t \lesssim 0.011 (\text{GeV}/c)^2$  since beyond this the interference effects are negligible and also because we assume a constant phase for the hadron-nucleon strong interaction amplitudes (i.e., the same value as at  $q=0$ ), an approximation which becomes less accurate away from the forward direction. In this  $-t$  region,  $\rho_n$  is insensitive to moderate variations in  $a_n$ . Therefore, we first calculate  $\rho_n$  by assuming that  $a_n = a_p$ . Then using this value of  $\rho_n$  we

can use the larger momentum transfer region  $-t \lesssim 0.05(\text{GeV}/c)^2$  to calculate  $a_n$ . Using this value for  $a_n$ , we can then recalculate  $\rho_n$  and perform this iteration until  $\rho_n$  and  $a_n$  do not change in value.

In our calculations the value of  $a_p$  are taken from Ref 22,  $\rho_p$  from Ref. 23 and values of  $\sigma_n$  and  $\sigma_p$  are from Ref. 24. At any particular energy we have interpolated between the experimentally measured values if necessary and the actual values used in our calculations are given in Table I. For the calculation of  $\rho_n$ , the angular distribution obtained from Eq. (2.18) was fitted to the proton-deuteron data by minimizing the chisquare with  $\rho_n$  being the only free parameter. The values of chisquare per data point in these fits vary from 0.6 to 2.5 and the typical error bars for  $\rho_n$  are  $\sim \pm 0.07$  which also include the effects of varying the various experimental parameters that we used within their statistical errors. It also includes an uncertainty of  $\sim \pm 0.01$  obtained by varying our Gaussian form factor of Eq. (2.28) to fit more closely the form factors given by the Reid hard core and Bressel-Kerman wave functions. The systematic errors in  $\rho_n$  can be as large as  $\pm 0.13$ , the main source being the proton-deuteron elastic scattering data<sup>14</sup>.

In Table II, we list the values of  $\rho_n$  obtained from various formulae by assuming  $a_n = a_p$ . The second column gives the results obtained from the extended charge expression Eq. (2.18) and also from Eq. (2.23). These two formulae yield

TABLE I

Input nucleon-nucleon parameters used for  
calculating  $\rho_n$  and  $a_n$ .

Momentum (GeV/c)	$a_p$ (GeV/c <sup>-2</sup> )	$\sigma_p$ (mb)	$\sigma_n$ (mb)	$\rho_p$
11.2	9.20	39.68	40.80	-0.326
15.9	10.30	39.25	39.54	-0.281
20.5	10.37	39.02	39.03	-0.249
26.5	10.50	38.72	38.80	-0.216
34.8	10.62	38.50	38.60	-0.185
48.9	10.85	38.46	38.45	-0.160
57.2	11.10	38.43	38.40	-0.136
60.8	11.07	38.44	38.51	-0.119
64.8	11.37	38.44	38.51	-0.105
70.2	11.48	38.44	38.51	-0.090

TABLE II. Results for  $\varrho_n$  and  $a_n$  from the analyses of pd data.

The second and fourth columns give the values of  $\varrho_n$  obtained by chisquare fits to the p-d elastic scattering data using either Eq. (2.18) (extended charge) or Eq. (2.23) (average phase) and point charge Eq. (2.19) with assumption  $a_n = a_p$ . The fifth column gives the results of Ref. 17 and the sixth column gives the result when the formula of Ref. 17 is used with the form factor given by Eq. (2.28). In the seventh column, we list the values of  $a_n$  obtained by using the values of  $\varrho_n$  from the second column as input. The results at 19.3 GeV/c are from the analysis of p-d elastic plus quasi-elastic scattering data and are given in the third and eighth columns.

P (GeV/c)	$\varrho_n$ Eqs.(2.18) and (2.23)	$\varrho_n$ Eq. (2.27)	$\varrho_n$ Eq. (2.19)	$\varrho_n$ Ref. 17	$\varrho_n$ Ref. 17 with Eq. (2.28)	$a_n$ (GeV/c) <sup>-2</sup> Eqs. (2.18) and (2.23)	$a_n$ (GeV/c) <sup>-2</sup> Eq.(2.27)
11.2	-0.29		-0.28	-0.21	-0.26	7.3	
15.9	-0.50		-0.49	-0.38	-0.46	7.0	
19.3		-0.32					10.25
20.5	-0.48		-0.47	-0.35	-0.44	6.5	
26.5	-0.45		-0.44	-0.35	-0.40	7.2	
34.8	-0.38		-0.37	-0.25	-0.34	8.3	
48.9	-0.33		-0.32	-0.14	-0.28	8.3	
57.2	-0.36		-0.35	-0.20	-0.31	8.7	
60.8	+0.06		+0.06		+0.14	11.7	
64.8	-0.05		-0.04	+0.13	-0.03	9.3	
70.2	-0.24		-0.23	-0.04	-0.18	8.4	

the same results to two significant figures. The fifth column gives the results of Beznogikh et al.<sup>14</sup> who used a formula similar to Eq. (2.23) in their analyses with the deuteron form factor given by<sup>25</sup>

$$S^2(\frac{1}{2}q) = \exp(-25.9q^2 + 60q^4). \quad (2.29)$$

There is a significant difference between the two values of  $\mathcal{F}_n$  which is not only due to the different formula but also due to the difference in the form factors used. The deuteron form factor given by Eq. (2.29) is a fit to the numerical values of  $S^2(q/2)$  obtained by fitting the formula of Ref. 14 to the proton-deuteron cross section data for  $0.002 \lesssim -t \lesssim 0.17$  (GeV/c)<sup>2</sup> from 10 to 26 GeV with the assumptions that  $\mathcal{F}_n = \mathcal{F}_p$  and  $a_n = a_p$ . This form factor for small momentum transfers is not consistent with the form factors obtained from the three "realistic" deuteron wave functions that we considered. In order to isolate the effects of the form factor, we have repeated the analyses of Ref. 14 with the deuteron form factor given by Eq. (2.28). The results are given in the sixth column and we find that the use of a more accurate form factor leads to a difference in  $\mathcal{F}_n$  of  $\sim 0.1$  on the average. We should also point out that even though data exist at 60.8 GeV/c, they were not used in Ref. 14 for calculating  $\mathcal{F}_n$  and  $a_n$ . The fourth column in Table II shows the results for  $\mathcal{F}_n$  obtained from Eq. (2.19) (point charge). If charge exchange effects are included (using the formula given in Appendix D), we find

that  $\rho_n$  changes by  $\lesssim 0.01$  at these energies.

We can now use the value of  $\rho_n$  obtained from Eq. (2.18) to calculate  $a_n$  by analyzing the data for  $0.002 \lesssim -t \lesssim 0.05$  (GeV/c)<sup>2</sup>. Again Eqs. (2.18) and (2.23) give identical results and the values of  $a_n$  are listed in the last columns of Table II. One can now perform an iteration to recalculate  $\rho_n$  and then  $a_n$  but the values change very little because  $\rho_n$  is relatively insensitive to variations in  $a_n$ . In our chisquare fit for  $a_n$ , the chisquare minimum varies from 1.0 to 2.3 per data point and typical results of our chisquare fit to the data are shown in Fig. 2.2. The error bars in  $a_n$  in Table II are  $\sim \pm 1.5$  and include the error due to the uncertainty in  $\rho_n$ . The smaller value of  $a_n$  compared to  $a_p$  are surprising since direct measurements<sup>26</sup> of  $a_n$  (from n-p scattering) and of  $a_p$  at larger momentum transfers seem to agree with each other. However, the value of  $a_n$  is quite sensitive to the input value of  $a_p$  in our analyses. If the values of  $a_p$  are lowered, the values of  $a_n$  increase by roughly the same amount. The input values of  $a_p$  that we have used are from Ref. 22 and are slightly higher than the recent Fermilab measurements in the overlapping energy region.

Since all the above results are based on the experiments of the same group, we have also used the elastic plus quasi-elastic scattering data at 19.3 GeV/c of Bellettini et. al.<sup>13</sup> to extract  $\rho_n$ . Using Eq. (2.27) with input parameters again from Refs. 22-24 (with values given in Fig. 2.3) we find  $\rho_n = -0.32$  and  $a_n \simeq a_p$ . The fit to the data

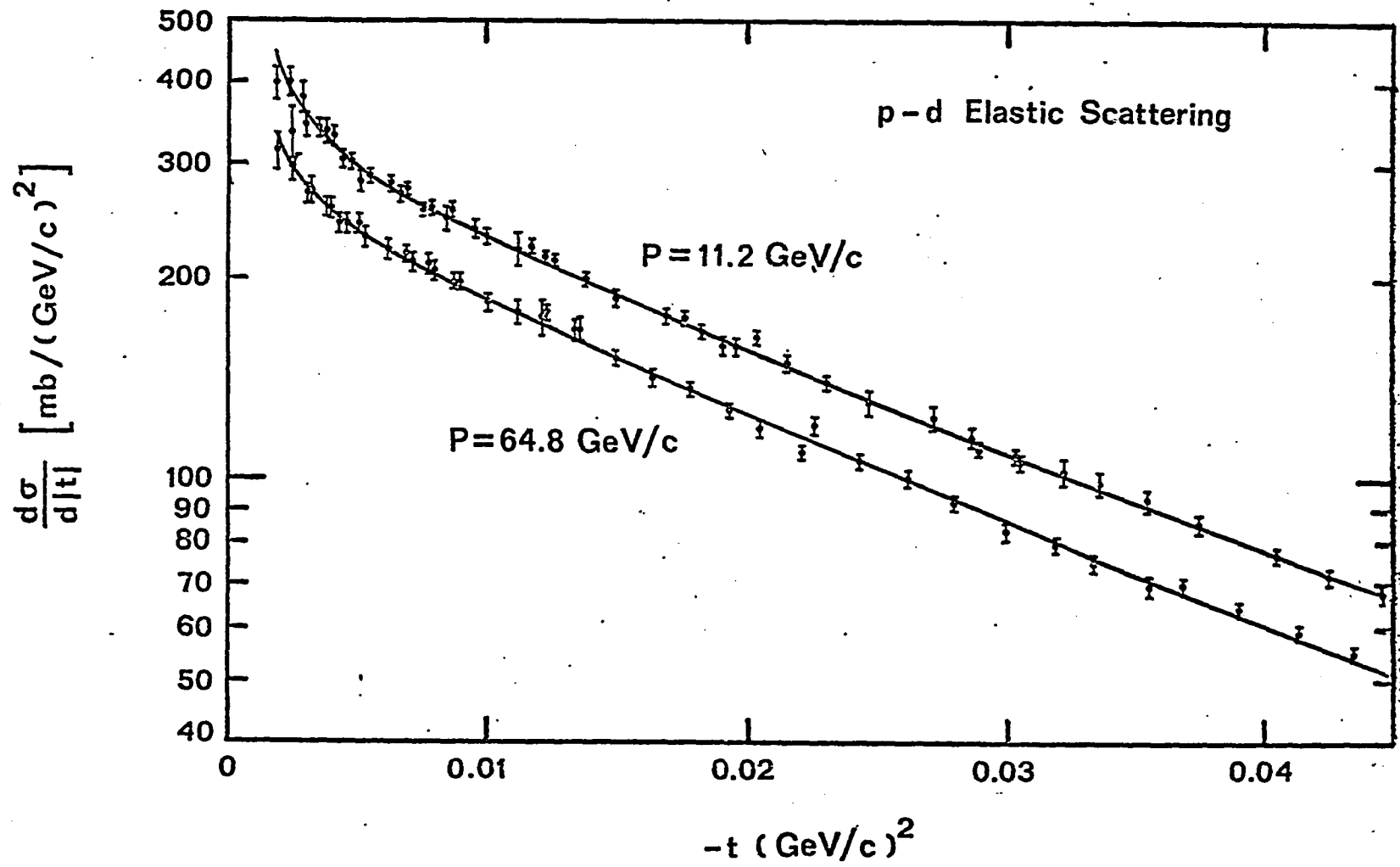


FIG. 2.2

is shown in Fig. 2.3. If we use the same input parameters as used in Ref. 13 ( $\sigma_n = \sigma_p = 38.9 \text{mb}$ ,  $a_n = a_p = 10(\text{GeV}/c)^{-2}$ ,  $\xi_p = -0.33$ ) we find  $\xi_n = -0.25$ . In Fig. 2.4 we show for comparison our calculated results for  $\xi_n$  together with dispersion relation calculations by Barashenkov and Toneev<sup>27</sup> and also by Carter and Bugg.<sup>28</sup>

We should point out that our theoretical results for p-d scattering do not include the effect of inelastic intermediate states<sup>29</sup> (for example, an  $N^*$  can be created coherently in the nucleus and then decay back into a proton) on the elastic scattering. The Glauber approximation can be extended to include these effects.<sup>30</sup> But quantitatively reliable calculations of these effects are lacking because they depend critically upon the phases of the production amplitudes which are not well known. On the other hand, rough estimates of the effect that are not included in the Glauber approximation can be obtained from the p-p, p-d and n-p total cross section measurements. Let us define the experimental cross section defect in deuterium by

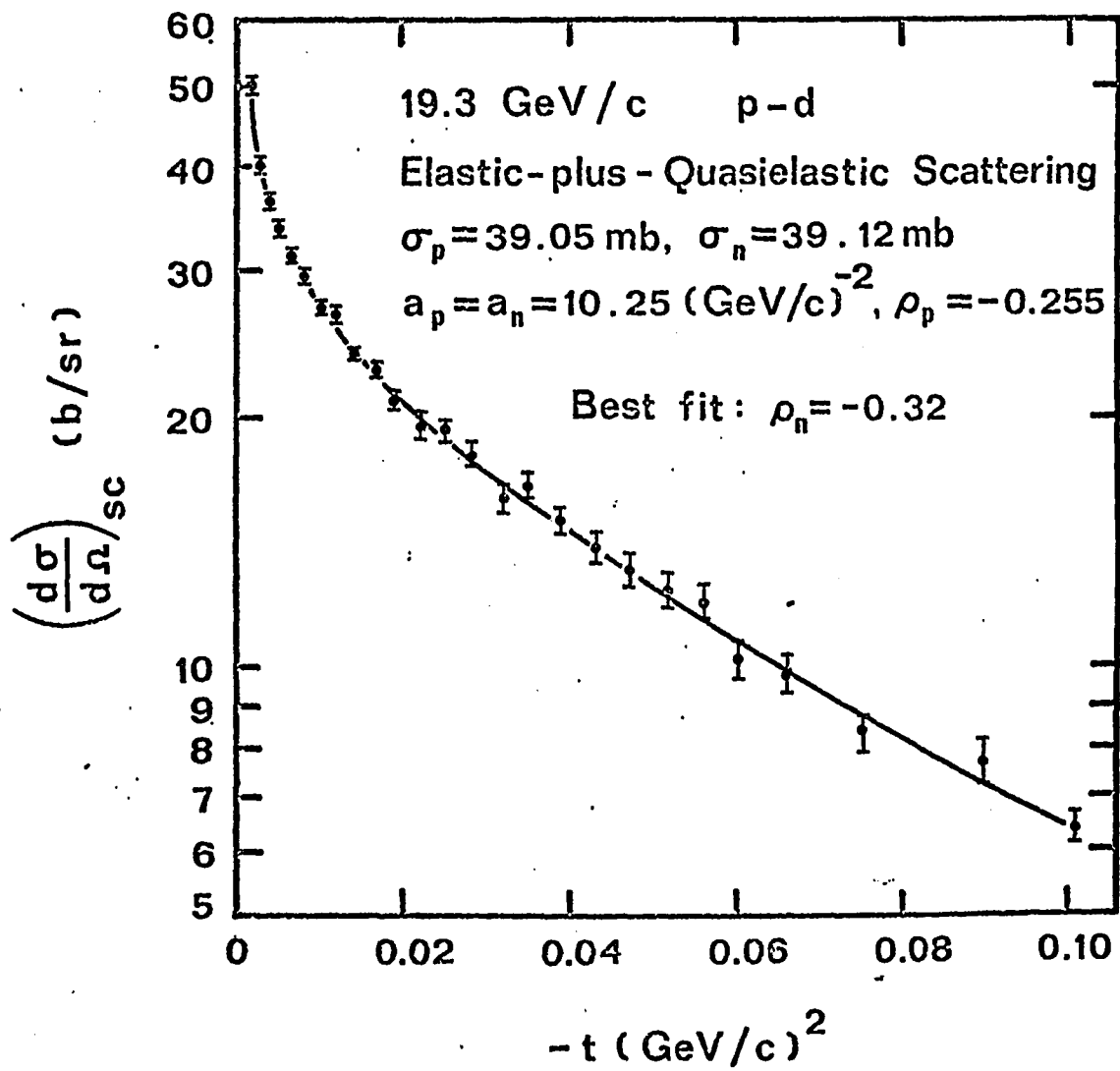
$$\delta \sigma_{\text{exp}} = \sigma_{np} + \sigma_{pp} - \sigma_{pd}$$

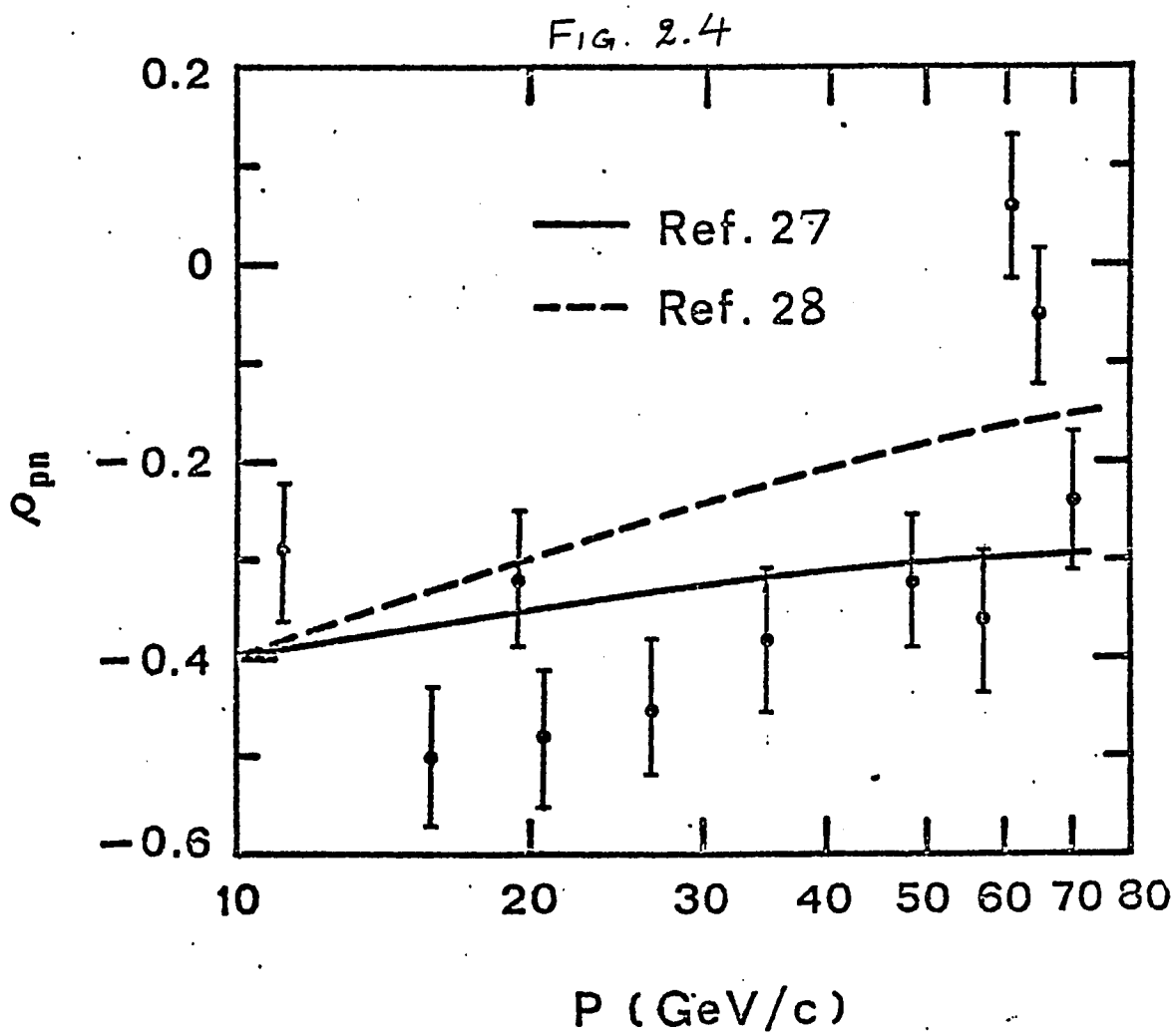
and the inelastic cross section defect by

$$\delta \sigma_{\text{inel}} = \delta \sigma_{\text{exp}} - \delta \sigma_{\text{tot}}$$

where  $\delta \sigma_{\text{tot}}$  is calculated from the double scattering term of the elastic scattering amplitude in the Glauber approximation. By using experimental data wherever they exist at

FIG. 2.3





roughly the same energy,<sup>24,31</sup> we find that  $|\delta\sigma_{inel}| \approx 0.1 \pm 0.9 \text{ mb}$  from 15 to 35 GeV. (For example, near 34 GeV,  $\delta\sigma_{exp} = 3.16 \text{ mb}$  and using the deuteron wave function given by the Reid hard core potential we find that  $\delta\sigma_{tot} = 3.05 \text{ mb}$ .) Since the effect of these inelastic processes on the invariant differential cross section  $(d\sigma/dt)_{pd}$  in the forward direction is roughly proportional to  $\delta\sigma_{inel}$ , these effects are quite small compared to the statistical errors in the p-d data and hence should have very little effect on our results. However, for much higher energies the intermediate production processes may have significant effect.

### III. Scattering of Charged Hadrons from Nuclei other than Deuterium

#### III (a). Introduction

The study of Coulomb effects is of considerable importance for the accurate description of collisions of charged hadrons from various nuclei and for the investigation of hadron-nucleon interactions by means of such collisions. The minima which occur in hadron-nucleus elastic scattering intensities are quite sensitive to  $\rho_n$  and hence the experimental measurements in that region can be used to determine  $\rho_n$ . However, the Coulomb effects play a significant role near the minima, and hence they must be treated accurately. In this section, we extend the formalism of Sec. II to derive hadron-nucleus scattering amplitudes, including the effects of the Coulomb interaction where the charged hadron and the bound proton are treated as extended charges. We shall also examine some approximate models where the Coulomb interaction is assumed to originate from the nucleus as a whole rather than from each individual proton.

#### III (b). Basic Formulas

The amplitude for elastic scattering between hadrons and nuclei with mass number  $A$  is given by

$$F(q) = \frac{ik}{2\pi} \int e^{i\vec{q}\cdot\vec{b}} \psi_A^*(\vec{r}_1, \dots, \vec{r}_A) \delta^3(A^{-1} \sum_{j=1}^A \vec{r}_j) \times \left\{ 1 - \prod_{j=1}^A [1 - \gamma_j(\vec{b} - \vec{s}_j)] \right\} \psi_A(\vec{r}_1, \dots, \vec{r}_A) d\vec{r}_1 \dots d\vec{r}_A d^2b \quad (3.1)$$

where  $\Psi_A$  is the ground state wave function of the nucleus and the other symbols are defined in preceding sections. The  $\delta$ -function in (3.1) represents the centre of mass constraint. Since we will only be comparing theoretical expressions to exhibit the charge distribution effects (and since accurate wave functions are needed only to reproduce the details of the structure in the differential cross section at large momentum transfers), we will assume that the nucleus can be described by a simple independent particle model where each nucleon is represented by a Gaussian, i.e.

$$|\Psi_A(\vec{r}_1, \dots, \vec{r}_A)|^2 = \prod_{j=1}^A |\phi_j(\vec{r}_j)|^2 = \prod_{j=1}^A \alpha^3 \pi^{-3/2} e^{-\alpha^2 r_j^2}, \quad (3.2)$$

where  $\alpha$  is related to the r.m.s. radius of the nucleus.

Now, using the result of Appendix H to eliminate the  $\delta$ -function, we obtain

$$F(q) = \frac{1}{2\pi} K(q) \int d^2b e^{i\vec{q} \cdot \vec{b}} \left\{ 1 - \prod_{p=1}^Z \langle \phi_p | [1 - \Gamma_p(\vec{b} - \vec{s}_p)] | \phi_p \rangle \prod_{n=1}^{A-Z} \langle \phi_n | [1 - \Gamma_n(\vec{b} - \vec{s}_n)] | \phi_n \rangle \right\}, \quad (3.3)$$

where  $Z$  is the atomic number of the target nucleus and  $K(q) = \exp(q^2/4A\alpha^2)$ . Again by writing

$$\Gamma_p(\vec{b} - \vec{s}_p) = \Gamma_c^{pt}(\vec{b} - \vec{s}_p) + e^{i\chi_c^{pt}(\vec{b} - \vec{s}_p)} \Gamma_c^E(\vec{b} - \vec{s}_p) + e^{i\chi_c(\vec{b} - \vec{s}_p)} \Gamma_{ps}(\vec{b} - \vec{s}_p), \quad (3.4)$$

we obtain

$$\begin{aligned}
 \langle \phi_p | [1 - \Gamma_p(\vec{b} - \vec{s}_p)] | \phi_p \rangle &= (2\alpha R)^{-2in} e^{-\alpha^2 b^2} \left[ \Gamma(1+in) \right. \\
 &\quad \times {}_1F_1(in+1; 1; \alpha^2 b^2) - \int_0^\infty e^{-x} x^{in} \Gamma_c^E(\sqrt{x}/\alpha) I_0(2\alpha b\sqrt{x}) dx \\
 &\quad - \frac{\Gamma_p(1-i\rho_p)}{4\pi a_p} \int_0^\infty e^{-x} x^{in} e^{i\chi_c^E(\sqrt{x}/\alpha)} I_0(2\alpha b\sqrt{x}) \\
 &\quad \times e^{-x/2a_p\alpha^2} dx \left. \right] \\
 &= (2\alpha R)^{-2in} A_p(b), \tag{3.5}
 \end{aligned}$$

$$\begin{aligned}
 \langle \phi_n | [1 - \Gamma_n(\vec{b} - \vec{s}_n)] | \phi_n \rangle &= 1 - \frac{\Gamma_n(1-i\rho_n)}{2\pi} \left( \frac{\alpha^2}{1+2a_n\alpha^2} \right) e^{-\alpha^2 b^2 / (1+2a_n\alpha^2)} \\
 &= A_n(b). \tag{3.6}
 \end{aligned}$$

Eq. (3.3), as it stands, converges very slowly because of the large impact parameter scattering by the Coulomb field and hence is not well suited for numerical evaluation. It can be made to converge rapidly by subtracting out the Coulomb amplitude due to a point nucleus of charge  $Ze$ . The Coulomb phase shift function,  $\chi_{cz}^{pt}(b)$ , due to the point nucleus is given by<sup>1</sup>

$$\chi_{cz}^{pt}(b) = 2\pi Z \ln(b/2R). \tag{3.7}$$

By adding and subtracting  $e^{i\chi_{cz}^{pt}}$  in the integrand of Eq. (3.3) we obtain

$$\begin{aligned}
 F(q) &= e^{-2\ln Z \ln(2kR)} K(q) \left\{ f_{cz}^{pt}(q) - ik \right. \\
 &\quad \times \int_0^\infty \left[ A_p(b)^Z A_n(b)^{A-Z} - (kb)^{2inZ} \right] J_0(qb) b db \left. \right\}, \tag{3.8}
 \end{aligned}$$

where  $f_{cz}^{pt}(q)$  is given by Eq. (2.10) with  $n$  replaced by  $Zn$ . Now the phase factor can be dropped as it does not contribute to the cross section.

If we consider the special case where the incident hadron and the bound proton are point charges,  $A_p(b)$  can be evaluated analytically and is given by

$$A_p(b) = (k/\alpha)^{2in} e^{-\alpha^2 b^2} \Gamma(1+in) \left[ {}_1F_1(in+1; 1; \alpha^2 b^2) - \frac{\sqrt{p}(1-i\rho_p)}{4\pi a_p} \left( \frac{2a_p \alpha^2}{1+2a_p \alpha^2} \right)^{in+1} {}_1F_1(in+1; 1; \frac{2a_p \alpha^4 b^2}{(1+2a_p \alpha^2)}) \right]. \quad (3.9)$$

This case has been considered in detail by Lesniak and Lesniak<sup>33</sup> for light nuclei.

Another way to include the Coulomb effects is by means of an approximation where one considers the Coulomb phase to originate from the nucleus as a whole rather than from each individual proton in the target. In that case the total phase shift function for the nucleus can be written as

$$\chi_{tot}(\vec{b}) = \chi_{cz}^{pt}(\vec{b}) + \chi_{cz}^E(\vec{b}) + \chi_s(\vec{b}) \quad (3.10)$$

where  $\chi_s(b)$  is the strong interaction phase shift function for the nucleus and  $\chi_{cz}^E(b)$  is the correction to the Coulomb phase shift due to the extended charge of the nucleus. One way to write the profile function for the nucleus is then

$$\Gamma_A(\vec{b}) = \left[ 1 - e^{i\chi_{cz}^{pt}(b)} \right] + e^{i\chi_{cz}^{pt}(\vec{b})} \left[ 1 - e^{i\chi_{cz}^E(\vec{b})} \right] + e^{i\chi_{cz}^{pt}(\vec{b}) + i\chi_{cz}^E(\vec{b})} \Gamma_s(\vec{b}) \quad (3.11)$$

where

$$\Gamma_s(\vec{b}) = \langle \psi_A | \{ 1 - e^{i\chi_s(\vec{b}, \vec{s}_1, \dots, \vec{s}_A)} \} | \psi_A \rangle.$$

This can be rearranged for convenience in numerical evaluation and the elastic scattering amplitude is given by

$$F(q) = K(q) \left\{ f_{c2}^{pt}(q) + i \int_0^\infty (kb)^{2inZ+1} \times [1 - e^{i\chi_{c2}^E(b)} (1 - \Gamma_s(b))] J_0(qb) db \right\} \quad (3.12)$$

where we have again dropped an unimportant overall phase factor.

Another formula which has been frequently used is that due to Bethe<sup>56</sup> who showed that, under certain assumptions, the elastic scattering intensity for charged hadron-nucleus collisions may be written as

$$d\sigma/d\Omega = |f_s(q) + f_e(q) e^{inZ\phi}|^2 \quad (3.13)$$

where  $f_s(q)$  is the strong interaction amplitude and  $f_e(q)$  is the Coulomb amplitude of the nucleus (apart from its phase). The amplitude  $f_e(q)$  includes the electromagnetic form factor of the nucleus. The relative phase was given by

$$\phi \approx -2 \ln(aq/1.06),$$

where  $a$  is related to the strong interaction radius of the nucleus. Using relativistic methods, West and Yennie<sup>56</sup>

obtained for the relative phase

$$\phi \approx -2 \ln(a'q) - C \quad (3.14)$$

with

$$a' = \frac{1}{2} (a^2 + R_1^2 + R_2^2)^{\frac{1}{2}}, \quad C = 0.577 \dots,$$

and where the charge form factors of the incident and target particles are given by  $e^{-R_1^2 q^2/4}$  and  $e^{-R_2^2 q^2/4}$ . For the case of point charge particles incident on a point nucleus, this reduces to the phase given by Bethe.

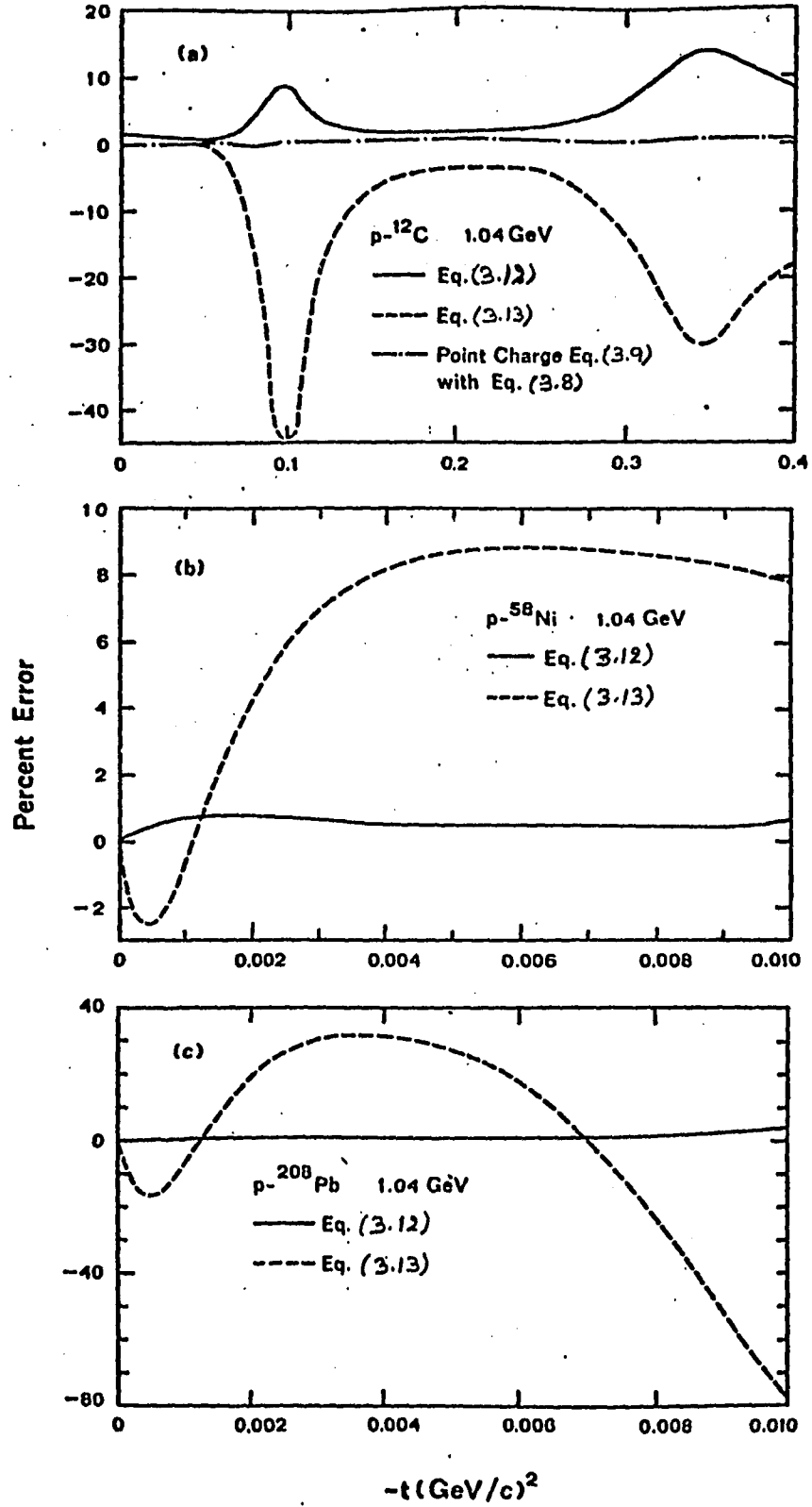
### III (c). Comparison of Approximate Models

Here we shall investigate the accuracy of the various approximate models. In Fig. 3.1 we show the percent error in the differential cross-sections obtained from the Eqs. (3.9), (3.12) and (3.13) compared to the 'exact' Glauber result given by Eq. (3.8). In Fig. 3.1(a) we show the results for  $p$ - $^{12}\text{C}$  elastic scattering at 1.04 GeV. For  $-t \lesssim 0.01 (\text{GeV}/c)^2$ , the error in the approximation given by Eq. (3.12) is  $\lesssim 0.8\%$  while the formula given by Eq. (3.13) (together with Eq. (3.14)) has errors of  $\lesssim 1.5\%$ . But at large momentum transfer the errors are as large as  $\sim 14\%$  and  $45\%$  for the two expressions.

We find that the assumption of point charge for each proton in the target (i.e. Eq. (3.9)), is quite accurate except at the diffraction minima. At 1.04 GeV, the percent error in this approximation is  $\lesssim 1\%$  near the minimum. However, at energies where the real part of the nucleon-nucleon amplitude is very small, almost the entire contribution to the cross sections near the minima is from the Coulomb scattering and the error in the point charge solution is larger. This error also depends on whether the Coulomb interaction is attractive or repulsive. For example at 180 MeV, the error at the first diffraction minimum in  $\pi^-$ - $^4\text{He}$  scattering is  $\sim 3\%$  while for  $\pi^+$ - $^4\text{He}$  scattering it is  $\sim 8\%$ .

In figures 3.1(b) and 3.1(c) we show the results for  $p$ - $^{58}\text{Ni}$  and  $p$ - $^{208}\text{Pb}$  scattering at small momentum transfers. We note that Eq. (3.13) becomes worse than it was for light

Fig. 3.1



nuclei, with rather large errors even at small momentum transfers. For  $-t \lesssim 0.01 \text{ (GeV/c)}^2$  the errors are  $\sim 8\%$  for p-Ni and  $\sim 30-80\%$  for p-Pb. However, in this region, the approximate phase result of Eq. (3.12) does reasonably well with errors  $\lesssim 1\%$  and  $4\%$  for the two nuclei. Near the first diffraction minimum, the error in Eq. (3.12) is  $\sim 7\%$  for both nuclei but increases at the other minima. For example, at  $-t \sim 0.25 \text{ (GeV/c)}^2$  the error in Eq. (3.12) for p-Ni scattering is  $23\%$ .

It is interesting to note that treating the protons as point charges instead of extended charges in the exact Glauber series, leads to a greater relative error in the scattering from deuterium than from other nuclei. The reason for this is that since in the heavier nuclei there are many protons close together, the point charge protons are smeared over the nuclear volume when the expectation value in the nuclear ground state is taken, and the result of smearing the extended charge protons is not much different. This is not true for the deuteron which has only one proton and is a loosely bound system. However, since the Coulomb effect itself is much smaller in deuterium, the point charge assumption does not lead to much error in the cross sections.

Among the other simpler formulae, the approximate amplitude of Eq. (3.12) is reasonable for small angles but leads to appreciable errors near the diffraction minima. At these larger angles one must consider the interference

of Coulomb effects with strong interaction effects of each nucleon separately instead of considering the overall Coulomb phase resulting from the nucleus as a whole. Eq. (3.13) is good only for light nuclei at very small angles. Its derivation uses the average Coulomb phase shift of nuclear scattering evaluated at  $q=0$  and neglects terms of  $O(Z^2 n^2)$ . It can be improved by introducing the  $q$  dependence of the phase but the formula will still be inaccurate for collisions where  $Zn \gtrsim 0.1$ . We should mention, for completeness, that Coulomb effects can also be included by means of the "optical limit". However, it was pointed out by Lesniak and Lesniak<sup>33</sup> that this approximation leads to significantly lower cross sections at large angles compared to those obtained from the full Glauber series with the assumption of each proton in the target being a point charge. Since we find that this point charge assumption is fairly accurate (except at the minima when the real parts of nucleon-nucleon amplitudes are small), our conclusions for the case of light nuclei are very similar to those of Ref. 33.

## IV. Scattering of Medium and High Energy

### Deuterons from Complex Nuclei

#### IV (a). Introduction

There have been some theoretical studies in the past, of deuteron-nucleus collisions.<sup>34-41</sup> However, except for the case of deuteron-deuteron collisions,<sup>6</sup> the analyses make a number of additional approximations and simplifications within the framework of the Glauber approximation. For example, in the case of  $d-^{12}\text{C}$  scattering, only terms up to fourth order in multiple scattering were included,<sup>41</sup> an approximation which is inadequate except at very small angles. The Coulomb interaction and the deuteron D-state were generally neglected and unrealistic wave functions were used for the deuteron.

Recently high energy deuteron-nucleus scattering experiments have been performed at Bevalac.<sup>42</sup> It is therefore important to undertake a careful theoretical study of deuteron-nucleus collisions. In the present analysis we retain the explicit multiple scattering form of the Glauber theory and express the deuteron-nucleus amplitude in terms of nucleon-nucleon amplitudes. Since the exact Glauber amplitude is difficult to evaluate for general forms of NN amplitudes and wave functions, we also consider some approximations and investigate their accuracies. The influence of the Coulomb field and the deuteron D-state on elastic scat-

tering intensities are also examined. Finally, the theoretical predictions are compared with the available data.

#### IV (b). Basic Formulas

The scattering amplitude operator for collisions between deuteron and nuclei with mass number  $A$ , can be written as

$$F_{dA}(\vec{q}, \vec{r}, \vec{r}_1, \dots, \vec{r}_A) = \frac{1}{2\pi} \int d^2b e^{i\vec{q}\cdot\vec{b}} \left[ 1 - e^{i\chi_{dA}(\vec{b}, \vec{r}, \vec{r}_1, \dots, \vec{r}_A)} \right], \quad (4.1)$$

where  $\vec{k}$  is the incident deuteron momentum,  $\vec{r}$  is the internal deuteron coordinate and  $\vec{r}_1, \dots, \vec{r}_A$  are the coordinates of the target nucleons. The deuteron-nucleus total phase shift function  $\chi_{dA}$  in turn, can be expressed in terms of the nucleon-nucleon phase shift  $\chi_{NN}$  by

$$\chi_{dA}(\vec{b}, \vec{r}, \vec{r}_1, \dots, \vec{r}_A) = \sum_{j=1}^A \left[ \chi_{pj}(\frac{1}{2}\vec{k}, \vec{b}_p - \vec{s}_j) + \chi_{nj}(\frac{1}{2}\vec{k}, \vec{b}_n - \vec{s}_j) \right], \quad (4.2)$$

where  $\vec{b}_p = \vec{b} + \frac{1}{2}\vec{s}$ ,  $\vec{b}_n = \vec{b} - \frac{1}{2}\vec{s}$  and we have explicitly written  $\frac{1}{2}k$  to indicate that the momentum for each incident nucleon is  $\vec{k}/2$ . Rewriting  $\chi_{NN}$  in terms of NN profile function, as in Sec. II, we obtain

$$e^{i\chi_{dA}} = \prod_{j=1}^A \left[ 1 - \Gamma_{pj}(\frac{1}{2}\vec{k}, \vec{b}_p - \vec{s}_j) - \Gamma_{nj}(\frac{1}{2}\vec{k}, \vec{b}_n - \vec{s}_j) + \Gamma_{pj}(\frac{1}{2}\vec{k}, \vec{b}_p - \vec{s}_j) \Gamma_{nj}(\frac{1}{2}\vec{k}, \vec{b}_n - \vec{s}_j) \right]. \quad (4.3)$$

The elastic scattering amplitude is again given by taking the expectation value of operator  $F_{dA}$  between the ground states of the deuteron and the target nucleus. For an independent particle model for the target nucleus, i.e.

$$|\Psi_A(\vec{r}_1, \dots, \vec{r}_A)|^2 = \prod_{j=1}^A |\phi_j(\vec{r}_j)|^2, \quad (4.4)$$

the elastic scattering amplitude becomes

$$F_{dA}(q) = K(q) \frac{i k}{2\pi} \int d^2b e^{i\vec{q}\cdot\vec{b}} \langle \gamma_d | \left\{ 1 - \prod_{j=1}^A [1 - \langle \Gamma_{pj} \rangle - \langle \Gamma_{nj} \rangle + \langle \Gamma_{pj} \Gamma_{nj} \rangle] \right\} | \gamma_d \rangle, \quad (4.5)$$

where  $K(q)$  is a centre of mass correlation function for the target nucleus described in Appendix H and

$$\begin{aligned} \langle \Gamma_{Nj} \rangle &= \langle \phi_j | \Gamma_{Nj}(\frac{1}{2}k, \vec{b}_N - \vec{s}_j) | \phi_j \rangle \\ &= \frac{2}{ik} \int_0^\infty (q' | \vec{b}_N |) f_{Nj}(\frac{1}{2}k, q') S_A(q') q' dq'; \quad N=p, n \end{aligned} \quad (4.6)$$

and similarly

$$\begin{aligned} \langle \Gamma_{pj} \Gamma_{nj} \rangle &= (i\pi k)^{-2} \int d^2q' e^{-i\vec{q}'\cdot\vec{b}_p} f_{pj}(\frac{1}{2}k, \vec{q}') \\ &\quad \times \int d^2q'' e^{-i\vec{q}''\cdot\vec{b}_n} f_{nj}(\frac{1}{2}k, \vec{q}'') S_A(\vec{q}' + \vec{q}''), \end{aligned} \quad (4.7)$$

$S_A(q)$  being the nuclear form factor. Now if we make the simplifying assumption that all NN amplitudes are equal (which is roughly true at high energies), i.e.

$$f_{pp} = f_{pn} = f_{np} = f_{nn} = f \quad (4.8)$$

Eq. (4.5) leads to

$$\begin{aligned} F_{dA}(q) &= -K(q) \frac{ik}{2\pi} \int d^2b e^{i\vec{q}\cdot\vec{b}} \langle \gamma_d | \left\{ \sum_{j=1}^A \binom{A}{j} \sum_{k=0}^j \binom{j}{k} \right. \\ &\quad \left. \times [-\langle \Gamma_{pj} \rangle]^{j-k} \sum_{\ell=0}^k \binom{k}{\ell} [-\langle \Gamma_{nj} \rangle]^{k-\ell} [\langle \Gamma_{pj} \Gamma_{nj} \rangle]^\ell \right\} | \gamma_d \rangle. \end{aligned} \quad (4.9)$$

In order to obtain analytic results, we shall represent the deuteron wave function by a sum of Gaussians

$$|\gamma_d(\vec{r})|^2 = \sum_{j=1}^N \alpha_j (4\pi\beta_j)^{-3/2} e^{-r^2/4\beta_j} \quad (4.10)$$

which corresponds to the deuteron form factor of Eq. (2.17).

For the target nucleus, we assume, for simplicity

$$|\Phi_j(\vec{r}_j)|^2 = \pi^{-3/2} R^{-3} e^{-r^2/R^2} \quad (4.11)$$

Although such a wave function is reasonable only for light nuclei, it describes the qualitative features of the scattering well and is quite useful for comparing different theoretical approximations. However, for comparing the theoretical predictions with the data, we shall use more realistic wave functions.

Using Eq. (4.10) and (4.11) and the high energy parameters of Eq. (2.14) for  $f(q)$ , the elastic scattering amplitude (4.9) reduces to

$$F_{\text{elA}}(q) = -K(q) i k \sum_{j=1}^A \binom{A}{j} \sum_{k=0}^j \binom{j}{k} \sum_{l=0}^k \binom{k}{l} \left[ \frac{-\sigma(1-i\epsilon)}{2\pi(R^2+2a)} \right]^{j-l} \times \left[ \frac{\sigma^2(1-i\epsilon)^2}{16\pi^2 a(R^2+a)} \right]^l \sum_{m=1}^N \alpha_m \frac{e^{-q^2} F(j, k, l, m)}{A(j, l) E(j, k, l, m)} \quad (4.12)$$

where

$$\begin{aligned} K(q) &= e \alpha p (q^2 R^2 / 4A) \quad (4.13) \\ F(j, k, l, m) &= \frac{1}{2A(j, k, l)} + \frac{\beta_m D^2(j, k, l)}{E(j, k, l, m)} \quad , \\ E(j, k, l, m) &= 1 - 2\beta_m \left[ \frac{B^2(j, k, l)}{A(j, l)} - \frac{2(j-k)}{R^2+2a} - \frac{l(R^2+2a)}{2a(R^2+a)} \right] \quad , \\ D(j, k, l) &= \frac{1}{2} - \frac{B(j, k, l)}{A(j, l)} \quad , \\ B(j, k, l) &= 2(j-k)/(R^2+2a) + l/(R^2+a) \\ A(j, l) &= 2(j-l)/(R^2+2a) + 2l/(R^2+a) \quad . \quad (4.14) \end{aligned}$$

This result, although exact within the framework of the Glauber approximation, is valid only for Gaussian wave functions. It is of considerable interest to investigate some approximations which lead to scattering amplitudes

that can be conveniently evaluated for general forms of deuteron and target nucleus wave functions and for more general NN amplitudes. In order to obtain the first approximation, we note that one can write

$$1 - e^{i\chi_{dA}} = (1 - e^{i\frac{\chi}{2}} \chi_{pA}) + (1 - e^{i\frac{\chi}{2}} \chi_{nA}) - (1 - e^{i\frac{\chi}{2}} \chi_{pA})(1 - e^{i\frac{\chi}{2}} \chi_{nA}) \quad (4.15)$$

Upon substitution in Eq. (4.1), this leads to

$$F_{dA}(\vec{q}) = \sum_{i=1}^3 F_i \quad , \quad (4.16)$$

$$F_1 = \langle \psi_d | \frac{\chi}{2\pi} \int d^2b e^{i\vec{q} \cdot \vec{b}} \langle \psi_A | \left\{ 1 - e^{i\frac{\chi}{2}} \chi_{pA}(\frac{1}{2}\vec{k}, \vec{b} + \frac{\vec{b}}{2} - \vec{s}_j) \right\} \times | \psi_A \rangle | \psi_d \rangle$$

$$= 2 F_{pA}(\frac{1}{2}\vec{k}, \vec{q}) S_d(-\frac{1}{2}\vec{q}) \quad , \quad (4.17)$$

where  $F_{NA}$  is the N-nucleus elastic scattering amplitude and  $S_d$ , the deuteron form factor. In a similar fashion

$$F_2 = 2 F_{nA}(\frac{1}{2}\vec{k}, \vec{q}) S_d(\frac{1}{2}\vec{q}) \quad . \quad (4.18)$$

The third term can be written as

$$F_3 = -\frac{\chi}{2\pi} \langle \psi_d | \int d^2b e^{i\vec{q} \cdot \vec{b}} \langle \psi_A | \left\{ 1 - e^{i\frac{\chi}{2}} \chi_{pA}(\vec{b} - \vec{s}_j) \right\} \times \sum_k | \psi_k \rangle \langle \psi_k | \left\{ 1 - e^{i\frac{\chi}{2}} \chi_{nA}(\vec{b} - \vec{s}_j) \right\} | \psi_A \rangle | \psi_d \rangle \quad ,$$

where we have introduced  $1 = \sum_k | \psi_k \rangle \langle \psi_k |$ ,  $| \psi_k \rangle$  being a complete set of states for the target nucleus. Now we make the approximation that, in the intermediate states, only the ground state  $| \psi_A \rangle$  of the target nucleus makes a significant contribution, i.e. we can write

$$\sum_k | \psi_k \rangle \langle \psi_k | \approx | \psi_A \rangle \langle \psi_A |$$

Such an approximation is expected to be reasonable because the deuteron is loosely bound and is more likely to break up rather than excite the target nucleus. This approximation should also be very good for uncorrelated nuclei. If one target nucleon is struck and the nucleus is excited, it can deexcite to ground state only if the same target nucleon is struck again by the other nucleon of the incident deuteron. The number of such double scattering (where same target nucleon is struck twice) is  $\frac{1}{A-1}$  times that of the other types of double scatterings. With this approximation:

$$F_3 = -\frac{\mu k}{2\pi} \langle \chi_d | \int d^2b e^{i\vec{q}\cdot\vec{b}} \Gamma_{pA}(\frac{1}{2}k, \vec{b} + \frac{1}{2}\vec{s}) \Gamma_{nA}(\frac{1}{2}k, \vec{b} - \frac{1}{2}\vec{s}) | \chi_d \rangle. \quad (4.19)$$

Rewriting the N-nucleus profile functions  $\Gamma_{NA}$  in terms of N-nucleus amplitude, we finally obtain

$$F_{dA}(\vec{q}) \simeq 2 F_{pA}(\frac{1}{2}k, \vec{q}) S_d(-\frac{1}{2}\vec{q}) + 2 F_{nA}(\frac{1}{2}k, \vec{q}) S_d(\frac{1}{2}\vec{q}) + \frac{2i}{\pi k} \int d^2q' S_d(\vec{q}') F_{pA}(\frac{1}{2}k, \frac{1}{2}\vec{q} - \vec{q}') F_{nA}(\frac{1}{2}k, \frac{1}{2}\vec{q} + \vec{q}'). \quad (4.20)$$

This result which we shall refer to as approximation I, expresses the deuteron-nucleus elastic scattering amplitude in terms of nucleon-nucleus scattering amplitudes. An alternative derivation of Eq. (4.20) is given in Refs. 34 and 35.

For  $f(q)$ ,  $S_d(q)$  and  $\phi_j(r_j)$  given by Eqs. (2.14), (2.17) and (4.11), we obtain

$$F_{dA}(q) \simeq e^{\frac{q^2 R^2}{4A}} \frac{\mu k}{2} (R^2 + 2a) \sum_{j=1}^A \frac{(-1)^j}{j} \binom{A}{j} \left[ \frac{\sigma(1-\alpha\rho)}{2\pi(R^2+2a)} \right]^j$$

$$\begin{aligned}
& \times e^{-\frac{q^2(R^2+2a)}{4j}} - \frac{1-k}{8} e^{q^2 R^2/8A} (R^2+2a)^2 \sum_{j=1}^A \binom{A}{j} \frac{1}{j} \sum_{k=1}^A \binom{A}{k} \frac{1}{k} \left[ \frac{\sigma(1-i\rho)}{2\pi(R^2+2a)} \right]^{j+k} \\
& \times \sum_{m=1}^N \frac{dm}{[G_+(j,k) + B_m \frac{R^2}{2A}]} \exp \left\{ -\frac{q^2}{4} \left[ G_+(j,k) - \frac{G_-^2(j,k)}{[G_+(j,k) + B_m \frac{R^2}{2A}]} \right] \right\} \quad (4.21)
\end{aligned}$$

where  $G_{\pm}(j,k) = \frac{(R^2+2a)}{4} \left[ \frac{1}{j} \pm \frac{1}{k} \right]$ .

The second approximation (Approximation II), we shall consider, was obtained first by Faldt and Pilkuhn<sup>40</sup>. In this alternative expansion of the Glauber series, the leading term corresponds to a configuration where both proton and neutron in the deuteron scatter at the same impact parameter (the impact parameter of the deuteron centre of mass) and higher order terms then correct for the true impact parameters. The formulas are given in Appendix D. They are generalizations of the results of Ref. 40 for the case of deuteron form factor given by a sum of Gaussians and for NN amplitudes having real parts different from zero.

#### IV (c) Total Cross sections

##### (i) Gaussian Wave Functions and Comparison of Theoretical Expressions

Deuteron-nucleus total cross sections may be obtained from the elastic scattering amplitude by means of the optical theorem

$$\sigma_{dA} = \frac{4\pi}{k} \text{Im} F_{dA}(0) \quad (4.22)$$

Using Eq. (4.12), we obtain

$$\sigma_{dA} = \sum_{j=1}^A g(j) \quad (4.23)$$

where

$$g(j) = 4\pi \operatorname{Re} \left( \binom{A}{j} \sum_{k=0}^j \binom{j}{k} \sum_{\ell=0}^k \binom{k}{\ell} \left[ -\frac{\sigma(1-\lambda\rho)}{2\pi(R^2+2a)} \right]^{j-\ell} \right. \\ \left. \times \left[ \frac{\sigma^2(1-\lambda\rho)^2}{16\pi^2 a(R^2+a)} \right]^\ell \sum_{m=1}^{\infty} \frac{d_m}{A(j,\ell) E(j,k,\ell,m)} \right) \quad (4.24)$$

For the scattering of deuterons from a heavy nucleus, there will be a large number of terms in the series (4.23). The series, however, converges quite rapidly. One can obtain a crude estimate of the number of terms needed in the series by using geometrical arguments similar to those in particle-nucleus scattering.<sup>44</sup> If we consider the incident deuterons as a particle traversing the nucleus, (and since at high energies almost all scattering is concentrated in forward direction) the number of significant terms in the series will be determined, roughly, by the number  $N$  of nucleons with which the incident deuteron collides. If we consider the nucleus as a uniform sphere of radius  $R$ , the number of nucleons/volume is  $3A/4\pi R^3$  while the effective volume swept by the deuteron through the nucleus is  $2R\sigma_{dN}$ ,  $\sigma_{dN}$  being the deuteron-nucleon interaction cross-section. Taking<sup>44</sup>  $R = \sqrt{\frac{2}{5}} 1.25 A^{1/3}$  fm is then equal to  $3A\sigma_{dN}/2\pi R^2$ . and  $\sigma_{dN} \simeq 83\text{mb}$  (at 2.1 GeV/n), we obtain  $N = 6.3A^{1/3}$ . For  $^{207}\text{Pb}$ , for example,  $N$  is 38. By evaluating the series (4.23) with deuteron form factor given by Eq. (2.28), we find that first 36 terms yield total crosssections which are accurate to six significant figures. In order to exhibit the rate of convergence more clearly, we define partial crosssections

$$\sigma_{dA}(j) = \sum_{k=1}^j g(j) \quad (4.25)$$

In Fig. 4.1 we plot  $\sigma_{dA}(j)$  as a function of  $j$  for target nuclei  ${}^{64}\text{Cu}$  and  ${}^{27}\text{Al}$ . It is clear that the series (4.23) converges very rapidly and requires less than  $6.3A^{1/3}$  terms for excellent accuracy. However, it is also evident that a premature truncation of the series can lead to quite erroneous results.

Figure 4.2 illustrates the percent errors in total cross sections predicted by approximation I (i.e.  $\sigma_{dA}$  from Eq. (4.21)) and approximation II (Eq. (D.1)) compared to the exact crosssections given by Eq. (4.23). Approximation I is quite accurate for the entire range of target nuclei with errors less than 1.6%. Approximation II is of comparable accuracy only for  $A \gtrsim 60$  and it can lead to inaccurate results for light nuclei with errors  $\sim 30\%$  for  ${}^4\text{He}$ ,  $\sim 13\%$  for  ${}^{12}\text{C}$  and  $\sim 10\%$  for  ${}^{16}\text{O}$ . This approximation, on the other hand, becomes quite accurate for  $A \gtrsim 100$ .

#### (ii) Realistic Wave Functions and Comparison with Data

Since we have seen that approximation I is extremely accurate, we shall use it to perform realistic calculations of  $\sigma_{dA}$  and compare it with the measurements. From Eqs. (4.20) and (4.22), we obtain

$$\sigma_{dA} = \frac{4\pi}{k} \text{Im} \left[ 2 F_{pA}(\frac{1}{2}k, 0) + 2 F_{nA}(\frac{1}{2}k, 0) + \frac{4k}{k} \int_0^{\infty} S_d(q') F_{pA}(\frac{1}{2}k, q') F_{nA}(\frac{1}{2}k, q') q' dq' \right], \quad (4.26)$$

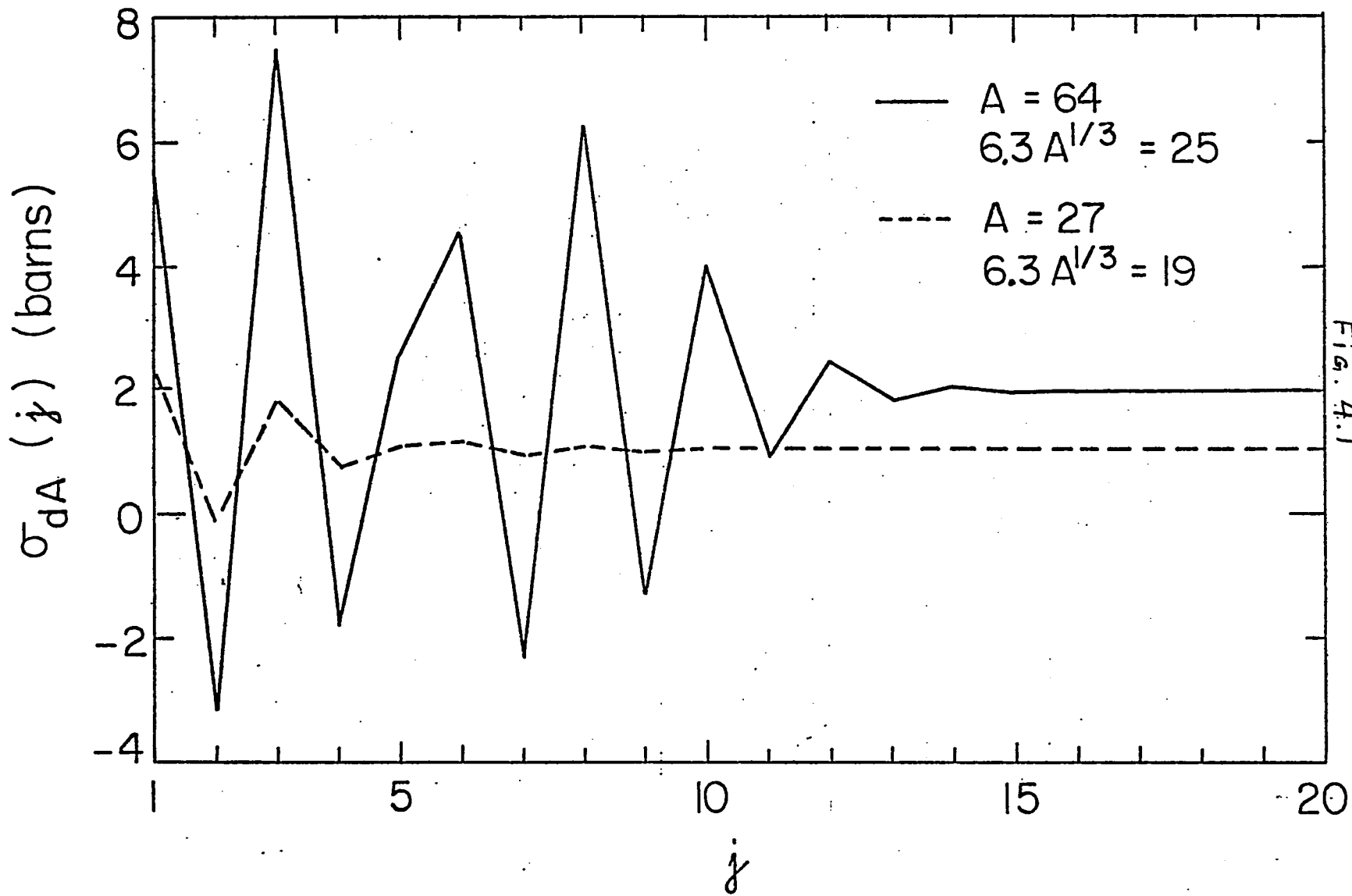


Fig. 4.1

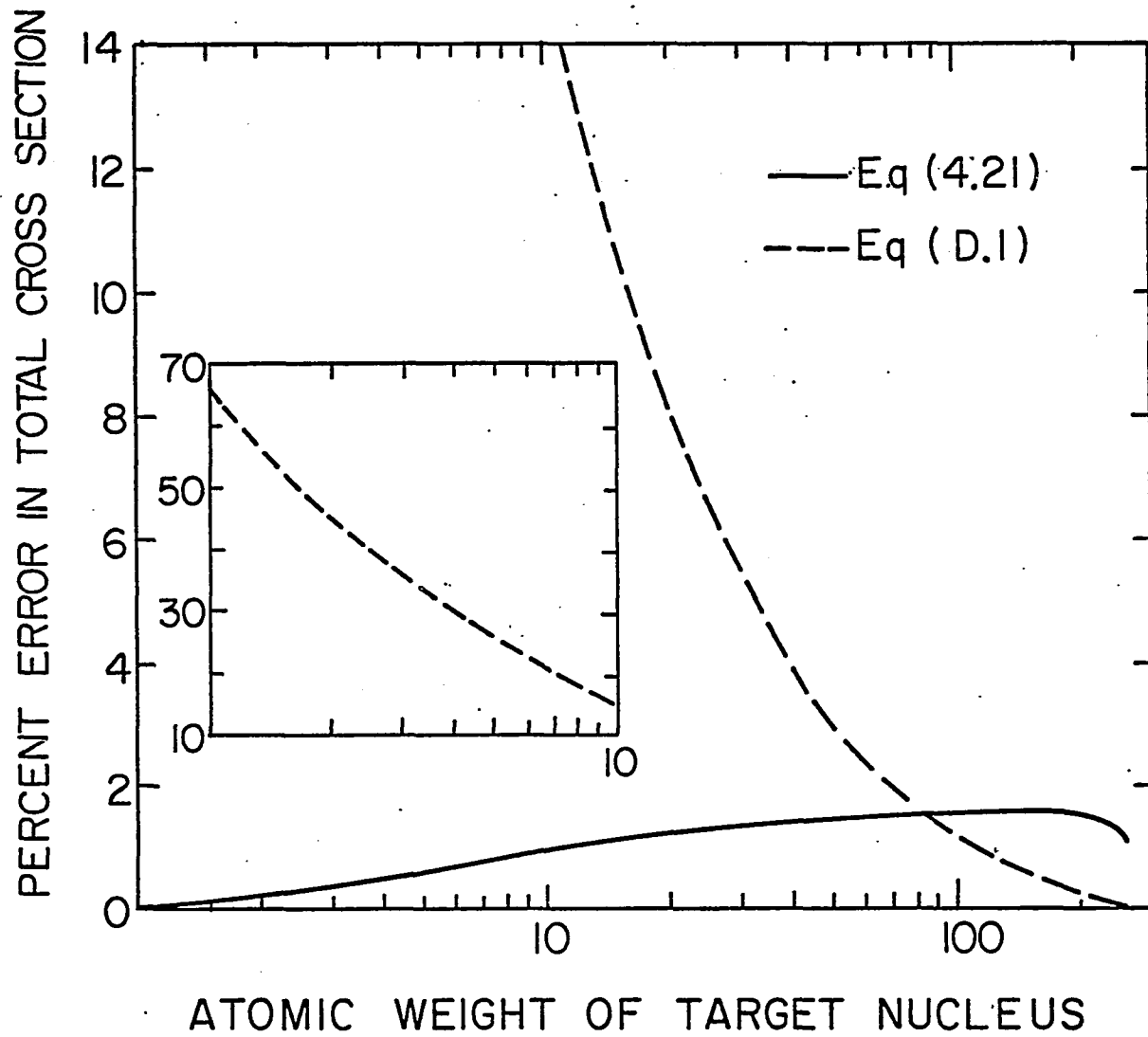


Fig. 4.2

where the first two terms can be readily recognized as p-nucleus and n-nucleus total cross-sections at momentum  $\hbar k/2$ . We shall now take the nuclear form factor to be

$$S_A(q) = (1 - \delta q^2) \exp(-q^2 R^2/4),$$

$$\delta = (A/6 - 2/3) R^2 A^{-1}. \quad (4.27)$$

Again assuming all NN amplitudes to be equal and of the form (2.14), the N-nucleus amplitude can be evaluated analytically with the result

$$F_{NA}(k', q) = -\frac{A k'}{2} e^{q^2 R^2/4A} (R^2 + 2a) \sum_{j=1}^A \binom{A}{j} \frac{1}{j} \left[ \frac{-\sigma(1-i\epsilon)}{2\pi(R^2+2a)} \right]^j$$

$$\times \sum_{k=0}^j \binom{j}{k} \left[ 1 - \frac{4\delta}{(R^2+2a)} \right]^{j-k} \left[ \frac{4\delta}{(R^2+2a)} \right]^k \frac{1}{j^k} k! e^{-q^2(R^2+2a)/4j}$$

$$\times L_k \left[ q^2(R^2+2a)/4j \right], \quad (4.28)$$

where  $L_k(z)$  is the Laguerre polynomial. Using Eq. (4.28) for  $F_{NA}$ , Eq. (4.26) can also be evaluated analytically if a sum of Gaussians is used for  $S_d$ . Alternatively, for general forms of  $S_d$ , Eq. (4.26) can be evaluated quite easily by numerical integrations. The parameter  $R$  in the nuclear form factor, upon making centre of mass and finite proton size corrections, is given by

$$R^2 = (\tau_A^2 - \tau_p^2) / \left[ \frac{5}{2} - \frac{2}{Z} - \frac{3}{2A} \right] \quad (4.29)$$

where  $\tau_p$  and  $\tau_A$  are the experimentally measured<sup>45</sup> rms radii of the proton and the nucleus.

We shall perform the calculations for  $\sigma_{dA}$  at 0.87 and 2.1 GeV/n, incident energies at which data have been obtained at Bevalac.<sup>42</sup> From Refs. 46 and 47, at 2.1 GeV/n we take  $a=6.2$  (GeV/c)<sup>-2</sup>,  $\delta=-0.28$ . Since different values

have been obtained for  $\sigma_{np}$  and  $\sigma_{pn}$ , we have used two different values 42.7 and 44mb for average NN total cross section  $\sigma$ . Similarly, at 0.87 GeV/n we take  $a=5.0$  (GeV/c)<sup>-2</sup>,  $\rho=-0.2$  and  $\sigma=42.4$  and 43.3mb. We have evaluated Eq. (4.26) by numerical integrations with the deuteron form factor obtained from the Gartenhaus-Moravcsik wave function. In Table III, we show the theoretical results together with the available experimental measurements. The agreement between them is quite good. Since  $\sigma_{dA}$  is calculated by using nuclear radius and NN scattering measurements, we have also estimated the total uncertainties in  $\sigma_{dA}$  by assuming uncertainties of  $\pm 0.1$ fm in  $r_A$ ,  $\pm 0.5$  (GeV/c)<sup>-2</sup> in  $a$ ,  $\pm 0.05$  in  $\rho$  and  $\pm 1$ mb in  $\sigma$ . The separate effects of these uncertainties for <sup>12</sup>C target is shown in Table IV. The largest effect is due to the nuclear radius; a change of  $\pm 0.1$ fm leads to a  $\sim 3\%$  change in  $\sigma_{dA}$ . The total uncertainty in  $\sigma_{dA}$  is, roughly  $\sim 5\%$ .

#### IV (d). Elastic Scattering Intensities:

##### (i) Comparison of Theoretical Cross sections

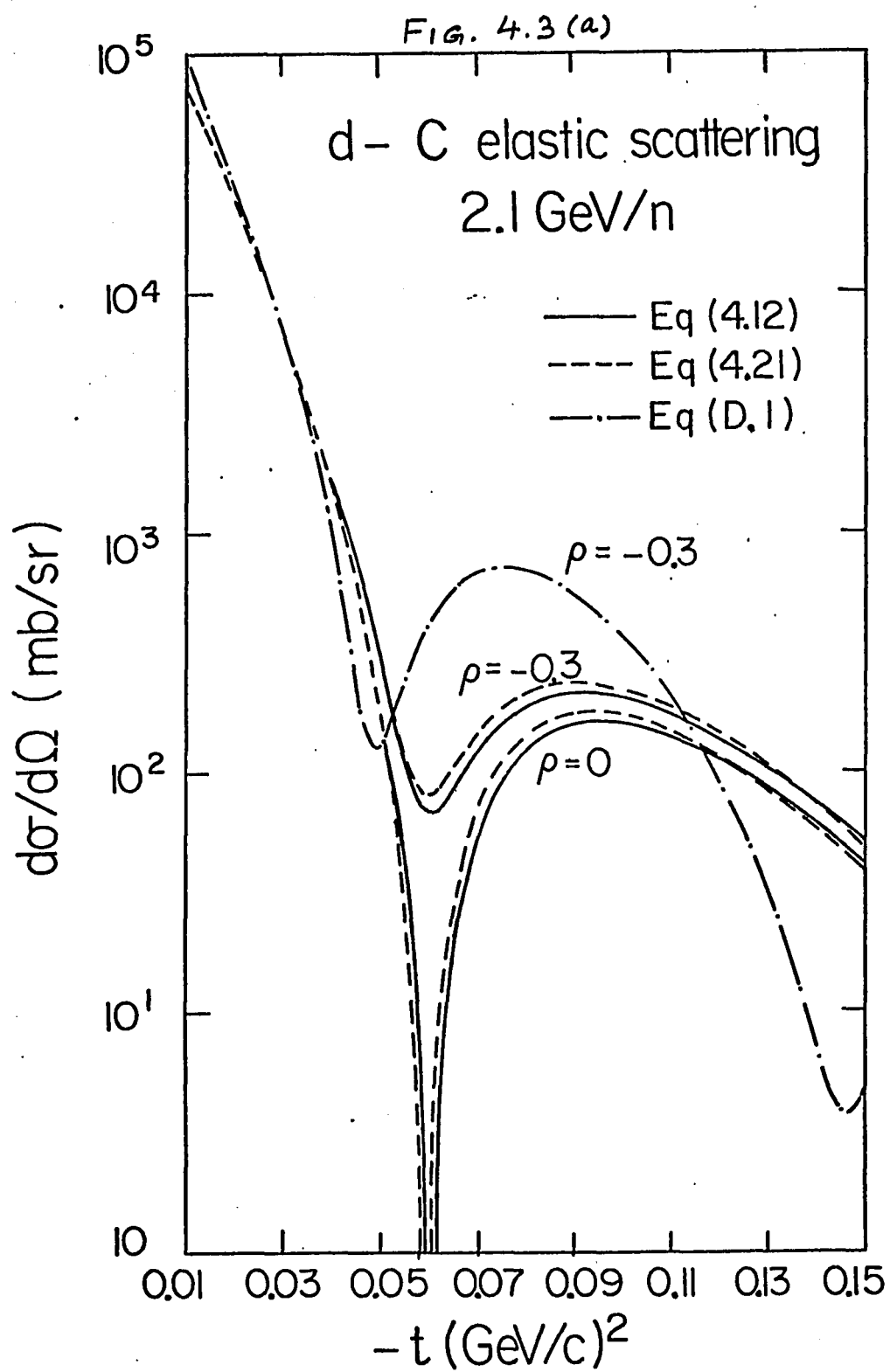
In this section we shall investigate the accuracy of the differential cross-sections predicted by approximation I and II, compared to the exact Glauber results given by Eq. (4.12). The differential cross sections for d-<sup>12</sup>C elastic scattering at 2.1 GeV/n are shown in Figs. 4.3(a) and 4.3(b). We see that approximation I agrees very well with the "exact" results out to the first diffraction minimum and agreement

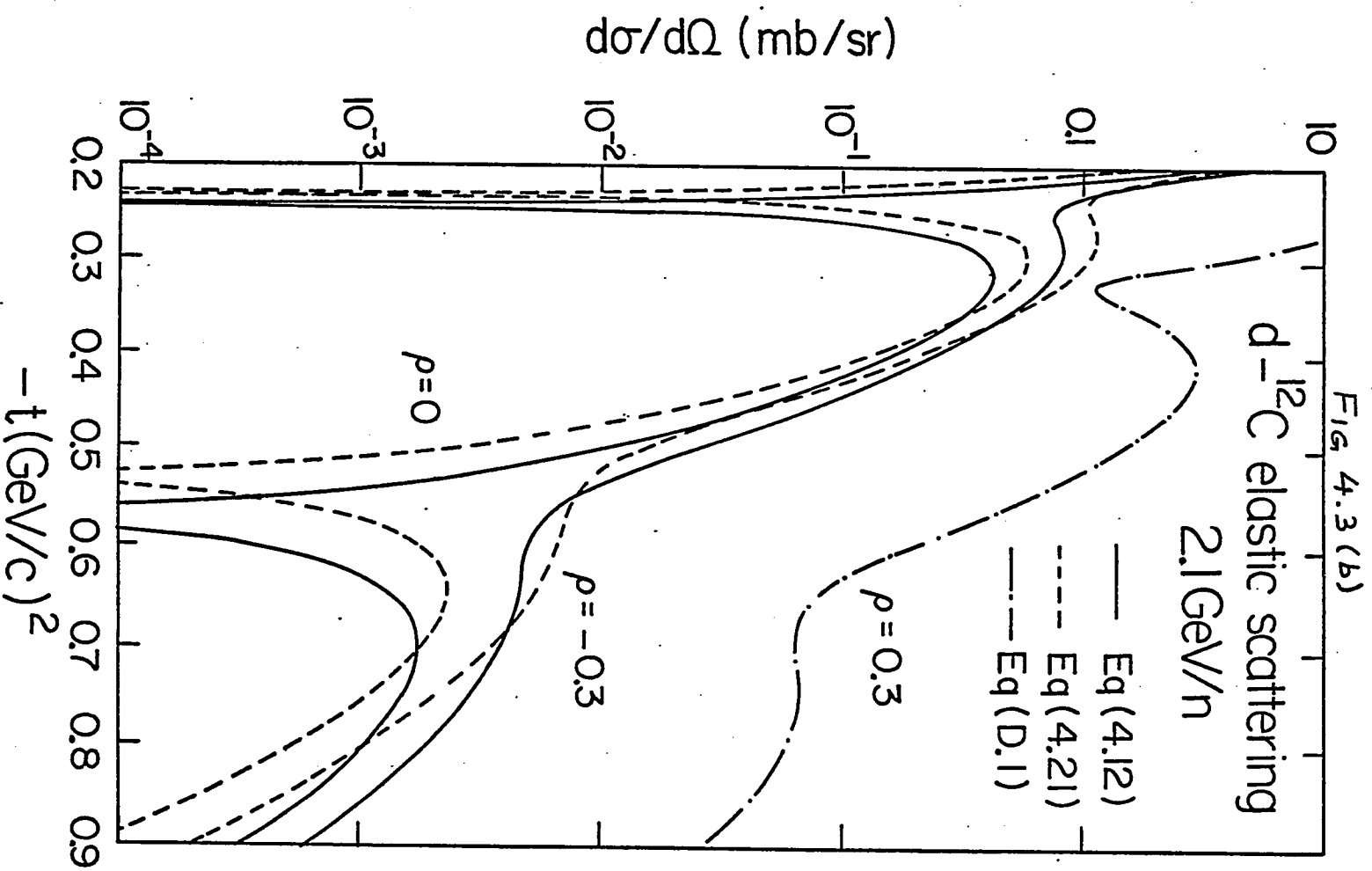
TABLE III. Deuteron-nucleus total cross sections, as predicted by Eq. (4.26), at 0.87 and 2.1 GeV/n together with the available measurements. (For d-d cross section the formula is derived in Appendix F.) The two theoretical values correspond to two different values of input NN total cross sections. The last column shows the total uncertainty in  $\sigma_{dA}$ , introduced by small variations in nuclear radii and NN scattering parameters.

Target Nucleus	$r_A$ (fm)	$\sigma_{dA}$ (mb)						$\Delta\sigma_{dA}$ (mb)
		2.1 GeV/n		Exp.	0.87 GeV/n		Exp.	
		Theory with $\sigma$ equal to				Theory with $\sigma$ equal to		
		42.7mb	44mb		42.4mb	43.3mb		
p	0.81	81.2	83.6	84.1±0.6	80.4	82.0	81.8±0.9	+1.9
D	-	152	156	156±0.8	149	152	151.6±1.1	+4
<sup>4</sup> He	1.71	255	262	266.9±2.4	250	254	254.8±2.9	+14
<sup>6</sup> Li	2.43	389	399		383	389		+17
<sup>9</sup> Be	2.42	511	522		501	508		+26
<sup>10</sup> B	2.45	544	556		533	540		+27
<sup>12</sup> C	2.453	603	612	630.5±4.6	590	597	618.2±6.1	+31
<sup>14</sup> N	2.48	659	671		644	652		+37
<sup>16</sup> O	2.71	757	771		741	750		+40

TABLE IV. The resulting uncertainties in deuteron-carbon total cross sections at 2.1 GeV/n arising from the separate uncertainties in the NN scattering parameters and in nuclear r.m.s. radii.

	$\Delta\sigma_{dA} \text{ (mb)}$
$\Delta\sigma = \pm 1.0 \text{ mb}$	$\pm 8$
$\Delta a = \pm 0.5 \text{ (GeV/c)}^{-2}$	$\pm 2$
$\Delta\rho = \pm 0.05$	$\pm 3$
$\Delta r_A = \pm 0.1 \text{ fm}$	$\pm 18$



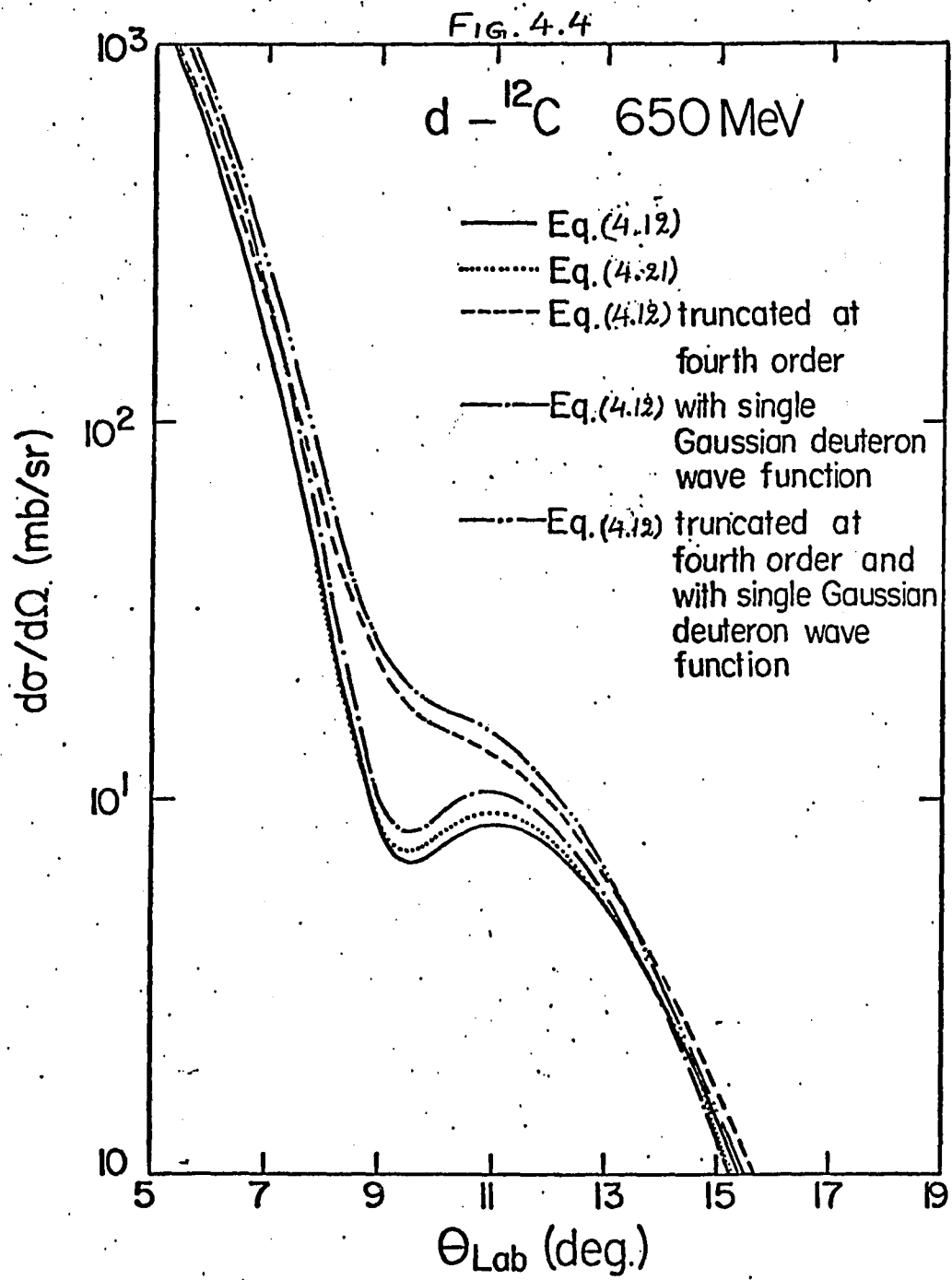


is reasonable out to the second minimum. The disagreement between the two curves increases with increasing momentum transfer. For example, for  $0.8 \lesssim q^2 \lesssim 2 \text{ (GeV/c)}^2$ , the predictions of approximation I are lower by a factor of  $\sim 2-6$ . Approximation II, on the other hand, is quite inaccurate even at small momentum transfers.

Another approximation has recently been used in Ref. 41, and good fit was obtained with 650 MeV  $d\text{-}^{12}\text{C}$  data. In this approximation only terms up to fourth order in multiple scattering were retained and an unrealistic wave function used for the deuteron. In Fig. 4.4 we show the curves obtained by making these approximations. Dashed curve is obtained by retaining terms only upto fourth order and the dot-dash curve is obtained from exact Eq. (4.12) with deuteron wave function of Ref. 41. The solid curve is the exact Glauber result of Eq. (4.12) with realistic deuteron form factor (2.28). We see that the two approximations made together in Ref. 41 can lead to substantial error in the cross sections. We also note that in the angular region where data exist, i.e.  $\theta_{\text{lab}} \lesssim 13^\circ$ , approximation I (dotted curve) is quite accurate.

#### (ii) Coulomb and Deuteron D-state Effects

In deuteron-nucleon collisions<sup>49</sup>, the deuteron D-state and in heavy ion collisions<sup>20</sup> the Coulomb interactions are important near the first minimum. In deuteron-nucleus collisions, since we have seen that approximation I is quite accurate out to the first minimum, we shall use it to investi-



gate these two effects. Assuming the Coulomb interaction to originate from the target nucleus as a whole, we can write for the scattering amplitude operator

$$F_{dA}(\vec{q}, \vec{s}) = 2 e^{-\frac{i}{2} \vec{q} \cdot \vec{s}} \left[ F_c(\frac{1}{2}k, \vec{q}) + e^{i\chi_{cp}} F_{pA}(\frac{1}{2}k, \vec{q}) \right] \\ + 2 e^{\frac{i}{2} \vec{q} \cdot \vec{s}} e^{i\chi_{cn}} F_{nA}(\frac{1}{2}k, \vec{q}) + \frac{2i}{\pi k} e^{i\chi_{cpn}} \\ \times \int d^2q' e^{i\vec{q}' \cdot \vec{s}} F_{pA}(\frac{1}{2}k, \frac{\vec{q}-\vec{q}'}{2}) F_{nA}(\frac{1}{2}k, \frac{\vec{q}+\vec{q}'}{2}), \quad (4.30)$$

where we have used an average phase approximation similar to the case of N-deuteron scattering of Sec. II. The average Coulomb phase shift functions  $\chi_{cp}$ ,  $\chi_{cn}$ , and  $\chi_{cpn}$  are given by the formulas of Appendix B, except that the NN amplitude  $f_{NN}(k, q)$  is replaced by N-nucleus amplitude

$$F_{NA}(\frac{1}{2}k, q). \quad F_c, \text{ the p-nucleus Coulomb amplitude is given by} \\ F_c(k, \vec{q}) = -\frac{2nk}{q^2} e^{-2i[n \ln(q/2k) - \arg \Gamma(1+in)]} \cdot \mathcal{F}_p(\vec{q}) \mathcal{F}_A(\vec{q}), \quad (4.31)$$

where  $n = Ze^2/\hbar v$  and  $\mathcal{F}_p$  and  $\mathcal{F}_A$  are the charge form factors of the proton and the target nucleus.

Now if the D-state is included, the deuteron wave function can be written as<sup>49</sup>

$$\psi_d^M(\vec{r}) = (4\pi)^{-\frac{1}{2}} r^{-1} [\mu(r) + \mathcal{S}^{-\frac{1}{2}} S_{12}(r) w(r)] \chi_1^M, \quad (4.32)$$

where  $\chi_1^M$  are spin-one spinors and  $S_{12}$  is the usual tensor operator. The differential cross section is then given by

$$\frac{d\sigma}{d\Omega} = \frac{1}{3} \sum_{M, M'} |\langle \psi_d^{M'} | F_{dA}(\vec{q}, \vec{s}) | \psi_d^M \rangle|^2 \\ = (d\sigma/d\Omega)_S + (d\sigma/d\Omega)_D, \quad (4.33)$$

where

$$\begin{aligned}
 (d\sigma/d\Omega)_S &= \left| F_{cpn}(\vec{q}) S_S(\frac{1}{2}\vec{q}) + \frac{2i}{\pi k} e^{i\chi_{cpn}} \right. \\
 &\quad \left. \times \int d^2q' S_B(\vec{q}') F_{pA}(\frac{1}{2}k, \frac{\vec{q}-\vec{q}'}{2}) F_{nA}(\frac{1}{2}k, \frac{\vec{q}+\vec{q}'}{2}) \right|^2, \\
 (d\sigma/d\Omega)_Q &= \frac{3}{4} \left| F_{cpn}(\vec{q}) S_Q(\frac{1}{2}\vec{q}) \right|^2 + \frac{1}{4} \left| F_{cpn}(\vec{q}) S_Q(\frac{1}{2}\vec{q}) \right. \\
 &\quad \left. + \frac{2i}{\pi k} e^{i\chi_{cpn}} \int d^2q' S_Q(\vec{q}') F_{pA}(\frac{1}{2}k, \frac{\vec{q}-\vec{q}'}{2}) \right. \\
 &\quad \left. \times F_{nA}(\frac{1}{2}k, \frac{\vec{q}+\vec{q}'}{2}) \right|^2, \quad (4.34)
 \end{aligned}$$

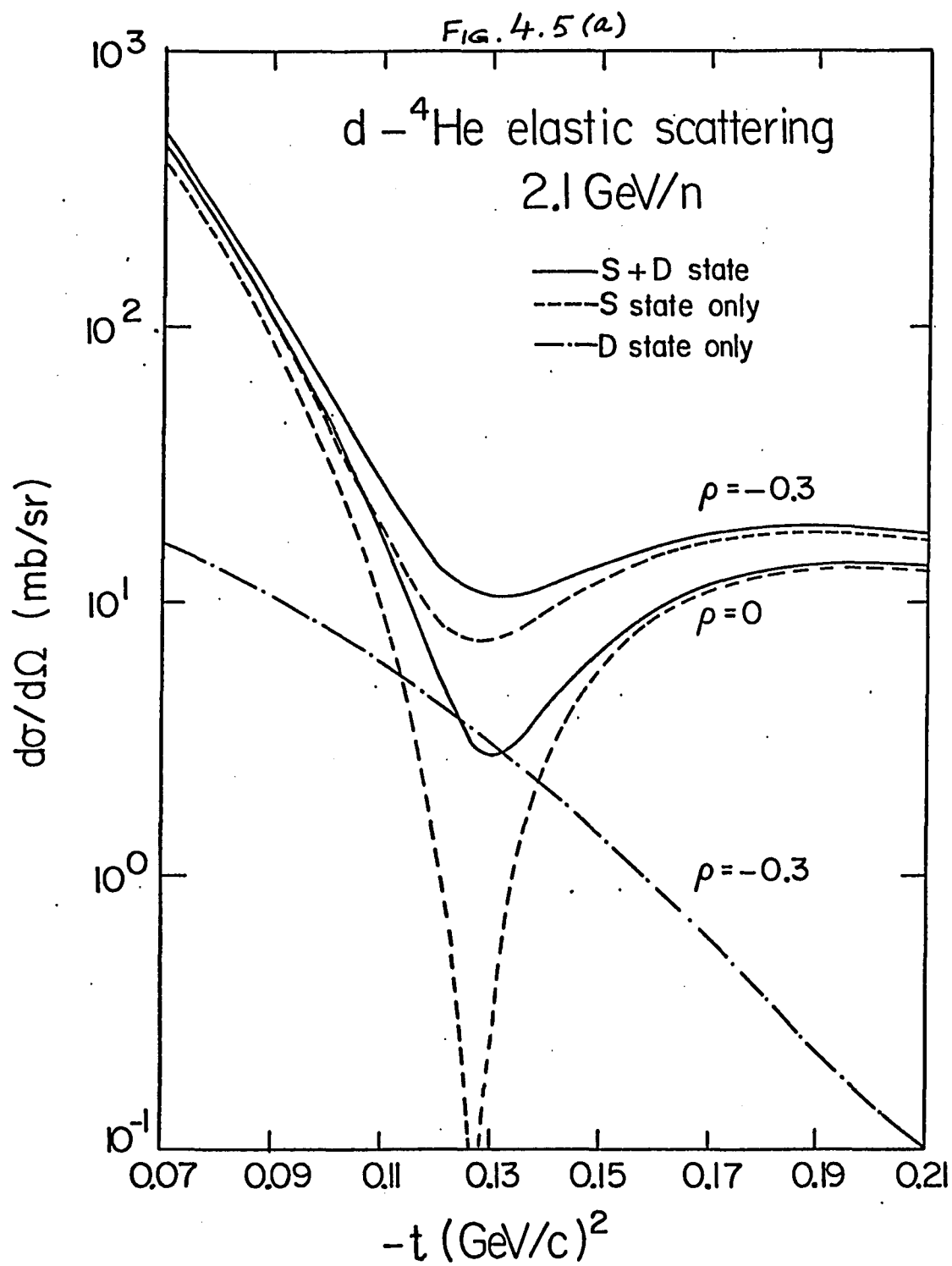
with

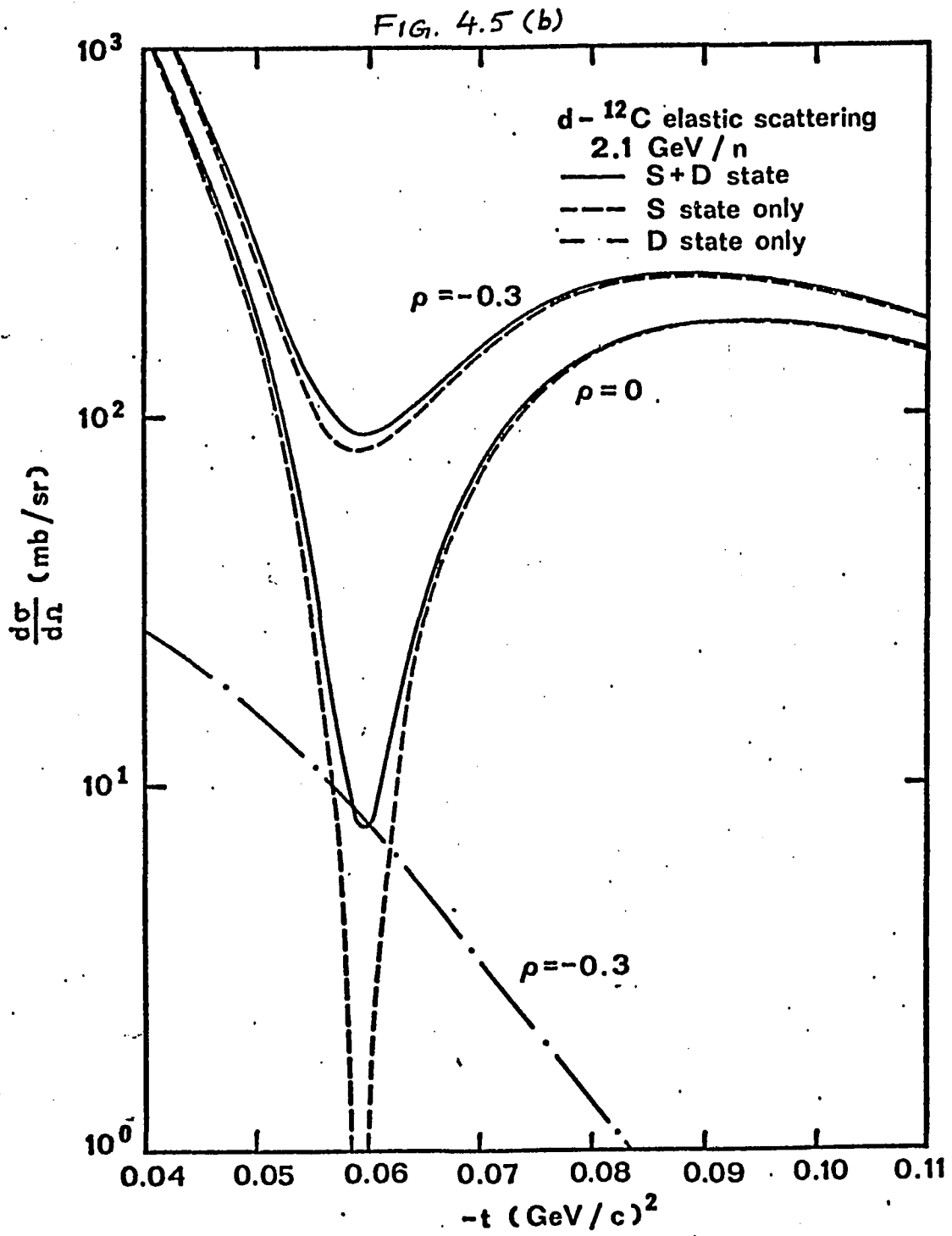
$$F_{cpn}(\vec{q}) = 2 \left[ F_C(\frac{1}{2}k, \vec{q}) + e^{i\chi_{cp}} F_{pA}(\frac{1}{2}k, \vec{q}) + e^{i\chi_{cn}} F_{nA}(\frac{1}{2}k, \vec{q}) \right],$$

and spherical and quadrupole form factors are defined as

$$\begin{aligned}
 S_S(q) &= \int_0^\infty j_0(qr) [u^2(r) + w^2(r)] dr, \\
 S_Q(q) &= 2 \int_0^\infty j_2(qr) w(r) [u(r) - 8^{-\frac{1}{2}} w(r)] dr.
 \end{aligned} \quad (4.35)$$

In order to illustrate the effects of the deuteron D-state clearly, we neglect the Coulomb interaction (i.e. let  $F_C$ ,  $\chi_{cp}$ ,  $\chi_{cn}$  and  $\chi_{cpn}$  go to zero) and take the nuclear wave functions as Gaussians. We obtain the deuteron form factors  $S_S$  and  $S_Q$  from the Gartenhaus-Moravcsik wave functions<sup>21</sup>. Figures 4.5(a) and (b) show the  $d$ - ${}^4\text{He}$  and  $d$ - ${}^{12}\text{C}$  differential cross sections at 2.1 GeV/n, with and without the D-state. The effect of D-state is significant in the case of  $d$ - ${}^4\text{He}$  scattering but it is less than that in case of  $d$ -N scattering. The effect is much smaller in case of  $d$ - ${}^{12}\text{C}$  scattering. The reason for this can be understood in the following manner. When





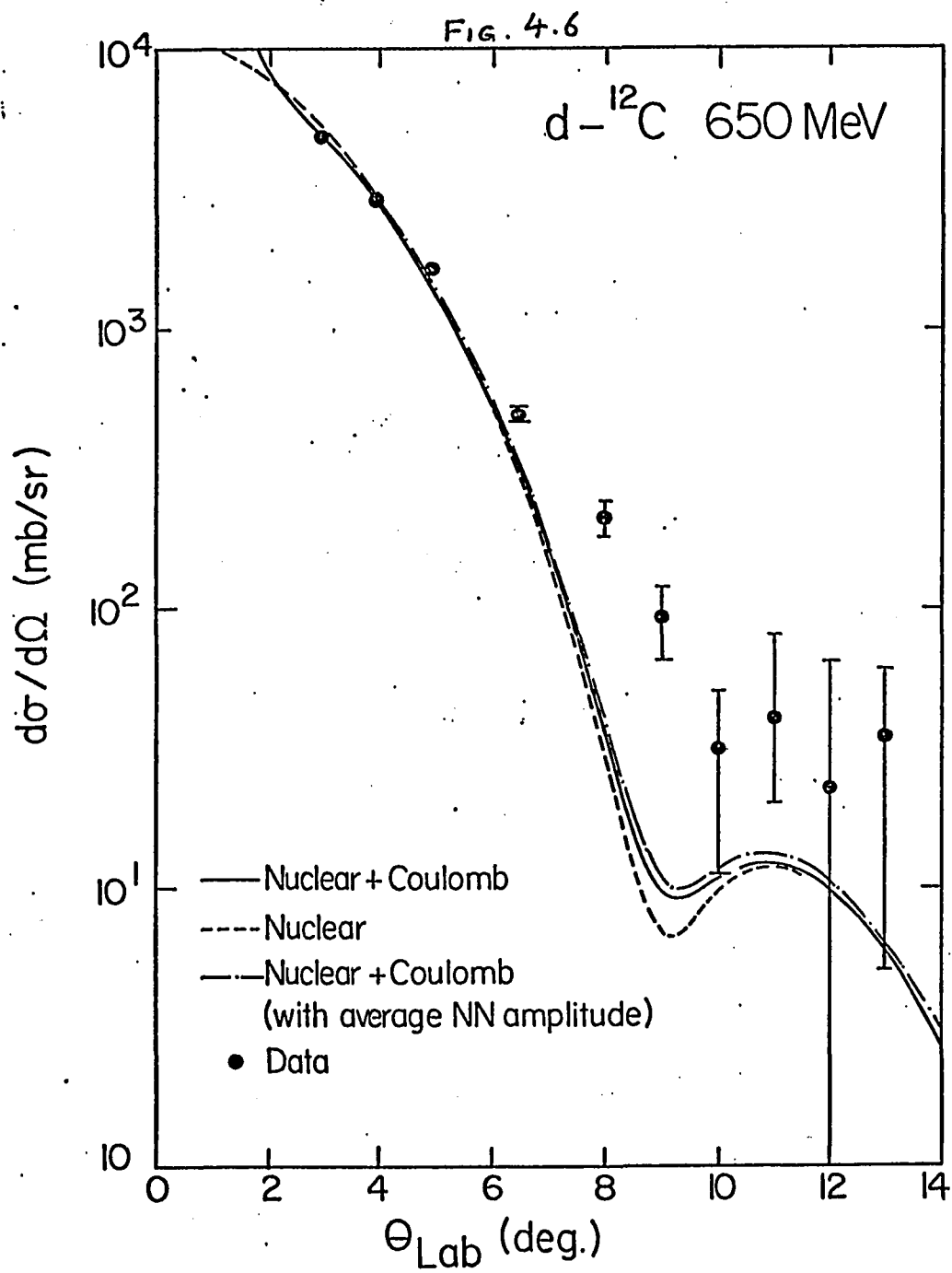
deuteron D-state is neglected, a minimum appears at  $q^2 \approx 0.33 \text{ (GeV/c)}^2$  in case of d-N scattering because of the destructive interference between the single and double scattering amplitudes. The cross sections before the minimum are predominantly due to single scattering and are proportional to  $S_s^2(\frac{1}{2}q)$ . When the D-state is included, the cross sections in this region become proportional to  $S_s^2(\frac{1}{2}q) + S_a^2(\frac{1}{2}q)$ . However, at  $q^2 \approx 0.33 \text{ (GeV/c)}^2$ ,  $S_a(\frac{1}{2}q)$  happens to be comparable in magnitude to  $S_s(\frac{1}{2}q)$  and therefore the minimum is almost completely filled. In the case of d- $^4\text{He}$  scattering, on the other hand, the minimum occurs at  $q^2 \approx 0.13 \text{ (GeV/c)}^2$ . At this value of  $q^2$ ,  $S_a^2(\frac{1}{2}q)$  is smaller than  $S_s^2(\frac{1}{2}q)$  by a factor of  $\sim 20$  and hence the minimum is only partially filled due to  $S_a$ . For heavier target nuclei, the position of the minimum moves to even smaller  $q^2$ . With decreasing momentum transfers,  $S_s$  increases (toward unity) and  $S_a$  decreases (toward zero) and, consequently, the effect of quadrupole form factor becomes less and less significant.

### (iii) 650 MeV d- $^{12}\text{C}$ Scattering

As mentioned earlier a good fit to the 650 MeV d- $^{12}\text{C}$  data was obtained in Ref. 41. But, as we have seen, the additional simplifications made in that calculation increase the cross sections substantially and hence lead to significant errors. We have performed the theoretical calculation again using Eqs. (4.33), (4.34) which include the Coulomb effects. The NN parameters at 325 GeV used are <sup>45,48</sup>

$\sigma_{pp} = 24.1 \text{ mb}$ ,  $a_{pp} = 0.35 \text{ (GeV/c)}^{-2}$ ,  $\rho_{pp} = 0.8$ ,  $\sigma_{np} = 33 \text{ mb}$ ,  
 $a_{np} = 2.8 \text{ (GeV/c)}^{-2}$  and  $\rho_{np} = 0.25$ . For deuteron S and D states we again use Gartenhaus-Moravcsik wave functions<sup>21</sup> and for carbon form factor we use Eq. (4.27). Figure 4.6 shows the theoretical results with the data. We see that, as expected, the Coulomb effects are important at small angles. They are, however, also noticeable at the minimum, even though the real parts  $\rho_{NN}$  are quite large. At energies where  $\rho_{NN}$  are small, Coulomb effects, near the minimum, become much more significant. Also shown in Fig. 4.6 is the curve obtained by assuming  $f_{pp} = f_{np}$  and using the mean values (as was done in Ref. 41). The error introduced by this procedure is not negligible except at very small angles and such an averaging should not be done in a detailed analysis of the data. From Fig. 4.6 we notice that the theoretical predictions, at larger angles, are systematically lower than the data, even though the error bars in data are large. For total cross sections we obtain 470mb which agrees well with the experimental value of  $456 \pm 18 \text{ mb}$ .

We should point out that this calculation can only be regarded as qualitative because of the use of a Gaussian form of NN amplitudes and the neglect of spin effects, both of which are not realistic at 325 MeV. Before conclusions regarding the validity of the theory are drawn or an attempt is made to extract information about nuclear correlations, spin dependent effects must be carefully included. The evaluation of exact Glauber amplitude with spin effects is quite



difficult. Such a calculation, however, can be carried out starting from the approximate Eq. (4.30), at least for angles out to the secondary maximum where Eq. (4.30) is a good approximation to the full Glauber series. This approximation can also be used to study deuteron-nucleus inelastic interactions, for example, deuteron dissociation from various nuclear targets.

## V. Medium and High energy Collisions between Heavy Ions

### V.(a). Introduction

Interest in heavy ion collisions at medium and high energies has increased rapidly in the past few years.<sup>6-9</sup> Many theoretical studies have involved the Glauber approximation or some variants of it. The full Glauber multiple scattering series is difficult to evaluate for general forms of nuclear wave functions and therefore an optical limit result has generally been used.<sup>7-9</sup> However, there are serious theoretical problems associated with the optical limit. It yields accurate results at small angles only when the centre of mass correction is used (although, technically this correction should go to unity in the optical limit), but on the other hand, this correction also leads to an unphysical rise in cross sections at larger angles. Furthermore, even for total cross sections, the recent  $^{12}\text{C}-^{12}\text{C}$  measurements show serious disagreement<sup>42</sup> with the prediction of the optical limit. In this section we study nucleus-nucleus scattering and the validity of the optical limit. The full Glauber amplitude is converted into a series where the first term is the optical limit amplitude. The higher order corrections are calculated and the results compared with the measurements.

## V (b). Basic Formulas

The elastic scattering amplitude for collisions between nuclei with mass numbers  $A_1, A_2$  can be written as

$$F_{A_1 A_2}(q) = K_{12}(q) \frac{\mu k}{2\pi} \int d^2b e^{i\vec{q}\cdot\vec{b}} \left[ 1 - e^{i\chi_{A_1 A_2}(\vec{b})} \right],$$

$$e^{i\chi_{A_1 A_2}(\vec{b})} = \langle \gamma_{A_1} \gamma_{A_2} | \prod_{\lambda=1}^{A_1} \prod_{j=1}^{A_2} \left[ 1 - \Gamma_{\lambda j}(\vec{b} - \vec{s}_\lambda + \vec{s}'_j) \right] | \gamma_{A_1} \gamma_{A_2} \rangle. \quad (5.1)$$

Here  $K_{12}(q)$  is a correction factor obtained by removing the  $\delta$ -function constraints due to the centers of mass (See Appendix H) and  $\vec{s}_i, \vec{s}'_i$  are the projection of the nucleon coordinates on the impact parameter plane.

If we define

$$f(\lambda) = \langle \gamma_{A_1} \gamma_{A_2} | \prod_{\lambda=1}^{A_1} \prod_{j=1}^{A_2} \left[ 1 - \lambda \Gamma_{\lambda j}(\vec{b} - \vec{s}_\lambda + \vec{s}'_j) \right] | \gamma_{A_1} \gamma_{A_2} \rangle,$$

we can write

$$i\chi_{A_1 A_2} = \ln f(\lambda) \Big|_{\lambda=1}$$

$$= i \left[ \chi_1 + \chi_2 + \chi_3 + \dots \right] \quad (5.2)$$

Now using the notation

$$f' \equiv \frac{\partial f(\lambda)}{\partial \lambda} \Big|_{\lambda=0}$$

and so on, we obtain

$$\begin{aligned} \chi_1 &= f', \\ \chi_2 &= \frac{1}{2} \left[ -f'^2 + f'' \right], \\ \chi_3 &= \frac{1}{6} \left[ 2f'^3 - 3f'f'' + f''' \right], \\ \chi_4 &= \frac{1}{24} \left[ -6f'^4 + 12f'^2f'' - 3f''^2 - 4f'f''' + f'''' \right], \end{aligned} \quad (5.3)$$

where (using the result  $2 \sum_{i < k} = \sum_{i \neq k}$ )

$$\begin{aligned}
f' &= - \sum_{\lambda=1}^{A_1} \sum_{j=1}^{A_2} \langle \gamma_{A_1} \gamma_{A_2} | \Gamma_{\lambda j} (\vec{b} - \vec{s}_\lambda + \vec{s}'_j) | \gamma_{A_1} \gamma_{A_2} \rangle, \\
f'' &= \sum'_{\lambda j k \ell} \langle \gamma_{A_1} \gamma_{A_2} | \Gamma_{\lambda j} \Gamma_{k \ell} | \gamma_{A_1} \gamma_{A_2} \rangle, \\
f''' &= - \sum_{\lambda j k \ell m n} \langle \gamma_{A_1} \gamma_{A_2} | \Gamma_{\lambda j} \Gamma_{k \ell} \Gamma_{m n} | \gamma_{A_1} \gamma_{A_2} \rangle, \quad (5.4)
\end{aligned}$$

etc. Here the prime over the summation sign indicates that no two pairs can be exactly equal, e.g. if  $i=k$  then  $j \neq 1$  and vice versa. If we now assume for simplicity, that all NN amplitudes are equal, we obtain<sup>55</sup>

$$\begin{aligned}
f' &= - A_1 A_2 C_1(b), \\
f'' &= A_1 A_2 \left[ (A_1-1)(A_2-1) C_1^2(b) + (A_2-1) C_2(b) + (A_1-1) C_3(b) \right], \\
f''' &= - A_1 A_2 \left[ (A_1-1)(A_1-2)(A_2-1)(A_2-1) C_1^3(b) + 3(A_1-1)(A_2-1) C_1(b) \right. \\
&\quad \times \left. \left\{ (A_2-2) C_2(b) + (A_1-2) C_3(b) \right\} + 6(A_1-1)(A_2-1) \right. \\
&\quad \times \left. C_4(b) + (A_2-1)(A_2-2) C_5(b) + (A_1-1)(A_1-2) C_6(b) \right], \\
f'''' &= A_1 A_2 \left[ (A_1-1)(A_1-2)(A_1-3)(A_2-1)(A_2-2)(A_2-3) C_1^4(b) \right. \\
&\quad + 6(A_1-1)(A_1-2)(A_2-1)(A_2-2) C_1^2(b) \left\{ (A_2-3) C_2(b) \right. \\
&\quad + (A_1-3) C_3(b) \left. \right\} + 4(A_1-1)(A_2-1) C_1(b) \left\{ (A_2-2)(A_2-3) \right. \\
&\quad \times C_5(b) + (A_1-2)(A_1-3) C_6(b) \left. \right\} + (A_1-1)(A_1-2)(A_2-1) \\
&\quad \times (A_2-2) \left\{ 24 C_1(b) C_4(b) + 6 C_2(b) C_3(b) \right\} \\
&\quad + 3(A_1-1)(A_2-1) \left\{ (A_2-2)(A_2-3) C_2^2(b) + (A_1-2)(A_1-3) C_3^2(b) \right. \\
&\quad + 4(A_2-2) C_7(b) + 4(A_1-2) C_8(b) + 2 C_9(b) \left. \right\} \\
&\quad + (A_2-1)(A_2-2)(A_2-3) C_{10}(b) + (A_1-1)(A_1-2)(A_1-3) C_{11}(b) \\
&\quad + 12(A_1-1)(A_2-1) \left\{ (A_2-2) C_{12}(b) + (A_1-1) C_{13}(b) \right\} \left. \right], \quad (5.5)
\end{aligned}$$

where  $C_i(b)$  can be expressed in terms of generalized

$$S_{A_i}^{jklm}(\vec{q}_1, \vec{q}_2, \vec{q}_3, \vec{q}_4) = \int d^3r_1 \dots d^3r_{A_i} e^{i(\vec{q}_1 \cdot \vec{r}_j + \vec{q}_2 \cdot \vec{r}_k + \vec{q}_3 \cdot \vec{r}_l + \vec{q}_4 \cdot \vec{r}_m)} \left| \Psi_{A_i}(\vec{r}_1, \dots, \vec{r}_{A_i}) \right|^2, \quad (1)$$

by

$$C_1(b) = (2\pi\lambda k_N)^{-1} \int d^2q_1 g(\vec{q}_1) S_{A_1}(\vec{q}_1, 0, 0, 0) S_{A_2}(-\vec{q}_1, 0, 0, 0),$$

$$C_2(b) = (2\pi\lambda k_N)^{-2} \int d^2q_1 g(\vec{q}_1) \int d^2q_2 g(\vec{q}_2) S_{A_1}(0, \vec{q}_1 + \vec{q}_2, 0, 0) S_{A_2}(-\vec{q}_1, -\vec{q}_2, 0, 0),$$

$$C_3(b) = C_2 [S_{A_1} \leftrightarrow S_{A_2}],$$

$$C_4(b) = (2\pi\lambda k_N)^{-3} \int d^2q_1 g(\vec{q}_1) \int d^2q_2 g(\vec{q}_2) \int d^2q_3 g(\vec{q}_3)$$

$$C_4(b) = (2\pi\lambda k_N)^{-3} \int d^2q_1 g(\vec{q}_1) \int d^2q_2 g(\vec{q}_2) \int d^2q_3 g(\vec{q}_3)$$

$$\times S_{A_1}(0, \vec{q}_1 + \vec{q}_2, \vec{q}_3, 0) S_{A_2}(0, -\vec{q}_2, -\vec{q}_1 - \vec{q}_3, 0),$$

$$C_5(b) = (2\pi\lambda k_N)^{-3} \int d^2q_1 g(\vec{q}_1) \int d^2q_2 g(\vec{q}_2) \int d^2q_3 g(\vec{q}_3)$$

$$\times S_{A_1}(0, 0, \vec{q}_1 + \vec{q}_2 + \vec{q}_3, 0) S_{A_2}(-\vec{q}_1, -\vec{q}_2, -\vec{q}_3, 0),$$

$$C_6(b) = C_5 [S_{A_1} \leftrightarrow S_{A_2}],$$

$$C_7(b) = (2\pi\lambda k_N)^{-4} \int d^2q_1 g(\vec{q}_1) \int d^2q_2 g(\vec{q}_2) \int d^2q_3 g(\vec{q}_3) \int d^2q_4 g(\vec{q}_4)$$

$$\times S_{A_1}(0, 0, \vec{q}_1 + \vec{q}_2 + \vec{q}_3, \vec{q}_4) S_{A_2}(0, -\vec{q}_2, -\vec{q}_3, -\vec{q}_1 - \vec{q}_4),$$

$$C_8(b) = C_7 [S_{A_1} \leftrightarrow S_{A_2}],$$

$$C_9(b) = (2\pi\lambda k_N)^{-4} \int d^2q_1 g(\vec{q}_1) \int d^2q_2 g(\vec{q}_2) \int d^2q_3 g(\vec{q}_3) \int d^2q_4 g(\vec{q}_4)$$

$$\times S_{A_1}(0, \vec{q}_1 + \vec{q}_2, 0, \vec{q}_3 + \vec{q}_4) S_{A_2}(0, 0, -\vec{q}_1 - \vec{q}_3, -\vec{q}_2 - \vec{q}_4),$$

$$C_{10}(b) = (2\pi\lambda k_N)^{-4} \int d^2q_1 g(\vec{q}_1) \int d^2q_2 g(\vec{q}_2) \int d^2q_3 g(\vec{q}_3) \int d^2q_4 g(\vec{q}_4)$$

$$\times S_{A_1}(0, 0, 0, \vec{q}_1 + \vec{q}_2 + \vec{q}_3 + \vec{q}_4) S_{A_2}(-\vec{q}_1, -\vec{q}_2, -\vec{q}_3, -\vec{q}_4),$$

$$C_{11}(b) = C_{10} [S_{A_1} \leftrightarrow S_{A_2}],$$

$$C_{12}(b) = (2\pi\lambda k_N)^{-4} \int d^2q_1 g(\vec{q}_1) \int d^2q_2 g(\vec{q}_2) \int d^2q_3 g(\vec{q}_3) \int d^2q_4 g(\vec{q}_4)$$

$$\times S_{A_1}(0, \vec{q}_1 + \vec{q}_2, 0, \vec{q}_3 + \vec{q}_4) S_{A_2}(0, -\vec{q}_2, -\vec{q}_1 - \vec{q}_3, -\vec{q}_4),$$

$$C_{13}(b) = C_{12} [ S_{A_1} \leftrightarrow S_{A_2} ],$$

$$g(\vec{q}) = e^{-i\vec{q}\cdot\vec{b}} f(\vec{q}) . \quad (5.6)$$

In the series expansion (5.2) for the nucleus-nucleus phase shift function, the first term, i.e.  $i\chi_1 = -A_1 A_2 C_1(b)$  is the usual 'optical limit' result of the Glauber theory. In order to illustrate the relative importance of the higher order terms, we shall take the independent particle model (4.4) for the nuclear wave functions so that

$$S_{A_i}(\vec{q}_1, \dots, \vec{q}_4) = S_{A_i}(\vec{q}_1) \dots S_{A_i}(\vec{q}_4) . \quad (5.7)$$

With  $S_{A_i}(q)$  given by  $\exp(-q^2 R_i^2/4)$  and NN amplitudes of form (2.14),  $C_1(b) \dots C_{13}(b)$  can all be evaluated analytically, and the explicit formulas are given in Appendix G.

#### V (c). Theoretical Results and Comparison with the Data

Before considering nucleus-nucleus scattering, let us first discuss briefly the case of particle-nucleus scattering. In this case (i.e.  $A_1=1$ ,  $A_2=A$ ,  $R_1^2=0$ ), we have from (5.3) and (5.4) in coordinate space

$$i\chi_1 = -A \int d^3\vec{r} \Gamma(\vec{b}-\vec{s}) \rho^{(1)}(\vec{r})$$

$$i\chi_2 = -\frac{1}{2} \int d^3\vec{r}_1 d^3\vec{r}_2 \Gamma_1(\vec{b}-\vec{s}_1) \Gamma_2(\vec{b}-\vec{s}_2) \times [A^2 \rho^{(1)}(\vec{r}_1) \rho^{(1)}(\vec{r}_2) - A(A-1) \rho^{(2)}(\vec{r}_1, \vec{r}_2)] , \quad (5.8)$$

where  $\rho^{(1)}$  and  $\rho^{(2)}$  are one and two particle densities. The coefficient of  $A^2$ , in  $i\chi_2$ , is the two-particle correlation function which vanishes for an uncorrelated nuclear wave function. The coefficient of remaining term in  $i\chi_2$  is

A (as in those of  $i\chi_1$ ). More explicitly, for Gaussian NN amplitudes and wave functions described in the preceding section, we have (with  $R^2 = R_2^2 + 2a$ )

$$\begin{aligned} \chi_1(b) &= -AY e^{-b^2/R^2}, & \chi_2(b) &= (\chi_1) \frac{Y}{2} e^{-b^2/R^2}, \\ \chi_3(b) &= (\chi_1) \frac{Y^2}{3} e^{-2b^2/R^2}, & \chi_4(b) &= (\chi_1) \frac{Y^3}{4} e^{-3b^2/R^2} \end{aligned} \quad (5.9)$$

where  $y = \sigma(1-ip)/2\pi R^2$ . Since  $R \propto A^{1/3}$ , we have  $y \propto A^{-2/3}$  and the optical limit result  $i\chi = i\chi_1$ , for particle-nucleus scattering, becomes a good approximation for large A.

This, however, is not the case with nucleus-nucleus scattering. In this case (assuming  $A_1 = A_2$ ), the coefficient of the surviving terms in  $i\chi_2$ , for uncorrelated nuclei, are proportional to  $A^3$  (whereas that for the term in  $i\chi_1$ , is  $\propto A^2$ ). The detailed expressions for  $i\chi_1, \dots, i\chi_4$  are given in Appendix G. For the special case  $A_1 = A_2 \gg 1$ ,  $R_1^2 = R_2^2 \gg a$ , we have

$$\begin{aligned} \chi_2(0) &\sim \chi_1(0) [-0.33 (AY)] & \chi_2(R) &\sim \chi_1(R) [-0.59 (AY)] \\ \chi_3(0) &\sim \chi_1(0) [0.33 (AY)^2] & \chi_3(R) &\sim \chi_1(R) [0.31 (AY)^2] \\ \chi_4(0) &\sim \chi_1(0) [-0.5 (AY)^3] & \chi_4(R) &\sim \chi_1(R) [-0.28 (AY)^3] \end{aligned} \quad (5.10)$$

One difference between (5.10) and (5.8) is that (5.10) is oscillatory. This is because of the occurrence of new types of multiple scattering in nucleus-nucleus case. Furthermore, the expansion parameter in this case is  $yA \propto A^{1/3}$  which may become greater than one for large A. In order to make qualitative estimates, let us first take  $R_1 = 1.25A_1^{1/3}$  fm,

( $i=1,2$ ). At incident energy of 2.1 GeV/n,  $\sigma=42.7$  mb, and we obtain  $yA \approx 0.22A^{1/3}$ . For the case  $^{208}\text{Pb}-^{208}\text{Pb}$  collisions, for example,  $yA \approx 1.3$ .

On the other hand, if we choose the parameter  $R_i^2$  to fit the rms radius  $r_i$  then  $R_i = \sqrt{\frac{2}{3}} r_i$ . For Pb,  $r_{\text{Pb}}=5.49$  fm which yields  $yA \sim 3.3$ . In fact in the limit  $A_1, A_2 \rightarrow \infty$  (with  $\sigma=\text{constant}$ ), the series (5.2) for the phase shift function appears to diverge. For  $A_1, A_2$  not too large, the series converges, but the optical limit result ( $i\chi = i\chi_1$ ) is still inaccurate. For light and medium nuclei, accurate results may be obtained by retaining sufficient number of terms in the series (5.2).

Before comparing our results with the data, we should comment briefly upon a frequently used approximation where<sup>7-10</sup> one takes  $f_{\text{NN}}(\vec{b}) \propto \delta^2(\vec{b})$ . (Equivalently  $f_{\text{NN}}(q) \rightarrow f_{\text{NN}}(0)$ , or for  $f_{\text{NN}}(q)$  of form (2.14),  $a \rightarrow 0$ .) That such an NN amplitude is not consistent with the Glauber approximation, is exhibited in multiple scattering terms of order four and higher. The term  $C_9(b)$  which corresponds to two nucleons of the projectile interacting with the same two nucleons of the target (for example, the quadruple scattering in deuteron-deuteron collisions) diverges in the limit  $a \rightarrow 0$ .

We have performed theoretical calculations at incident energies of 0.87 and 2.1 GeV/n using the formulas given in Appendix G. The functions  $\chi_1, \dots, \chi_4$  were calculated by means of Eqs. (5.3), (5.5) and (G.1). Tables V-VII show the theoretical predictions for nucleus-nucleus total cross

sections, slope parameters of nucleus-nucleus forward elastic scattering amplitude and total inelastic cross sections, together with the available measurements. The agreement between them is quite good and the correction terms give significant contributions. The earlier large discrepancy<sup>42</sup> between theory and data for  $^{12}\text{C}-^{12}\text{C}$  total cross section does not indicate a breakdown of the Glauber approximation but rather indicates the breakdown of the approximations leading to the optical limit result. In Figs. 5.1(a) and (b) we show the elastic scattering angular distribution for  $^4\text{He}-^4\text{He}$  and  $^{12}\text{C}-^{12}\text{C}$  collisions at 2.1 GeV/n. Again the errors are quite large if one uses the optical limit. However, accurate results can be obtained by retaining sufficient number of terms in the series (5.2). For He-He collisions, for example, terms upto  $\chi_4$  lead to excellent convergence in the total and inelastic cross sections, in the forward slope parameter, and in the elastic scattering differential cross sections out to the second minimum. Convergence can be obtained at larger momentum transfers by considering the higher order terms in (5.2).

Before concluding we should comment briefly upon the validity of the optical limit for the case of hadron-hadron collisions. If one considers the hadrons to be made up of an infinite number of constituents<sup>50</sup>  $x$  (or equivalently a continuum of hadronic matter), the appropriate limit in (5.2) is  $\sqrt{\sigma_{xx}} \rightarrow 0$  as  $A_1, A_2 \rightarrow \infty$  with  $\sqrt{\sigma_{xx}} A_1 A_2 \rightarrow \text{constant}$ . In this limit we have  $yA \sim \frac{\sqrt{\sigma_{xx}}}{R^2} A \sim \frac{\text{const.}}{R^2 A}$ . We see that, in this

case,  $i\chi \rightarrow i\chi_1$  (the optical limit) for  $A_1, A_2 \rightarrow \infty$ . If we make the further assumption that the hadron form factors are much more sharply peaked in forward direction, than the x-x scattering amplitudes, the optical limit result becomes identical to the Chou-Yang model<sup>51</sup>, which has been quite successful in fitting, for example, the high energy p-p cross section data.

TABLE V. Nucleus-nucleus total cross sections at 2.1 GeV/n

The values in parantheses are the total crosssections at 0.87 GeV/n. The quoted experimental errors are statistical only. The two experimental values in the second row correspond to  ${}^4\text{He}-{}^{12}\text{C}$  and  ${}^{12}\text{C}-{}^4\text{He}$  scattering respectively. The nucleon-nucleon parameter used in our calculations  $\sigma=42.7$  mb,  $a=6.2$  (GeV/c) $^{-2}$ ,  $\rho=-0.28$  at 2.1 GeV/n, and  $\sigma=42.4$  mb,  $a=5$  (GeV/c) $^{-2}$ ,  $\rho=-0.2$  at 0.87 GeV/n.

Nuclei	$\sigma_{\text{tot}}$ (mb) with $\chi_{A_1 A_2}$ equal to				$\sigma_{\text{tot}}$ (mb)
	$\chi_1$	$\chi_1+\chi_2$	$\chi_1+\chi_2+\chi_3$	$\chi_1+\chi_2+\chi_3+\chi_4$	Experiment
${}^4\text{He}-{}^4\text{He}$	{ 429 (420)	384 (373)	387 (377)	386 (375)	408 $\pm$ 2.5 (390 $\pm$ 4.2)
${}^4\text{He}-{}^{12}\text{C}$	{ 909 (885)	788 (767)	810 (792)	802 (781)	835 $\pm$ 5, 826 $\pm$ 5.9 (820 $\pm$ 13, 790 $\pm$ 0.7)
${}^4\text{He}-{}^{16}\text{O}$	1097	961	989	979	
${}^4\text{He}-{}^{24}\text{Mg}$	1387	1217	1260	1244	
${}^4\text{He}-{}^{40}\text{Ca}$	1939	1720	1778	1757	
${}^{12}\text{C}-{}^{12}\text{C}$	{ 1605 (1580)	1365 (1329)	1453 (1430)	1420 (1384)	1347 (1256 $\pm$ 31)
${}^{12}\text{C}-{}^{16}\text{O}$	1880	1599	1712	1669	
${}^{12}\text{C}-{}^{24}\text{Mg}$	2272	1931	2086	2026	
${}^{12}\text{C}-{}^{40}\text{Ca}$	3010	2584	2786	2709	
${}^{16}\text{O}-{}^{16}\text{O}$	2180	1855	1996	1942	
${}^{16}\text{O}-{}^{24}\text{Mg}$	2607	2212	2406	2332	
${}^{16}\text{O}-{}^{40}\text{Ca}$	3402	2916	3165	3071	
${}^{24}\text{Mg}-{}^{24}\text{Mg}$	3077	2607	2861	2765	
${}^{24}\text{Mg}-{}^{40}\text{Ca}$	3949	3385	3698	3577	
${}^{40}\text{Ca}-{}^{40}\text{Ca}$	4941	4307	4662	4512	

TABLE VI. The slope parameter of nucleus-nucleus forward elastic scattering cross sections. The other details are the same as in Table V.

Nuclei	Slope [(GeV/c) <sup>-2</sup> ] with $\chi_{AA_2}$ equal to				Slope [(GeV/c) <sup>-2</sup> ] Experiment
	$\chi_1$	$\chi_1+\chi_2$	$\chi_1+\chi_2+\chi_3$	$\chi_1+\chi_2+\chi_3+\chi_4$	
<sup>4</sup> He- <sup>4</sup> He	73.4 (72.0)	71.4 (69.9)	71.8 (70.3)	71.8 (70.4)	70 ± 4 (63 ± 10)
<sup>4</sup> He- <sup>12</sup> C	121.9 (120.0)	116.9 (114.8)	117.7 (115.7)	117.8 (115.9)	129±4, 117±2.4 (120±13, 117±3)
<sup>4</sup> He- <sup>16</sup> O	143.5	137.3	138.4	138.4	
<sup>4</sup> He- <sup>24</sup> Mg	173.8	165.5	167.0	167.0	
<sup>4</sup> He- <sup>40</sup> Ca	235.0	223.4	225.4	225.2	
<sup>12</sup> C- <sup>12</sup> C	192.1 (189.5)	179.8 (176.8)	183.0 (180.3)	182.5 (179.8)	204 ± 11 (254 ± 18)
<sup>12</sup> C- <sup>16</sup> O	221.3	206.4	210.7	209.8	
<sup>12</sup> C- <sup>24</sup> Mg	261.8	242.8	248.9	247.3	
<sup>12</sup> C- <sup>40</sup> Ca	340.8	315.4	324.1	321.5	
<sup>16</sup> O- <sup>16</sup> O	253.0	235.2	240.7	239.3	
<sup>16</sup> O- <sup>24</sup> Mg	296.8	274.3	282.3	279.8	
<sup>16</sup> O- <sup>40</sup> Ca	381.3	351.6	363.0	359.2	
<sup>24</sup> Mg- <sup>24</sup> Mg	344.9	316.6	328.3	324.2	
<sup>24</sup> Mg- <sup>40</sup> Ca	436.9	399.4	416.6	410.6	
<sup>40</sup> Ca- <sup>40</sup> Ca	540.6	492.6	517.2	509.1	

TABLE VII. Nucleus-nucleus inelastic cross sections. The other details are the same as in Table V.

Nuclei	$\sigma_{inel}$ ((mb) with $\chi_{A_1 A_2}$ equal to				$\sigma_{inel}$ (mb) Experiment
	$\chi_1$	$\chi_1 + \chi_2$	$\chi_1 + \chi_2 + \chi_3$	$\chi_1 + \chi_2 + \chi_3 + \chi_4$	
${}^4\text{He}-{}^4\text{He}$	305 (301)	282 (275)	283 (278)	283 (277)	276±3.7 (262±13)
${}^4\text{He}-{}^{12}\text{C}$	583 (576)	534 (522)	543 (534)	541 (530)	547±3, 423±4.6 (542±16, 516±5.3)
${}^4\text{He}-{}^{16}\text{O}$	698	641	652	649	
${}^4\text{He}-{}^{24}\text{Mg}$	863	795	810	806	
${}^4\text{He}-{}^{40}\text{Ca}$	1184	1099	1118	1113	
${}^{12}\text{C}-{}^{12}\text{C}$	973 (963)	880 (862)	910 (899)	902 (887)	888±19 (939±17)
${}^{12}\text{C}-{}^{16}\text{O}$	1128	1021	1058	1049	
${}^{12}\text{C}-{}^{24}\text{Mg}$	1344	1218	1265	1253	
${}^{12}\text{C}-{}^{40}\text{Ca}$	1759	1603	1622	1647	
${}^{16}\text{O}-{}^{16}\text{O}$	1296	1174	1219	1207	
${}^{16}\text{O}-{}^{24}\text{Mg}$	1529	1385	1443	1428	
${}^{16}\text{O}-{}^{40}\text{Ca}$	1972	1796	1869	1850	
${}^{24}\text{Mg}-{}^{24}\text{Mg}$	1784	1612	1689	1669	
${}^{24}\text{Mg}-{}^{40}\text{Ca}$	2265	2054	2153	2128	
${}^{40}\text{Ca}-{}^{40}\text{Ca}$	2807	2548	2680	2649	

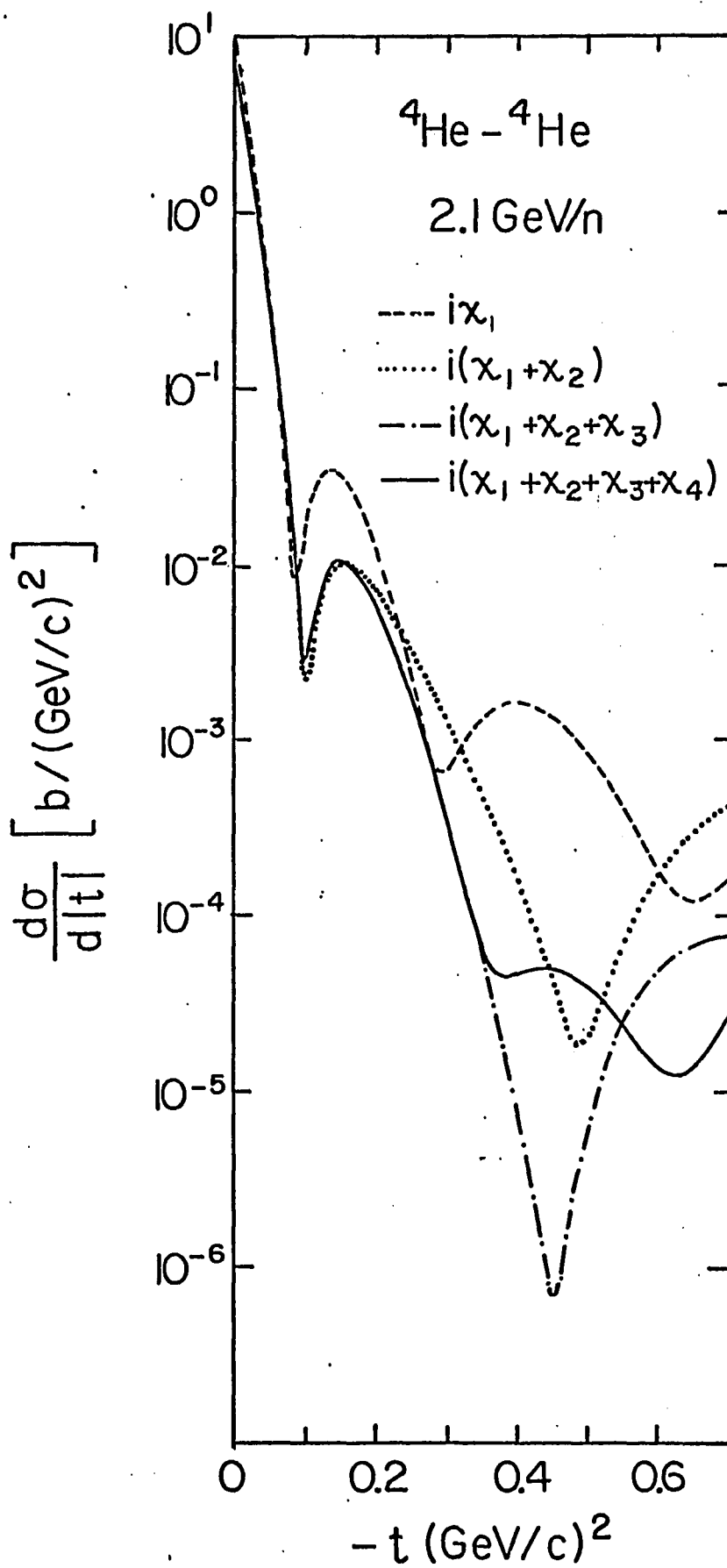
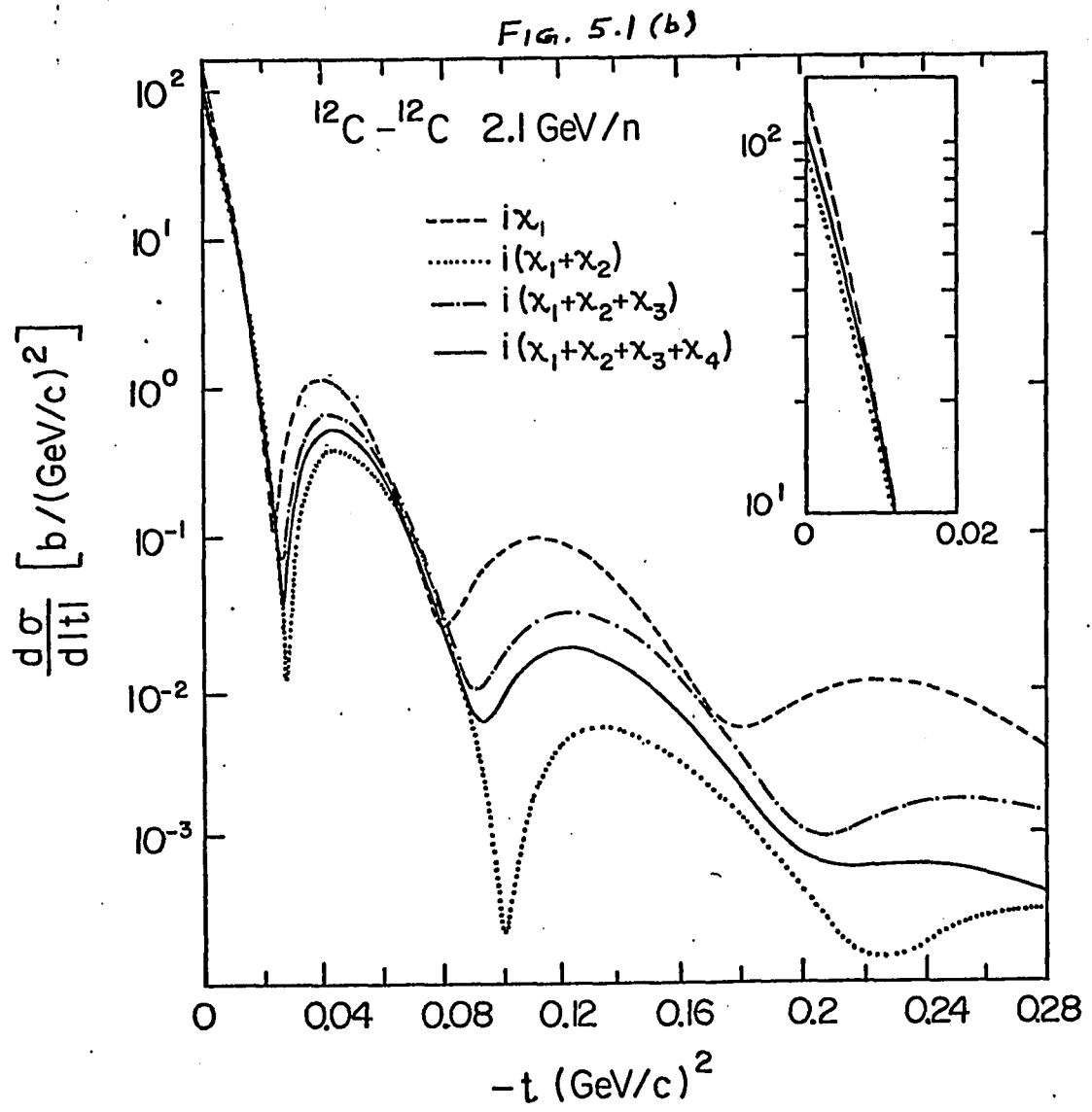


FIG. 5.1 (a)



## VI. Summary of Results

Since Coulomb-nuclear interference studies are important for obtaining  $\rho_n$  and  $a_n$  indirectly from p-d scattering measurements, we have examined various approximate formulas together with the exact results within the diffraction theory. We find that the average phase approximation Eq. (2.23) gives results almost identical to the more accurate expressions given by Eq. (2.18), and together with Eq. (2.27) for  $(d\sigma/d\Omega)_{sc}$ , provides simple analytic formulas for the study of charged hadron-deuteron elastic and elastic-plus-quasielastic scattering. In this approximation one can easily include the effects of the quadrupole deformation of the deuteron, the momentum transfer dependence of  $\rho$ , charge-exchange effects, and spin dependent effects which are important at medium energies. Using the experimental p-d measurements from 10 to 70 GeV, we have calculated the parameters  $\rho_n$  and  $a_n$  for the p-n forward scattering amplitude. Our theoretical results have also been used recently to analyze the high energy p-d data obtained at Fermi Lab.<sup>52</sup>

For hadron-nucleus scattering, we find that the formula obtained by Bethe and subsequently modified by West and Yennie gives reasonable results for light nuclei at very small angles. The approximate phase result of Eq. (3.12), where the Coulomb effects are considered to originate from the nucleus as a whole works well for all

nuclei at small angles but gives too large a cross section in the vicinity of the diffraction minima. However, if the Coulomb effects are incorporated in each proton, then the assumptions of point charges for the bound protons and the incident hadron is much more accurate than the previous approximations. Nevertheless, at the diffraction minimum this approximation can lead to errors ranging from  $\sim 0.5$  to  $\sim 8\%$  depending on the charge of the hadron and the real parts of the hadron-nucleon amplitudes. Therefore, in any analysis of hadron-nucleus scattering data, to obtain the real parts of the hadron-nucleon amplitudes, the "exact" Eq. (3.8) should be used.

Deuteron-nucleus scattering has been treated within the framework of the Glauber theory without any further approximations. For simple wavefunctions, the total cross sections and the elastic scattering intensities are expressed as finite series which converge rapidly. An approximation, where the deuteron-nucleus scattering amplitude is expressed in terms of nucleon-nucleus amplitudes, is found to be fairly accurate for total cross sections and for differential cross sections at small momentum transfers. The Coulomb effects are found to be significant near the diffraction minimum but the effects of the deuteron D-state are found to become less important as the target nucleus becomes heavier. The theoretical predictions agree very well with the deuteron-nucleus total cross section data at incident energies of 0.325, 0.87 and 2.1

GeV/n. However, at 0.325 GeV/n the theoretical calculations (without spin effects) do not agree well with the  $d-^{12}\text{C}$  elastic scattering data at larger angles. We also show that a recent impressive fit<sup>41</sup> to this data is due to the additional approximations made in that calculation.

Since high energy nucleus-nucleus cross section data<sup>42</sup> have now become available, we have also studied the problem of nucleus-nucleus scattering. The observed disagreement<sup>42</sup> between theory and measurements is found to be due to the failure of the optical limit rather than of the Glauber approximation. The optical limit result which is considered to become accurate for collisions between large nuclei, is in fact found to be the first term of a series of phase shift functions which diverges for large nuclei. We have derived corrections to the optical potential (or the optical phase shift function) which provide a basis for realistic calculations. The theoretical predictions (with the corrections) agree well with the 0.87 and 2.1 GeV/n data on nucleus nucleus total and inelastic cross sections and on the slope of nucleus-nucleus scattering amplitudes.

APPENDIX A: Exact Multiple Scattering Series for  
Nucleus-nucleus Collisions

For collisions between nuclei with mass numbers  $A_1$  and  $A_2$ , the Schrödinger equation can be written as

$$(H_{A_1} + H_{A_2} + V)|\Psi\rangle = E|\Psi\rangle. \quad (\text{A.1})$$

The free Green's function with outgoing boundary condition is

$$G_1 = (E - H_{A_1} - H_{A_2} + i.0)^{-1}, \quad (\text{A.2})$$

which leads to

$$|\Psi\rangle = |\phi\rangle + G_1 V |\Psi\rangle. \quad (\text{A.3})$$

Here  $|\phi\rangle$  is the solution of (A.1) without the interaction  $V$ . We define a wave operator  $\Omega$  such that

$$\Omega |\phi\rangle = |\Psi\rangle. \quad (\text{A.4})$$

The transition matrix is then given by

$$\begin{aligned} \langle \vec{k}' | T | \vec{k} \rangle &= \langle \vec{k}' | V | \Psi_{\vec{k}} \rangle = \langle \vec{k}' | V \Omega | \vec{k} \rangle \\ \text{or } T &= V \Omega. \end{aligned} \quad (\text{A.5})$$

Upon substituting (A.4) in (A.3), we obtain

$$\Omega = 1 + G_1 V \Omega \quad (\text{A.6})$$

When operated upon by  $V$  from left, this yields

$$T = V + V G_1 T, \quad (\text{A.7})$$

which is the Lippmann-Schwinger equation for the T matrix. Now for

$$V = \sum_i \sum_j V_{ij} \quad (\text{A.8})$$

we have

$$\begin{aligned} T &= \sum_{ij} V_{ij} + \sum_{ij} V_{ij} G T \\ &= \sum_{ij} P_{ij}, \end{aligned} \quad (\text{A.9})$$

where

$$\begin{aligned} P_{ij} &= V_{ij} + V_{ij} G \sum_{kl} P_{kl} \\ &= V_{ij} + V_{ij} G P_{ij} + V_{ij} G \sum_{k,l \neq i,j} P_{kl} \end{aligned} \quad (\text{A.10})$$

Therefore, we can write

$$\begin{aligned} (1 + V_{ij} G) P_{ij} &= V_{ij} + V_{ij} G \sum_{k,l \neq i,j} P_{kl} \\ \text{or } P_{ij} &= (1 + V_{ij} G)^{-1} V_{ij} + (1 + V_{ij} G)^{-1} V_{ij} G \sum_{k,l \neq i,j} P_{kl}. \end{aligned} \quad (\text{A.11})$$

The matrix  $t'_{ij}$  for scattering of the  $i$ th bound nucleon of projectile with  $j$ th bound nucleon of the target satisfies the equation

$$\begin{aligned} t'_{ij} &= V_{ij} + V_{ij} G t'_{ij} \\ \text{or } t'_{ij} &= (1 - V_{ij} G)^{-1} V_{ij}. \end{aligned} \quad (\text{A.12})$$

With this Eq. (A.11) becomes

$$P_{ij} = t'_{ij} + t'_{ij} G \sum_{k,l \neq i,j} P_{kl} \quad (\text{A.13})$$

and finally (A.9) yields

$$T = \sum_{ij} t'_{ij} + \sum_{\substack{ijkl \\ k,l \neq i,j}} t'_{ij} G t'_{kl} + \dots \quad (\text{A.14})$$

The multiple scattering series (A.14) represents an exact formal solution to the nucleus-nucleus scattering problem. It reduces to the Watson series for the case of a single incident particle. At this stage, one can also make a weak binding approximation

$$t'_{ij} \approx t_{ij} , \quad (\text{A.15})$$

where the free nucleon-nucleon matrix  $t_{ij}$  satisfies an equation parallel to Eq. (A.12) with  $H_{A_1}$  and  $H_{A_2}$  (in G) replaced by the corresponding kinetic energy operators.

APPENDIX B: Coulomb Phase Shift Function for Extended Charges

For collisions between point charges  $Z_p e$  and  $Z_t e$ , we have

$$\chi_c^{pt}(\vec{b}) = 2\eta \ln(b/2R), \quad (\text{B.1})$$

where  $\eta = Z_p Z_t e^2 / \hbar v$ . If the projectile and the target are considered to have extended charge distributions  $\rho_p$  and  $\rho_t$ , the Coulomb phase shift function becomes

$$\chi_c(\vec{b}) = \frac{2}{\hbar v} \int d^3r d^3r' \rho_p(\vec{r}) \rho_t(\vec{r}') \ln\left(\frac{|\vec{b} - \vec{s} + \vec{s}'|}{2R}\right), \quad (\text{B.2})$$

where  $r^2 = s^2 + z^2$  and  $r'^2 = s'^2 + z'^2$ . For the case

$$\rho_i(\vec{r}) = Z_i e \pi^{-3/2} d_i^{-3} e^{-r^2/d_i^2}, \quad i = p, t, \quad (\text{B.3})$$

Eq. (B.2) becomes

$$\chi_c(\vec{b}) = 2\eta (\pi d_p d_t)^{-2} \int d^2s d^2s' e^{-\frac{s^2}{d_p^2} - \frac{s'^2}{d_t^2}} \ln\left(\frac{|\vec{b} - \vec{s} + \vec{s}'|}{2R}\right). \quad (\text{B.4})$$

Letting  $\vec{s} - \vec{s}' = \vec{x}$  and utilizing the results<sup>53</sup>

$$\int_0^{2\pi} e^{i\lambda \cos\phi} d\phi = 2\pi I_0(\lambda), \quad \int_0^\infty e^{-\lambda x^2} I_0(2\beta x) x dx = \frac{e^{-\beta^2/\lambda}}{2\lambda},$$

we obtain

$$\chi_c(\vec{b}) = \chi_c^{pt}(\vec{b}) + \frac{\eta}{\pi(d_p^2 + d_t^2)} \int_0^\infty \int_0^{2\pi} e^{-\frac{x^2}{d_p^2 + d_t^2}} \ln\left(1 + \frac{x^2}{b^2} - \frac{2x}{b} \cos\phi\right) x dx d\phi. \quad (\text{B.5})$$

Now with the result

$$\int_0^{2\pi} \ln(1 + a^2 - 2ax \cos\phi) d\phi = 2\pi \ln a^2, \quad a^2 > 1 \\ = 0, \quad a^2 < 1$$

Eq. (B.5) yields ( $E_1(z)$  being the exponential integral<sup>53</sup>)

$$\chi_c(\vec{b}) = \chi_c^{pt}(\vec{b}) + \eta E_1\left(\frac{b^2}{d_p^2 + d_t^2}\right). \quad (\text{B.6})$$

## APPENDIX C: Average Phase Shift Functions

In this Appendix we obtain an approximation to Eq. (2.11) which leads to analytic results for both elastic and elastic plus quasi-elastic scattering by deuterium. In terms of profile functions, Eq. (2.11) can be written as (apart from the unimportant phase factor)

$$F_d(\vec{q}, \vec{s}) = e^{-\frac{i}{2}\vec{q}\cdot\vec{s}} \left[ f_c^{pt}(q) + i \int_0^\infty J_0(qb) (kb)^{2ln+1} \Gamma_c^E(b) db \right] \\ + \frac{1-k}{2\pi} \int d^2b e^{i\vec{q}\cdot\vec{b}} e^{i\chi_c^E(\vec{b}+\frac{1}{2}\vec{s})} \left[ \Gamma_{ps}(\vec{b}+\frac{1}{2}\vec{s}) \right. \\ \left. + \Gamma_n(\vec{b}-\frac{1}{2}\vec{s}) - \Gamma_{ps}(\vec{b}+\frac{1}{2}\vec{s}) \Gamma_n(\vec{b}-\frac{1}{2}\vec{s}) \right]. \quad (C.1)$$

Since for high-energy hadron-proton scattering  $n$  is small (for example, for  $\pi^\pm$ -p or p-p scattering  $n < 10^{-2}$  at medium and high energies), we can write, to  $O(n)$ ,

$$\Gamma_c^E(b) = 1 - \exp[-in E_1(b^2/r^2)] \\ \approx -in E_1(b^2/r^2), \quad r^2 = c^2 + d^2, \quad (C.2)$$

where we have assumed that the form factors  $F_x(q)$  and  $F_p(q)$  for the incident hadron and the bound proton are given by  $e^{-d^2q^2/4}$  and  $e^{-c^2q^2/4}$  respectively. The Coulomb amplitude in Eq. (C.1) is then given by

$$f_c(q) = f_c^{pt}(q) + i \int_0^\infty J_0(qb) (kb)^{2ln+1} [-ln E_1(b^2/r^2)] db. \quad (C.3)$$

The integration can be performed by expanding the Bessel function in a power series and we obtain

$$f_c(q) = f_c^{pt}(q) + n(kr)^{2ln+1} \frac{r}{2} \sum_{m=0}^{\infty} \frac{(-1)^m (qr)^{2m} \Gamma(ln+m+1)}{2^{2m} m! (ln+m+1) \Gamma(m+1)}. \quad (C.4)$$

For  $f_c^{pt}(q)$  given by Eq. (2.10), by dropping terms of  $O(n^2)$ , we obtain

$$\begin{aligned} f_c(q) &= f_c^{pt}(q) \left\{ 1 + \sum_{m=0}^{\infty} (-1)^{m+1} \frac{(q^2 r^2/4)^{m+1}}{(m+1)!} \right\} \\ &= f_c^{pt}(q) \exp(-q^2 r^2/4) \\ &= f_c^{pt}(q) F_x(q) F_p(q). \end{aligned} \quad (C.5)$$

The last three terms in Eq. (C.1) can also be approximated.<sup>57</sup> In these terms since the strong interaction profile functions become negligible for impact parameters which are larger than the sum of the deuteron size and the hadron-nucleon interaction radius, the long range part of the Coulomb interaction has little effect; and over the range of impact parameters where these terms are not negligible, the Coulomb phase shift varies slowly. We can therefore use Coulomb phase shift functions averaged over the appropriate profile functions and the deuteron ground state. They are defined as

$$\chi_{cp} = \langle i | \int \chi_c(\vec{b}_p) \Gamma_{ps}(\vec{b}_p) d^2b | i \rangle / \langle i | \int \Gamma_{ps}(\vec{b}_p) d^2b | i \rangle, \quad (C.6)$$

$$\chi_{cn} = \langle i | \int \chi_c(\vec{b}_p) \Gamma_n(\vec{b}_n) d^2b | i \rangle / \langle i | \int \Gamma_n(\vec{b}_n) d^2b | i \rangle, \quad (C.7)$$

$$\chi_{cpn} = \langle i | \int \chi_c(\vec{b}_p) \Gamma_{ps}(\vec{b}_p) \Gamma_n(\vec{b}_n) d^2b | i \rangle / \langle i | \int \Gamma_{ps}(\vec{b}_p) \Gamma_n(\vec{b}_n) d^2b | i \rangle, \quad (C.8)$$

where  $\vec{b}_p = \vec{b} + \vec{s}/2$ ,  $\vec{b}_n = \vec{b} - \vec{s}/2$  and  $|i\rangle$  refers to the ground state of the deuteron. We will evaluate  $\chi_{cpn}$ , which is the most complicated of the three, explicitly. For nucleon-nucleon amplitudes given by Eq. (2.14) we obtain

For  $f_c^{pt}(q)$  given by Eq. (2.10), by dropping terms of  $O(n^2)$ , we obtain

$$\begin{aligned} f_c(q) &= f_c^{pt}(q) \left\{ 1 + \sum_{m=0}^{\infty} (-1)^{m+1} \frac{(q^2 r^2/4)^{m+1}}{(m+1)!} \right\} \\ &= f_c^{pt}(q) \exp(-q^2 r^2/4) \\ &= f_c^{pt}(q) F_x(q) F_p(q). \end{aligned} \quad (C.5)$$

The last three terms in Eq.(C.1) can also be approximated.<sup>57</sup> In these terms since the strong interaction profile functions become negligible for impact parameters which are larger than the sum of the deuteron size and the hadron-nucleon interaction radius, the long range part of the Coulomb interaction has little effect; and over the range of impact parameters where these terms are not negligible, the Coulomb phase shift varies slowly. We can therefore use Coulomb phase shift functions averaged over the appropriate profile functions and the deuteron ground state. They are defined as

$$\chi_{cp} = \langle i | \int \chi_c(\vec{b}_p) \Gamma_{ps}(\vec{b}_p) d^2b | i \rangle / \langle i | \int \Gamma_{ps}(\vec{b}_p) d^2b | i \rangle, \quad (C.6)$$

$$\chi_{cn} = \langle i | \int \chi_c(\vec{b}_p) \Gamma_n(\vec{b}_n) d^2b | i \rangle / \langle i | \int \Gamma_n(\vec{b}_n) d^2b | i \rangle, \quad (C.7)$$

$$\chi_{cpn} = \langle i | \int \chi_c(\vec{b}_p) \Gamma_{ps}(\vec{b}_p) \Gamma_n(\vec{b}_n) d^2b | i \rangle / \langle i | \int \Gamma_{ps}(\vec{b}_p) \Gamma_n(\vec{b}_n) d^2b | i \rangle, \quad (C.8)$$

where  $\vec{b}_p = \vec{b} + \vec{s}/2$ ,  $\vec{b}_n = \vec{b} - \vec{s}/2$  and  $|i\rangle$  refers to the ground state of the deuteron. We will evaluate  $\chi_{cpn}$ , which is the most complicated of the three, explicitly. For nucleon-nucleon amplitudes given by Eq. (2.14) we obtain

$$\Gamma_n(\vec{b}) = \frac{\sigma_n(1-i\rho_n)}{4\pi} e^{-b^2/2a_n}, \quad (C.9)$$

$$\Gamma_{ps}(\vec{b}) = \frac{\sigma_p(1-i\rho_p)}{4\pi} e^{-b^2/2a_p}. \quad (C.10)$$

Now using the relation

$$\int_{-\infty}^{\infty} |\phi(\vec{r})|^2 d\vec{z} = (2\pi)^{-2} \int e^{-\vec{r} \cdot \vec{q}} S(q) d^2q, \quad (C.11)$$

where  $\phi(\vec{r})$  is the wave function for the deuteron ground state, we may express  $\chi_{cpn}$  as

$$\chi_{cpn} = \frac{\int_0^{\infty} \chi_c(b) e^{-b^2/2a_p} b db \int_0^{\infty} e^{-a_n q^2/2} J_0(qb) S(q) q dq}{a_p \int_0^{\infty} S(q) e^{-(a_n+a_p)q^2/2} q dq}. \quad (C.12)$$

For the special case in which the form factor is a sum of Gaussians, as in Eq. (2.17),  $\chi_{cpn}$  reduces to

$$\chi_{cpn} = \frac{\sum_{j=1}^N (\alpha_j / A_j) \int_0^{\infty} \chi_c(b) e^{-b^2(\alpha_j^{-1} + A_j^{-1})/2} b db}{a_p \sum_{i=1}^N (\alpha_i / H_i)}, \quad (C.13)$$

where  $A_i = a_n + 2\beta_i$  and  $H_i = a_n + a_p + 2\beta_i$ .

With  $f_c^{pt}$  as defined in Eq. (2.10), the phase shift function  $\chi_c(b)$  for Gaussian charge distributions Eqs. (B.3) and (B.6) is (see Appendix B)

$$\chi_c(b) = 2n \ln(kb) + n E_1(b^2/r^2), \quad (C.14)$$

where  $r^2 = c^2 + d^2$  and  $n = Z_1 Z_2 e^2 / \hbar v$ . To evaluate  $\chi_{cpn}$  with this expression for  $\chi_c(b)$ , we note that

$$\int_0^\infty e^{-\alpha b^2} [2n \ln(kb) + n E_1(b^2/r^2)] b db = \frac{n}{2\alpha} \left\{ \ln \left[ k^2 \left( r^2 + \frac{1}{\alpha} \right) \right] - C \right\}, \quad (C.15)$$

where  $C$  is Euler's constant,  $C = 0.577\dots$ . Using this result in Eq. (C.13), we obtain

$$\chi_{cpn} = n \sum_{i=1}^N \alpha_i H_i^{-1} \ln \left[ k^2 \left( r^2 + \frac{2a_p A_i}{H_i} \right) \right] / \sum_{i=1}^N \alpha_i H_i^{-1} - nC. \quad (C.16)$$

In a similar fashion, we find

$$\chi_{cp} = n \ln [k^2 (r^2 + 2a_p)] - nC, \quad (C.17)$$

$$\chi_{cn} = n \sum_{i=1}^N \alpha_i \ln [k^2 (r^2 + 2A_i)] - nC. \quad (C.18)$$

Using these approximations for  $e^{i\chi_c(\vec{b}_p)}$  in Eq. (C.1) together with Eq. (C.5), we obtain as an approximation to Eq. (C.1), the result

$$F_d^{av}(\vec{q}, \vec{s}) = e^{-\frac{i}{2} \vec{q} \cdot \vec{s}} f_c(q) + \frac{i k}{2\pi} \int d^2 b e^{i \vec{q} \cdot \vec{b}} \left[ e^{i\chi_{cp}} \Gamma_{ps}(\vec{b}_p) + e^{i\chi_{cn}} \Gamma_n(\vec{b}_n) - e^{i\chi_{cpn}} \Gamma_p(\vec{b}_p) \Gamma_n(\vec{b}_n) \right], \quad (C.19)$$

which leads to Eq. (2.21).

## APPENDIX D: Charge Exchange Effects

In this Appendix, we show that the effects of charge exchange in collisions of hadrons of isospin  $\frac{1}{2}$  with deuterons can be easily incorporated in the average phase approximation. Since we are considering elastic scattering where no net transfer of charge occurs, we have to allow for a pair of successive collisions with two cancelling exchanges of charge. For elastic scattering; therefore, Eq.(2.21) can be rewritten<sup>54</sup> as<sup>0</sup>

$$\begin{aligned}
 F_{el}^{av}(q) = & \left[ f_c(q) + e^{i\chi_{cp}} f_{ps}(q) + e^{i\chi_{cn}} f_n(\vec{q}) \right] S(\frac{1}{2}q) \\
 & + \frac{i}{2\pi k} e^{i\chi_{cpn}} \int S(\vec{q}') \frac{1}{2} \left[ f_{ps}(\frac{1}{2}\vec{q} + \vec{q}') f_n(\frac{1}{2}\vec{q} - \vec{q}') \right. \\
 & \left. + f_n(\frac{1}{2}\vec{q} + \vec{q}') f_{ps}(\frac{1}{2}\vec{q} - \vec{q}') - f_{ce}(\frac{1}{2}\vec{q} + \vec{q}') f_{ce}(\frac{1}{2}\vec{q} - \vec{q}') \right] d^2q'
 \end{aligned} \tag{D.1}$$

where  $f_{ce}(\vec{q}) = f_{ps}(\vec{q}) - f_n(\vec{q})$ . Using the forms for  $S(q)$ ,  $f_{ps}$  and  $f_n$  given in Sec. II, we obtain, upon integration, the result

$$\begin{aligned}
 F_{el}^{av}(q) = & \left[ f_c(q) + e^{i\chi_{cp}} f_{ps}(q) + e^{i\chi_{cn}} f_n(q) \right] S(\frac{1}{2}q) \\
 & + \frac{i}{k} e^{i\chi_{cpn}} \left[ 2c_n c_p e^{-(a_p + a_n) q^2/8} \sum_{j=1}^N \frac{d_j}{H_j} e^{(a_p - a_n) q^2/8 H_j} \right. \\
 & \left. - \frac{1}{4} \sum_{j=1}^N d_j \left\{ \frac{c_p^2 e^{-a_p q^2/4}}{(a_p + \beta_j)} + \frac{c_n^2 e^{-a_n q^2/4}}{(a_n + \beta_j)} \right\} \right].
 \end{aligned} \tag{D.2}$$

## APPENDIX E: Approximation II for d-A Scattering

In this appendix we describe the theoretical results of an approximation first used by Faldt and Pilkuhn. The details of derivation are given in Ref. 40. Generalizing the results to deuteron wave function of Eq. (4.10), and NN amplitude of Eq. (2.14), we obtain

$$F_{dA}(q) \simeq F_0(q) + F_e(q) \quad (\text{E.1})$$

where

$$F_0(q) = \mu k \int_0^\infty J_0(qb) [1 - e^{-\sigma' T(b)}] b db \\ + \frac{i k}{4} \sigma' \int_0^\infty J_0(qb) e^{-\sigma' T(b)} \Delta T(b) b db \sum_{m=1}^N \alpha_m \beta_m, \\ F_e(q) = -\frac{\mu k \sigma'^2}{16 \pi} \int_0^\infty J_0(qb) T(b) e^{-\sigma' T(b)} \sum_{m=1}^N (\alpha + \beta_m)^{-1}, \quad (\text{E.2})$$

with  $\sigma' = \sigma(1 - ip)$ .

For nuclear wave functions given by Eqs. (4.4) and (4.11),

$$T(b) = \frac{A}{\pi R^2} e^{-b^2/R^2} \\ \Delta T(b) = \frac{4A}{\pi R^4} \left[ \frac{b^2}{R^2} - 1 \right] e^{-b^2/R^2} \quad (\text{E.3})$$

## APPENDIX F: Deuteron-Deuteron Cross sections

Deuteron-deuteron scattering is studied in detail in Ref. 6. Here we can obtain it as a special case of the results of Sec. IV. We have

$$e^{i\chi_{dd}(\vec{b}, \vec{s}, \vec{s}')} = [1 - \Gamma_{pp}(\vec{b} + \frac{1}{2}\vec{s} - \frac{1}{2}\vec{s}')] [1 - \Gamma_{pn}(\vec{b} + \frac{1}{2}\vec{s} + \frac{1}{2}\vec{s}')] \\ \times [1 - \Gamma_{np}(\vec{b} - \frac{1}{2}\vec{s} - \frac{1}{2}\vec{s}')] [1 - \Gamma_{nn}(\vec{b} - \frac{1}{2}\vec{s} + \frac{1}{2}\vec{s}')] . \quad (\text{F.1})$$

Now assuming that all NN amplitudes are equal, Eq. (4.1) leads to

$$F_{dd}(q) = 8f(q)S_d^2(\frac{1}{2}q) + \frac{2i}{\pi k} \left[ 4S_d(\frac{1}{2}q) \int d^2q' S_d(\vec{q}') f(\frac{1}{2}\vec{q} - \vec{q}') \right. \\ \left. \times f(\frac{1}{2}\vec{q} + \vec{q}') + 2 \int d^2q' S_d^2(\vec{q}') f(\frac{1}{2}\vec{q} - \vec{q}') f(\frac{1}{2}\vec{q} + \vec{q}') \right] \\ - \frac{8}{\pi^2 k^2} \int d^2q' S_d(\vec{q}') f(\frac{1}{2}\vec{q} - \vec{q}') \int d^2q'' S_d(\vec{q}'') f(\frac{1}{2}\vec{q} - \vec{q}'') f(\frac{1}{2}\vec{q} + \vec{q}'') \\ - \frac{2i}{(\pi k)^3} \int d^2q' S_d(\vec{q}') \int d^2q'' S_d(\vec{q}'') \int d^2q''' f(\vec{q}''') \\ \times f(\frac{1}{2}\vec{q} - \vec{q}' - \vec{q}''') f(\frac{1}{2}\vec{q} + \vec{q}'' - \vec{q}''') f(\vec{q}' - \vec{q}'' + \vec{q}''') , \quad (\text{F.2})$$

where  $f(q) = f(\frac{1}{2}k, q)$ . With NN amplitudes and deuteron form factor, given by Eqs. (2.14), (2.17) respectively, this reduces to

$$F_{dd}(q) = 8f_0 S_d^2(\frac{1}{2}q) e^{-\frac{1}{2}aq^2} + \frac{4if_0^2}{k} e^{-\frac{1}{4}aq^2} \left[ 2S_d(\frac{1}{2}q) \sum_{i=1}^N \frac{\alpha_i}{(a+\beta_i)} \right. \\ \left. + \sum_{i,j} \frac{\alpha_i \alpha_j}{(a+\beta_i+\beta_j)} \right] - \frac{32}{k^2} f_0^3 e^{-\frac{1}{4}aq^2} \sum_{i,j} \frac{\alpha_i \alpha_j}{\alpha_{ij}} e^{\frac{a^2 q^2 (a+\beta_i+\beta_j)}{4\alpha_{ij}}} \\ - \frac{16if_0^4}{k^3 a} e^{-\frac{1}{8}aq^2} \sum_{i,j} \alpha_i \alpha_j / (2\beta_i+a)(2\beta_j+a) , \quad (\text{F.3})$$

where  $f_0 = k\sigma(i+\rho)/4\pi$  and  $\alpha_{ij} = 4(\beta_i+a)(\beta_j+a) - a^2$ .

## APPENDIX G: Nucleus-Nucleus Cross sections

For the case of NN amplitudes and nuclear form factors given by Eqs. (2.14) and (5.7) respectively, the multiple integrations in Eq. (5.6) can be performed analytically with the results

$$\begin{aligned}
C_1(b) &= (\sigma'/R^2) e^{-b^2/R^2}; \quad \sigma' = \frac{\sigma(1+e)}{2\pi}, \quad R^2 = R_1^2 + 2a + R_2^2, \\
C_2(b) &= (\sigma'^2/\alpha_1) e^{-2b^2/(R^2+R_1^2)}; \quad \alpha_1 = R^4 - R_1^4, \\
C_3(b) &= C_2 [1 \leftrightarrow 2], \\
C_4(b) &= (\sigma'^3/R^2\alpha_{12}) \exp\left[-\frac{2b^2}{R^2}\left(1 + \frac{2a^2}{\alpha_{12}}\right)\right]; \quad \alpha_{12} = \alpha_1 - R_2^4, \\
C_5(b) &= (\sigma'^3/\alpha_1\beta_1) \exp\left[-\frac{b^2}{R^2}\left(1 + \frac{2\beta_1^2}{\alpha_1}\right)\right]; \quad \beta_1 = R^2 - R_1^2, \\
C_6(b) &= C_5 [1 \leftrightarrow 2], \\
C_7(b) &= (\sigma'^4/R^2P_1\alpha_1) \exp\left[-b^2\left(\frac{2}{R^2} + \frac{\beta_1^2}{R^2\alpha_1} + \frac{\alpha_1^2}{P_1}\right)\right]; \\
&\quad P_1 = R^{-2}[\alpha_{12} - \beta_1^2 R_1^4 \alpha_1^{-1}], \quad \alpha_1 = R^{-2}[2a - \beta_1^2 R_1^2 \alpha_1^{-1}], \\
C_8(b) &= C_7 [1 \leftrightarrow 2], \\
C_9(b) &= (\sigma'^4/R^2\alpha_{12}T) \exp\left\{-b^2\left[\frac{2}{R^2+R_1^2} + \frac{\alpha_1}{R^2\alpha_{12}}\left(\frac{\beta_1}{R^2} + \frac{\beta_1 R_1^2 R_2^2}{\alpha_1 R^2} + \frac{S^2}{T}\right)\right]\right\}, \\
&\quad S = 1 - R_2^2 \beta_1 \alpha_1^{-1} - R^{-4} \alpha_{12}^{-1} (\alpha_1 \beta_2 + R_1^2 R_2^2 \beta_1) (R_1^2 + R_1^2 R_2^4 \alpha_1^{-1}), \\
&\quad T = R^2 \alpha_{12} \alpha_1^{-1} - \alpha_1 R^{-2} \alpha_{12}^{-1} (R_1^2 + R_2^4 \alpha_1^{-1})^2, \\
C_{10}(b) &= \frac{\sigma'^4 R^2}{V_1(\alpha_1^2 - R_1^4 \beta_1^2)} \exp\left\{-b^2\left[\frac{2}{R^2+R_1^2} + \frac{U_1^2}{V_1} + \frac{\beta_1 U_1}{\alpha_1}\right]\right\}, \\
&\quad U_1 = \frac{\beta_1(\alpha_1 - \beta_1 R^2)}{R^2(\alpha_1 + \beta_1 R^2)}, \quad V_1 = \frac{1}{R^2}\left[\alpha_1 - \frac{2\beta_1^2 R_1^4}{(\alpha_1 + \beta_1 R^2)}\right], \\
C_{11}(b) &= C_{10} [1 \leftrightarrow 2], \\
C_{12}(b) &= \frac{\sigma'^4}{R^2\alpha_1\delta_1} \exp\left[-b^2\left(\frac{1}{R^2} + \frac{2}{R^2+R_1^2} + \frac{\gamma_1^2}{\delta_1}\right)\right];
\end{aligned}$$

$$\gamma_1 = \frac{B_1}{R^2} - \frac{R_2^2}{R^2 + R_1^2}, \quad \delta_1 = \frac{\alpha_1}{R^2} - \frac{R^2 R_2^4}{\alpha_1},$$

$$C_{13}(b) = C_{12} [1 \leftrightarrow 2]. \quad (G.1)$$

The total phase shift function  $\chi_{A_1 A_2}$  is now given by Eqs. (5.2), (5.3) and (5.5). For the special case  $A_1 = A_2 \gg 1$ ,  $R_1^2 = R_2^2 \gg a$ , we obtain

$$i \chi_1(b) \rightarrow -A^2 \gamma e^{-b^2/R^2}, \quad \gamma = \sigma(1 - \epsilon)/2\pi R^2,$$

$$i \chi_2(b) \rightarrow i \chi_1(b) (A\gamma) \left[ e^{-b^2/R^2} - 1.33 e^{-b^2/3R^2} \right],$$

$$i \chi_3(b) \rightarrow i \chi_1(b) (A\gamma)^2 \left[ 1.67 e^{-2b^2/R^2} - 4 e^{-4b^2/3R^2} + 2 e^{-b^2/R^2} + 0.67 e^{-b^2/2R^2} \right],$$

$$i \chi_4(b) \rightarrow i \chi_1(b) (A\gamma)^3 \left[ 3.5 e^{-3b^2/R^2} - 12 e^{-7b^2/3R^2} + 4 e^{-5b^2/3R^2} + 8 e^{-2b^2/R^2} + 2.67 e^{-3b^2/2R^2} - 6.4 e^{-7b^2/5R^2} - 0.27 e^{-3b^2/5R^2} \right]. \quad (G.2)$$

The nucleus-nucleus total cross sections is now given by

$$\sigma_{tot} = \frac{4\pi}{k} \text{Im} F_{A_1 A_2}(0) = 2 \text{Re} \int d^2b [1 - e^{i \chi_{A_1 A_2}(b)}], \quad (G.3)$$

and the inelastic cross section by

$$\sigma_{inel} = \sigma_{tot} - \sigma_{el} = 2\pi \int_0^\infty \{1 - |e^{i \chi_{A_1 A_2}(b)}|^2\} b db. \quad (G.4)$$

If the nucleus-nucleus forward scattering amplitude, is taken to be

$$F_{A_1 A_2}(q) = F_0 e^{-\frac{1}{2} B q^2},$$

the slope parameter is given by

$$B = \lim_{q \rightarrow 0} \left[ -2 \frac{(\partial F_{A_1 A_2} / \partial q^2)}{F_{A_1 A_2}} \right] \rightarrow \frac{\int_0^\infty \Gamma_{A_1 A_2}(b) b^3 db}{2 \int_0^\infty \Gamma_{A_1 A_2}(b) b db}. \quad (G.5)$$

We should point out that in obtaining Eq. (G.4), for con-

venience in numerical calculations, in  $\sigma_{e1}$  we have neglected the c.m. correlation function  $K_{12}(q)$ . This approximation is expected to be good since nucleus-nucleus amplitudes are sharply peaked in forward direction and the dominant contributions to  $\sigma_{e1}$  come from very small  $q$  region, where  $K_{12}(q)$  has little effect.

## APPENDIX H: Center of Mass Correction

For harmonic oscillator wave functions, the center of mass correlation function is given by<sup>32</sup>

$$K_1(q) = \exp(q^2 R^2 / 4A) \quad . \quad (H.1)$$

However, in Sections III-V, use has been made of the fact that (H.1) is the correct form for Gaussian wave functions. That this is so, will be demonstrated in this section.

Utilizing the expansion

$$1 - \prod_{j=1}^A \{1 - \Gamma_j\} = \sum_{j=1}^A \Gamma_j - \sum_{j \neq k} \Gamma_j \Gamma_k + \dots \quad , \quad (H.2)$$

the hadron-nucleus amplitude (3.1) (without the  $\delta$ -function) can be rewritten as

$$\begin{aligned} F_A(q) = & \lambda k_A \left[ (\lambda k_N)^{-1} \sum_j \int d^2 q_1 f_j(\vec{q}_1) S_A(q_1) \delta^2(\vec{q} - \vec{q}_1) \right. \\ & - (\lambda k_N)^{-2} (2\pi)^{-1} \sum_{j \neq k} \int d^2 q_1 d^2 q_2 f_j(\vec{q}_1) f_k(\vec{q}_2) S_A(q_1) \\ & \left. \times S_A(q_2) \delta^2(\vec{q} - \vec{q}_1 - \vec{q}_2) + \dots \right] \quad . \quad (H.3) \end{aligned}$$

Now let us consider the  $\delta$ -function constraint due to c.m.

With

$$\begin{aligned} |\Psi(\vec{r}_1, \dots, \vec{r}_A)|^2 \delta^3\left(\sum_j \vec{r}_j\right) &= \left[ \left(\frac{\pi R^2}{A}\right)^{3/2} \prod_{j=1}^A |\phi_j(\vec{r}_j)|^2 \right] (2\pi)^{-3} \int d^3 \lambda e^{i \sum_j \vec{\lambda} \cdot \vec{r}_j / A} \\ &= \left(\frac{\pi R^2}{A}\right)^{3/2} (2\pi)^{-3} \int d^3 \lambda \prod_{j=1}^A \left[ |\phi_j(\vec{r}_j)|^2 e^{i(\vec{\lambda}_1 \cdot \vec{r}_j + \lambda_2 z_j) / A} \right] \quad (H.4) \end{aligned}$$

in (3.1) we will obtain a series for  $F_A$  similar to (H.3) with  $S_A(\vec{q}_1) \rightarrow S_A(\vec{q}_1 + \frac{\vec{\lambda}_1}{A})$  and factors of type  $\exp(-N\lambda_1^2 R^2 / 4A^2)$  [ $N=(A-1)$ ,  $(A-2)$  and so on, for first, second terms etc.].

With Gaussian form (4.11) for  $|\phi_j|^2$ , we have  $S_A(\vec{q}_i + \frac{\vec{\lambda}_i}{A})$   
 $= S_A(\vec{q}_i) \exp(-R^2 \lambda_{1i}^2 / 4A^2 - R^2 \vec{q}_i \cdot \vec{\lambda}_{1i} / 2A)$ . Upon performing  
 integration over  $\vec{\lambda}$ , we obtain a series exactly like (H.3)  
 except that there are additional factors  $e^{q_1^2 R^2 / 4A}$  in first  
 term,  $e^{(\vec{q}_1 + \vec{q}_2)^2 R^2 / 4A}$  in second term and so on. But due  
 to the  $\delta$ -functions occurring in (H.3), this leads to a  
 contribution of  $\exp(q^2 R^2 / 4A)$  from each term. Therefore,  
 the net effect of introducing the c.m. constraint is to  
 multiply the amplitude by the factor  $K_1(q)$  given by (H.1).  
 This result can be extended to nucleus-nucleus collisions,  
 in a straight forward manner, to yield a correction term

$$K_{12}(q) = \exp(q^2 R_1^2 / 4A_1 + q^2 R_2^2 / 4A_2) .$$

(H.5)

## BIBLIOGRAPHY

1. R.J. Glauber, Lectures in Theoretical Physics, edited by W.B. Brittin et al. (Wiley-Interscience, New York, 1959), Vol.I., p. 315.
2. K.M. Watson, Phys. Rev. 89,575 (1953); K.M. Watson and M.L. Goldberger, Collision Theory (John Wiley & Sons, N.Y. 1964).
3. See, for example, C. Carlson, Phys. Rev. C2,1224(1970).
4. A.K. Kerman, H. McManus and R.M. Thaler, Ann. Phys. 8, 551 (1959).
5. R.H. Landau, S.C. Phatak and F. Tabakin, Ann. Phys. 78, 299 (1973) and references therein.
6. V. Franco, Phys. Rev. 175, 1376 (1968); Phys. Rev. Lett. 32, 911 (1974).
7. W. Czyż and L.C. Maximon, Ann. Phys. 52, 59 (1969).
8. A. Dar and Z. Kirzon, Phys. Lett. 37B, 166 (1971); Nuclear Physics A237, 319 (1975).
9. W.L. Wang, Phys. Lett. 52B, 143 (1974); W.L. Wang and R.G. Lipes, Phys. Rev. C9, 814 (1974).
10. S. Barshay, C.B. Dover and J.P. Vary, Phys. Rev. C11, 360 (1975).
11. See, for example, J.P. Vary and C.B. Dover, Phys. Rev. Lett. 31, 1510 (1973).
12. D.R. Harrington, Phys. Rev. 184, 1745 (1969).
13. T.A. Osborn, Ann. Phys. 58, 417 (1970).
14. J.M. Eisenberg, Ann. Phys. 71, 542 (1972).

15. V. Franco and R.J. Glauber, Phys. Rev. 142, 1195 (1966).
16. G. Bellettini et al., Phys. Lett. 19, 341 (1965); L.M.C. Dutton et al., Phys. Lett. 25B, 245 (1967); Phys. Rev. Lett. 21, 1416 (1968), and Nucl. Phys. B9, 594 (1969).
17. G.G. Beznogikh et al., Sov. J. Nucl. Phys. 18, 179 (1974).
18. G.G. Beznogikh et al., Nucl. Phys. B54, 97 (1973).
19. V. Franco, Phys. Rev. Lett. 27, 1541 (1971).
20. V. Franco and G.K. Varma, Phys. Rev. C12, 225 (1975); Phys. Rev. Lett. 33, 44 (1974).
21. R.V. Reid, Ann. Phys. 50, 411 (1968); J.M. Humberston and J.B.C. Wallace, Nucl. Phys. A141, 362 (1970); C.N. Bressel, A.K. Kerman and B. Rouben, Nucl. Phys. A124, 624 (1969); T. Hamada and I.D. Johnston, Nucl. Phys. 34, 382 (1962); M.J. Moravcsik, Nucl. Phys. 7, 113 (1958).
22. G.G. Beznogikh et al., Phys. Lett. 43B, 85 (1973).
23. G.G. Beznogikh et al., Phys. Lett. 39B, 411 (1972).
24. S.P. Denisov et al., Phys. Lett. 36B, 415 (1971).
25. L.S. Zolin et al., Sov. J. Nucl. Phys. 18, 30 (1974).
26. J. Engler et al., Nucl. Phys. B62, 160 (1973).
27. V.S. Barashenkov and V.D. Toneev, Preprint R2-3850, JINR, 1968.
28. A.A. Carter and D.V. Bugg, Phys. Lett. 20, 203 (1966).
29. J. Pumplin and M. Ross, Phys. Rev. Lett. 21, 1778 (1968); V.N. Gribov, Sov. Phys. JETP 29, 483 (1969).

30. See, for example, J.S. Trefil, Phys. Rev. D3, 1615 (1971); M. Ikeda, Phys. Rev. C6, 1608 (1972).
31. J. Engler et al., Phys. Lett. 31B, 669 (1970); L.W. Jones et al., Phys. Lett. 36B, 509 (1971); M.J. Longo et al., Phys. Rev. Lett. 33, 725 (1974).
32. L.J. Tassie and F.C. Barker, Phys. Rev. 111, 940 (1958).
33. H. Lesniak and L. Lesniak, Nucl. Phys. B38, 221 (1972).
34. L. Zamick, Ann. Phys. (N.Y.) 21, 550 (1963).
35. M.L. Rustgi, Nucl. Phys. 59, 460 (1964); Phys. Lett. 24B, 229 (1967).
36. L.M.C. Dutton et al., Phys. Lett. 16, 331 (1965).
37. J.F. Reading, Phys. Rev. 156, 1110 (1966).
38. T. Sawada, Nucl. Phys. 74, 289 (1965).
39. A. Tekou, Nucl. Phys. B46, 141 (1972).
40. G. Fäldt and H. Pilkuhn, Ann. Phys. (N.Y.) 58, 454 (1970).
41. K.S. Chadha and V.S. Varma, Phys. Rev. C13, 715 (1976).
42. J. Jaros, Ph.D. Thesis, University of California (1975); Lawrence Berkeley Laboratory Report LBL-3849.
43. A formula similar to Eq. (4.23) was also obtained in Ref. 39.
44. V. Franco, Phys. Rev. C6, 748 (1972).
45. H.R. Collard, L.R.B. Elton and R. Hofstadter, in Nuclear Radii, edited by H. Schopper (Springer Verlag, Berlin-Hedelberg-New York, 1967).
46. O. Benary et al., UCRL Report No. UCRL-20000NN, (1970);

- W.N. Hess, Rev. Mod. Phys. 30, 368 (1958).
47. D.V. Bugg et al., Phys. Rev. 146, 980 (1966); R.E. Mischke et al., Phys. Rev. Lett. 25, 1724 (1970).
48. L.M.C. Dutton et al., Nucl. Phys. B9, 594 (1969).  
In this Ref.  $\rho_{pn}=0.05\pm 0.20$ . But the formula used in this Reference for d-p scattering is erroneous. We, therefore, take  $\rho_{pn}=0.25$  as predicted by dispersion relations (Ref. 28).
49. D.R. Harrington, Phys. Rev. Lett. 21, 1496 (1968); V. Franco and R.J. Glauber, Phys. Rev. Lett. 22, 370 (1969).
50. See, for example, D.R. Harrington and A. Pagnamenta, Phys. Rev. 184, 1908 (1969).
51. T.T. Chou and C.N. Yang, Phys. Rev. 170, 1591 (1968); 175, 1832 (1968).
52. Y. Akimov et al., Phys. Rev. D12, 3399 (1975).
53. I.S. Gradshteyn and I.M. Ryzhik; Table of Integrals, Series and Products (Academic, N.Y., 1965).
54. R.J. Glauber and V. Franco, Phys. Rev. 156, 1685 (1967).
55. In obtaining Eq. (5.5), the independent particle model (5.7) has been used.
56. The approximations of Bethe and of West and Yennie have been studied by V. Franco, Phys. Rev. D7, 215 (1973).
57. V. Franco, Phys. Rev. Lett., 16, 944 (1966).